NASA Contractor Report 187471

CONTROL-STRUCTURE-INTERACTION (CSI) TECHNOLOGIES AND TRENDS FOR FUTURE NASA MISSIONS

Photon Research Associates
Cambridge Research Division

LAWRENCE LIVERMORE NATIONAL LABORATORY
Livermore, California

Purchase Order L-44566C
December 1990

National Aeronautics and
Space Administration

Langley Research Center
Hampton, Virginia 23665-5225

CR-R-059

CONTROL-STRUCTURE-INTERACTION (CSI) TECHNOLOGIES AND TRENDS FOR FUTURE NASA MISSIONS

FINAL REPORT

SUBMITTED TO:
LAWRENCE LIVERMORE NATIONAL LABORATORY
P.O. BOX 5012
LIVERMORE, CA 94550

SUBMITTED BY:
PHOTON RESEARCH ASSOCIATES
CAMBRIDGE RESEARCH DIVISION
1033 MASSACHUSETTS AVENUE
CAMBRIDGE, MA 02138
(617) 354-1522

IN RESPONSE TO:
CONTRACT NO.
B063679

PREFACE

This is the final report for the Lawrence Livermore National Laboratory, LLNL contract number B063679, entitled "Control-Structure-Interaction (CSI) Technologies and Trends for Future NASA Missions". This report covers work performed during the period from 9 December 1988 through 16 December 1989.

Contributions to the program were made by the entire staff of Photon Research Associates, Cambridge Division. Dr. James Turner acted as program manager and principal investigator. The engineering staff included Dr. Hon Chun, Dr. James Keat, Ms. Laura Larkin, Dr. Leslie Matson, Dr. Keto Soosaar, and Ms. Karen Swiech.

TABLE OF CONTENTS

LIST OF FIGURES

LIST OF TABLES

1.0 GOAL OF THE STUDY

The objective of the study has been to review Control-Structure-Interaction (CSI) issues which are relevant for NASA systems. This goal has been achieved by: 1) reviewing large space structures (LSS) technologies to provide a background and survey of the current state-of-the-art (SOA) 2) analytically studying a focus mission to identify opportunities where CSI technology may be applied to enhance or enable future NASA spacecraft and, 3) expanding a portion of the focus mission, the large antenna, to provide in-depth trade studies, scaling laws, and methodologies which may be applied to other NASA missions.

NASA anticipates several classes of missions which may experience CSI. To make the conclusions as broadly applicable as possible, the first portion of the study has considered generic mission requirements and reviewed: CSI design methodology including model reduction, system identification, and modern control techniques, as well as the community's experimental heritage.

The focus mission chosen for the second portion of the study has been the Earth Observation Sciences Geostationary Platform Bus (EOS-GPB). Three finite element models with varying degrees of complexity and flexibility have been analyzed to reveal potential CSI. A variety of disturbance sources have been examined and applied to the models. This numerical study has shown the importance of early preliminary system definition in order to examine potential CSI effects.

The third portion of the study expands on part of the Geoplat structure, the large antenna. Since many NASA missions will be either primarily a large antenna or a platform which includes a large antenna, this type of structure is of great interest. Most likely these antennas and their supporting structures will be flexible. This segment of the study provides insight into the more generic CSI issue by developing a new CSI methodology for assessing potential spacecraft behaviors in terms of mass, operational (electromagnetic) frequency and control approach (e.g., passive vs. active control).

The report is presented in several sections. Section 1 defines CSI issues and presents an overview of the relevant modeling and control issues for Large Space Structures. Section 2 presents the results of the three phases of the CSI study. Section 2.1 gives the results of a CSI study conducted with the Geostationary Platform (Geoplat) as the focus mission. Section 2.2 contains an overview of the CSI control design methodology available in the technical community. Included is a survey of the CSI ground-based experiments which have been conducted to verify theoretical performance predictions. Section 2.3 presents and demonstrates a new CSI scaling law methodology for assessing potential CSI with large antenna systems.

1.1 Definition Of The CSI Problem

CSI has existed since the earliest launches of satellites into space. In the beginning, however, the satellites were small and structurally stiff. Because the structures were stiff, a significant gap existed which separated the disturbance and structural frequency bandwidths, leading to vehicles which did not develop troublesome induced structural responses. Over time, however, as satellites have become larger they have tended to become more flexible. There are several reasons for the increased structural flexibility. First, launch weight constraints require that vehicles weigh as little as possible because of the high cost per pound to place satellites on-orbit. A byproduct of the launch weight constraints is that the structural designs tend to minimize the amount of material used to construct the structures. Because the structural frequencies are inversely proportional to the weight of the vehicle, the overall vehicle frequencies become lower, which increases the potential for resonant interactions with the controller. In addition to the launch weight constraints satellites must be efficiently packaged in order to fit within the launch volume constraints. These constraints lead to design requirements for structures with small cross sectional areas, which again leads to lower structural frequencies.

As vehicles become larger, their structural behavior can be shown to scale nonlinearly with size, while the associated performance requirements tighten (See Figure 1). How severe these problems become depends on the operational frequency of the main sensor which is frequently an antenna. For example, antenna systems which operate at long wavelengths may be able to function with significant induced structural behavior, whereas systems which operate at optical wavelengths may be able to tolerate only microns of induced motions.

There are many potential sources of on-board and environmental disturbances. For example, on-board disturbances can include: mass imbalances in rotating machinery, thruster station keeping and attitude control firings, cryocoolers, fluid sloshing motions, crew motions, as well as changing system parameters due to expendable fuels. On the other hand, external environmental disturbances can include: gravity gradient torques, solar radiation pressure, atmospheric drag, and thermal loads. For systems where the open-loop structural behavior (with no control system) exceeds the allowable tolerances, advanced technologies can beneficially be applied to reduce the system responses to acceptable levels.

There are two basic approaches for resolving potential control/structure interactions. First, one can invoke passive techniques which attempt to modify the structural behavior in such a way that the resulting open-loop behavior remains within the

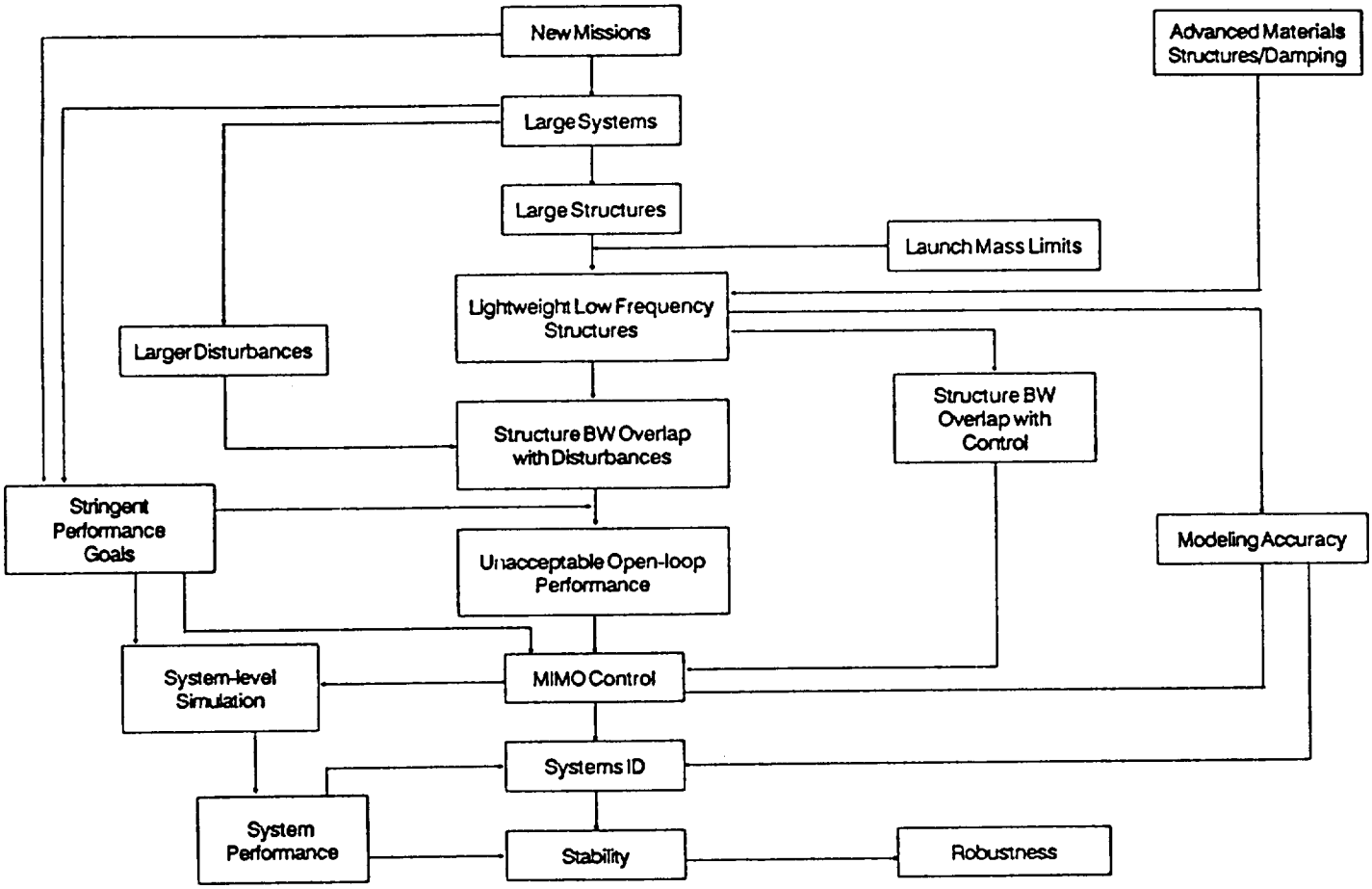

Figure 1: CSI GENESIS

mission tolerances. Examples of this approach include: 1) modifying the structure to increase its stiffness, 2) isolating disturbance sources from the structure, 3) adding passive damping treatments to remove energy from the structure when a forced response has been excited, and 4) use of so-called smart structure concepts for defining local member damping mechanisms.

For systems where passive solution approaches fail to bring the system response to within prescribed performance tolerances one must resort to active means. When active means are used, various control approaches can be applied to reduce the induced system response. Unlike passive techniques active approaches define corrective inputs based on observing the system response by using a priori systems models to define the control laws which seek to suppress the induced responses. A fundamental difference between passive and active control approaches is that active systems have the potential for exciting a response if the control is improperly designed.

There are several potential mechanisms by which a control can induce an unanticipated structural response. For example, the models used for the control design represent idealizations of the real physical vehicle. Idealizations are necessary because the governing equations of motion are rigorously defined by Partial Differential Equations (PDE's), which are difficult to deal with either analytically or numerically. To solve PDE models one makes use of two levels of modeling approximations to generate a workable description. The first approximation consists of replacing the PDE description in terms of a finite element description of the structure. In this approach the structure is viewed as an assemblage of interconnected spatial domains which possess internal degrees of freedom to account for elastic behavior. The resulting mathematical description is now defined in terms of Ordinary Differential Equations (ODE's) rather than the more fundamental and complicated PDE model. The accuracy of the ODE model depends on the finite element grid size used in the modeling of the structural elements. These approximations represent the first level of idealization in the development of the mathematical model. The second level of mathematical idealization arises because the finite model (e.g., consisting typically of hundreds to thousands of subdomains) must be reduced in size in order to be useful for simulation purposes. The standard approach is to transform the physical space finite element model (i.e., all degrees of freedom retained for each subdomain) into an equivalent modal space model where the system response is described in terms of the uncoupled system vibration modes. By developing disturbance models and performance metrics the system response can be assessed in terms of the participation of various structural vibration modes. The selection of a suitable math model for the structure is known as a reduced-order model (ROM) methodology. The selection of a ROM represents a second level of approximation in that the high frequency behavior of the structure is truncated, though low

frequency modes can also be deleted if they can be shown not to affect the performance metrics which define the mission design goals. The ROM and control design process is typically accomplished iteratively to insure stability and performance when the final control design is tested on a "truth model" consisting of all of the modes defined by the finite element model.

Because the control design process for LSS is complicated, it is of interest to develop systematic approaches for evaluating the potential for applying CSI technology (i.e., advanced control designs and systems) in large platform, antenna, and optical systems. The availability of top-level evaluation tools can be a great aid if they can be used to assess how close a system concept is to requiring active control to achieve mission objectives (e.g., line-of-sight (LOS) pointing stability). An early assessment and detection of any detrimental interactions can be helpful in weeding out impractical concepts and helping define technology programs to insure that the hardware is available to support planned operational systems.

1.2 Issues Relevant To NASA Missions

A complete understanding of the CSI issues and technologies for LSS requires that five basic and interrelated issues are thoroughly understood. As shown in Table 1, the five key technical issues are: modeling accuracy, control law design, sensors and actuators, system identification, and system validation.

Model accuracy is important because control systems can only be expected to perform well when they are designed with a full knowledge of the structural behavior to be suppressed. Uncertainty in the knowledge of the structural frequencies and mode shapes can lead to two harmful effects. First, the control system has to work hard in order to achieve the performance goals. Second, the control system can completely fail to achieve the desired tolerances and in the worst case can lead to instability in the system performance.

Control law designs are an integral part of developing an effective strategy for maintaining system performance within appropriate bounds. There are two basic approaches that one can employ in addressing the control law synthesis process: classical and modern control methodologies. Classical approaches have been used for many years and are well understood. The limitation of these methods is that the designer must think in terms of a single input and a single output which is uncoupled from other control inputs which may be applied to the system. This restriction is particularly important for spacecraft applications which have many vibration modes which must be controlled. Modern control methods,

TABLE 1: KEY CSI TECHNICAL ISSUES

Technical Issues	Potential Concerns	Resolution/Tradeoff
Modeling Accuracy	- Nonlinear Effects - Fluid Motion - Stability - Performance	- Material, Nonlinear Joint, Fluid Motion Models Increased Fidelity vs. Computational cost - Ground Testing - System ID, Adaptive Control
Control Law Design	- ROM Spillover - Robustness - Performance	- Improved Model Selection/ROM - Robust Design Techniques - Nonconservative Analysis Techniques - Distributed Control Approaches - Adaptive Control
Sensors & Actuators Actuators	- Poor Performance Due to Bandwidth, Saturation, Resolution, Noise, Nonlinearity, Placement - Failures	- New Technology (Fiber Optics, Electro-Optics, Piezoelectrics) - Optimal Placement Methods - Testing and Refinement - Redundancy Management
System Identification	- Resolution of Closely Spaced Modes - Computational Complexity - Sensor Resolution and Bandwidth - Nonlinearities	- Stochastic Methods - Adaptive Methods - Parallel Processing
System Validation	- Testing in 1-G - Facilities for LSS - Suspension & Scaling - Cost	- Develop Space-Validated Analytical Tools - Novel, Active 0-G Suspension - Scaling Laws - New Facilities

on the other hand, can deal with the multi-input/multi-output(MIMO) nature of spacecraft applications directly. The challenge for modern control methods is that high performance can only be achieved when the parameters defining the structure are well-known. Potential sources of errors include assumed estimates for: mass, stiffness, thermal properties, boundary conditions at joints, as well as the purely mathematical idealizations involved in developing the ROM. To overcome the intrinsic sensitivity of modern controllers many researchers have attempted to develop so-called robust control design approaches which can tolerate modest levels of uncertainty in the math model for the structure.

Sensors and actuators provide the means for observing and controlling the system response. These elements possess their own internal dynamic characteristics which can interact with the structure to be controlled. The key issues are bandwidth, saturation levels, and resolution. Improper placement of these devices on a structure can corrupt the interpretation of observed signals and lead to incorrect controls being applied to the structure. For many applications the capabilities of these devices represent the "Achilles heel" in the development of operational control systems. The development of new and improved device concepts is a technical area which deserves to receive continued support in the future.

System identification seeks to improve the performance of a control system by establishing improved estimates for the parameters which arise in the equations of motion. These new estimates are then used to compute new control parameters which are used by the control system. In principle, system identification algorithms can correct the math models for all errors arising from modeling idealizations and approximate parameter values. Currently, this methodology is limited to linear system analysis.

Before a satellite is launched into space it is important to validate the system performance. This is accomplished by conducting a series of ground-based tests. Ground testing cannot duplicate the on-orbit environmental conditions exactly because of the effects of gravity and atmospheric drag, as well as support structure interactions with the operational vehicle. Nonetheless, critical elements can be tested and verified to perform properly. Because of the size of LSS concepts it is necessary to consider scaled models in order to obtain information regarding the performance of the full-scale systems. The ground test is important because it can be used to confirm both the hardware performance and the analytical software prediction tools which can be adjusted to account for the on-orbit environmental conditions. As systems become larger, it becomes increasingly important to have space verified software tools, particularly when extrapolations from scaled systems are in doubt.

1.3 Net National Mission Model

CSI technology involves many disciplines which must effectively integrate concepts and technologies to achieve solutions. To define the magnitude of the problem for different systems, the problem must be divided into more manageable pieces. The first step consists of considering the range of operational frequencies which can be encountered in typical applications. As shown in Table 2 the short wavelengths correspond to optical systems and the long wavelengths correspond to radar systems. The control goals are defined in terms of the ratio of open-loop performance over closed-loop performance for various design objectives such as pointing stability and wavefront control. Defined in this way, a numerical value of 100 for a ratio of open-loop to closed-loop performance, implies that the closed-loop control must reduce the open-loop response by a factor of greater than 100 in order to achieve the mission objectives.

Structural deformation performance tolerances are typically defined in terms of fractions of the operational wavelength. Optical systems have the tightest requirements because of the short operational wavelength. The control requirements, however, for these systems have much larger bandwidths because any induced motions beyond essentially infinitesimal values exceed the performance tolerances. It should be recognized, however, that these systems represent generic applications, which only provide top-level bounds for defining the complexity of the active control problem. Properly used, however, these bounds can be employed to guide the theoretical and experimental demonstrations necessary for developing the required technology.

From Table 2 it can also be seen that active control approaches must be able to address different classes of disturbance inputs. For example, optical systems can be dominated by slew and periodic inputs, whereas the radar systems may have to deal with scanning inputs. As shown in Table 3, the classes of disturbance inputs are categorized in terms of periodic disturbances, random disturbances, and slew and attitude control. Requirements for achieving important mission goals have also been defined and compared with predicted capabilities from theory and experiment. Though the theoretical capabilities are seen to be in close agreement with the mission requirements, further comparison with experimentally demonstrated methods is disappointing. Section 2.2.4 describes many experiments which have been undertaken to demonstrate the active control technology required for handling CSI for LSS.

Tables 4 and 5 define the mission and theoretical capabilities required for modeling accuracy in structures, dynamics, and disturbances, and system identification. This data represents a reduction and synthesis of the information contained in References

TABLE 2: NET NATIONAL MISSIONS - ACTIVE STRUCTURES GOALS

	SHORT λ - OPTICAL	LONG λ - RADAR
OPERATING PARAMETERS		
Diameter	15m	100m
Wavelength	1μm	3 cm
TOLERANCES		
Surface	0.03	0.4 mm
Defocus	0.2	0.2
Pointing	10 nrad	10 mrad
Disturbances	Periodic, random, slew	Scan, slew, periodic
CONTROL REDUCTION GOALS*		
LOS	10^2 - 10^4	10 - 10^2
Wavefront	0 - 10	10 - 10^2
STRUCTURAL MODEL		
Modes in BW	100	50
Controlled Modes	30	30
Control BW (Hz)	50	5

* Reduction necessary to achieve performance, i.e., open-loop response/closed-loop response.

TABLE 3: PROGRESS IN CONTROL DESIGN METHODOLOGY

TYPE OF PROBLEM	REQUIREMENT	THEORY AND EXPERIMENT	LAB DEMONSTRATION	FLIGHT TESTED
PERIODIC DISTURBANCE	5 Hz, 10 Hz			
Modes of Interest	150	150	13	
Controlled Modes	25	30	2 Rigid, 5 Flex	NONE
Bandwidth of Control (Hz)	26	25	45	
Reduction Level	10^4	10^5	10^1	
RANDOM DISTURBANCE				
Disturbance BW (Hz)	DC to 15	DC to 15		
Modes of Interest	150	150		
Controlled Modes	30		NONE	NONE
Bandwidth of Control (Hz)	40	40		
Reduction Level	10^3	10		
SLEW AND ATTITUDE CONTROL				
Disturbance	10^o in 1 sec	10^o in 1 sec	3^o in 3 sec	
Modes of Interest	150	150	7	
Controlled Modes	100	100	3	
Bandwidth of Control (Hz)	130	130	80	UNKNOWN
Reduction Level	10^4	10^4 -5 x torque 10^2 -2 x torque	10^2	

74-85. Clearly many of these technical areas require a significant amount of work before the significant gaps separating mission requirements and theoretical
capabilities can be closed. For example, if 150 modes are required for a control system to function properly, a very practical question arises as to whether the control system can tolerate the expected levels of modeling accuracy errors in the frequencies mode shapes, and damping levels. Advanced theoretical developments and experimental demonstrations should be developed with these requirements in mind.

Figure 2 presents a paradigm for the integration of CSI technology with the development cycle of a typical mission. Once a basic engineering concept is mature enough to be modeled and simulated, existing CSI technology can be used to develop a control system which meets the mission performance objectives. A preliminary assessment of the proposed design establishes whether existing or projected capabilities will solve any observed CSI problems or whether new research and development programs are necessary in order to meet the program objectives. If new programs are required then parallel efforts can be established which conduct the required research, develop prototypes, and demonstrate experimentally that workable approaches will resolve the previously identified CSI problem.

1.4 Study Approach

The study is divided into three distinct sections. The first section reviews the potential for CSI technology applications in the EOS-Geostationary Platform focus mission. In Section 2.1 the basic methods available for developing active control models are presented and associated ground-based experiments are discussed.

Section 2.2 describes in detail the model which has been used in this study. Geoplat is of interest because it consists of a platform which has many independent instruments which must be pointed at either points on the earth or stars in space. The platform has two large antennas which provide low structural frequency dynamics behavior. The small antenna is a 7.5 m solid and the large antenna is a 15m mesh structure. Though instruments are distributed throughout the platform, there is a central instrument deck where all of the high pointing accuracy devices are located. The CSI technology benefit question addressed by the study is to establish whether any instrument pointing problems are likely to arise when the Geostationary Platform structure is subjected to disturbances expected to exist during on-orbit operational conditions. The results of this effort are described in Sections 2.2.4 and 2.2.5.

TABLE 4: MODELING ACCURACY: STRUCTURES, DYNAMICS, AND DISTURBANCES

AREA OF CONCERN	REQUIREMENT	THEORETICAL CAPABILITY
STRUCTURES		
Number of Modes	150	
Frequency Accuracy	Unknown	1-1%, 2-5% 10-30%
Modeshape Accuracy	Unknown	1-2%, 2-10% 10-60%
Damping Accuracy	Unknown	50%
DYNAMICS		
"Fixed Configuration"	Rings, Trees	Trees, 20 DOF
Deploying Configuration	100 DOF 100 DOF	NONE
DISTURBANCES		
Environmental	Problem Dependent	No Problems
On-Board	Problem Dependent	Some Problem for Optical Systems

TABLE 5: SYSTEM IDENTIFICATION

	REQUIREMENT	STATE OF ART*
TOTAL NUMBER OF MODES	50	30
CONTROLLED MODES	20	10
BANDWIDTH (Hz)	30	20
DAMPING	Unkown	Unknown
TIME TO PROCESS	< 30 min	<30 min
MODES IN CONTROL BW	1 to 10	3 to 25
MODES OUT OF CONTROL BW	20 to 50	25 to 50

* TRW-ACOSS

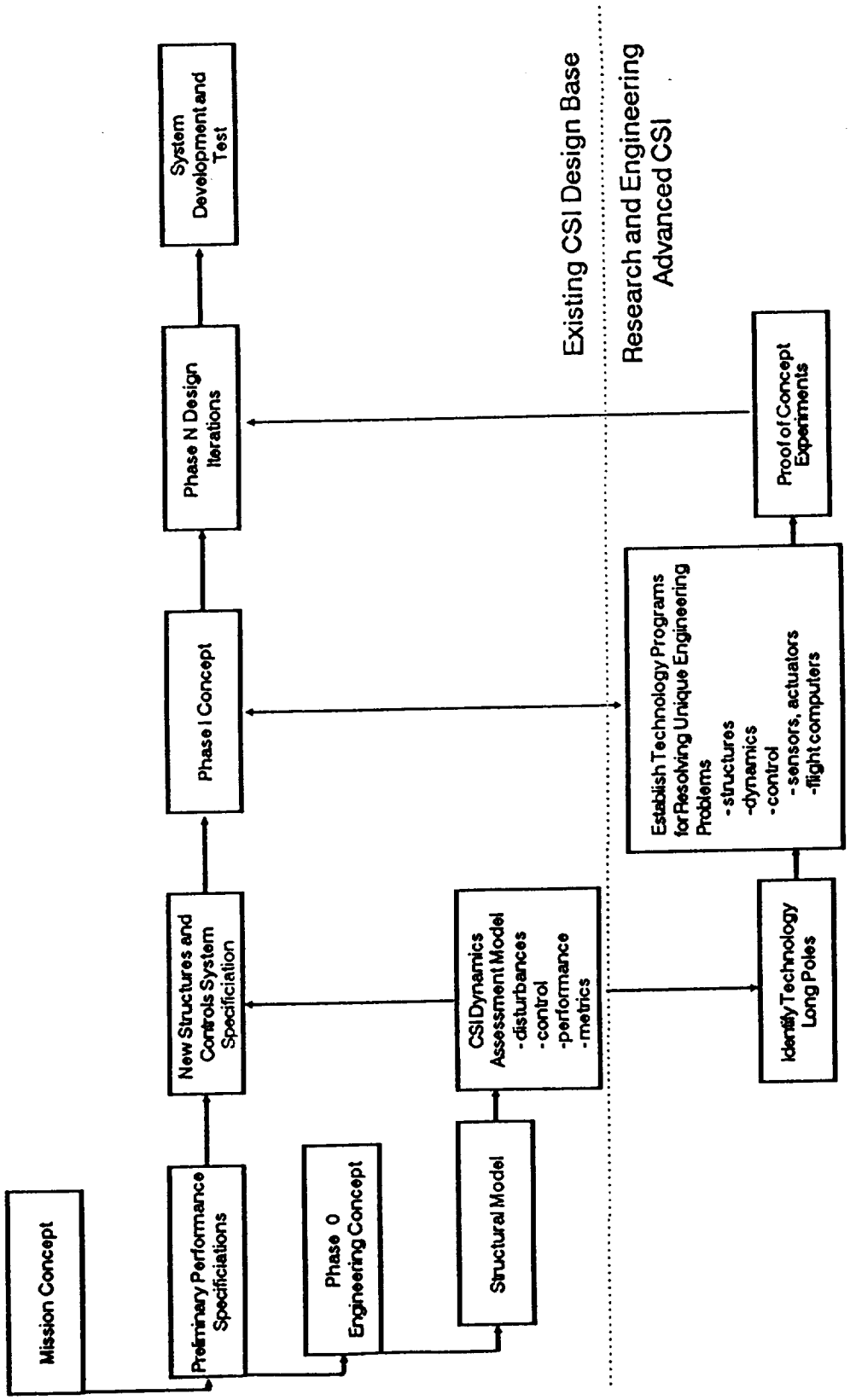

Figure 2: CSI DESIGN PROCESS

Section 2.3 presents a new top-level CSI methodology for conducting preliminary assessments for large antenna systems. The specific application is derived from the Geostationary Platform focus mission, though the assessment approach is generically useful. The trade studies allow the system size, operational frequency, and launch weight to be quickly varied in order to understand how the demonstrated capabilities of modern active control methods impact various decisions.

2.0 CSI BENEFIT STUDY

The CSI benefit study consists of three basic activities. First, the Geostationary Platform focus mission concept is studied and assessed for potential CSI problems. This material is presented in Section 2.1. Second, the integrated technologies required for developing high performance modern control designs are presented in Section 2.2. Also reviewed are the numerous ground-based experiments which have been conducted for demonstrating various aspects of control related technology. Third, a new top-level CSI evaluation methodology is presented in Section 2.3. This new methodology permits rapid parametric trade studies to be conducted while investigating the complex interactions between control capabilities, operational system frequencies, and antenna design sizes.

2.1 Geostationary Platform Baseline Structures

This section presents a preliminary CSI assessment for the Geostationary Platform focus mission configuration. The CSI study is carried out by using a finite element model developed by NASA for the structure and developing appropriate disturbance models which are applied to the structure. Based on the response obtained from the structure, the goal of the effort is to investigate potential control based solutions for minimizing the system response.

Three finite element models have been developed at NASA Langley and employed during the course of the study. Table 6 presents a summary description of the models. The first model (GEORIG) treated the solar arrays as rigid and lumped the antenna mass and inertia at the attach points on the structure. These idealizations, however, produced an artificially stiff structure which was not affected by disturbance inputs many times greater than anticipated. The second model (GEORED) added flexible solar array booms while retaining the lumped mass and inertial models assumed for the antenna. This model had the correct low frequency behavior due to the solar arrays, though the modeling assumptions for the antenna still eliminated the possibility of studying any interactions between the antenna feed boom assemblies and the pointing of the platform instruments. The final model (FULLFORD) extended the second model to include full scale antenna models and feed boom assemblies. This model provides the best overall physics representation for the Geostationary Platform (at this time) and has been used for the remainder of the CSI study.

A description of the structural model is presented in Section 2.1.1. A description of the Geoplat sensor suite is presented in Section 2.1.2. The finite element model and representative eigenvalue and eigenvector data is presented in Section 2.1.3. Descriptions of the disturbance models considered are provided in Section 2.1.4. The CSI assessment is presented in Section 2.1.5.

TABLE 6: GEOSTATIONARY PLATFORM STRUCTURAL MODEL DATA

MODEL	DESCRIPTION	NO. OF NODES	NO. OF MODES	FREQUENCY RANGE (Hz)
GEORIG	FLEXIBLE STRUCTURE; RIGID BOOMS	79	36	0 - 46.
GERED	BOOM FLEXIBILITY ADDED	94	46	0 - 22
FULL FORD	ANTENNA FLEXIBILITY ADDED	395	46	0 - 13

2.1.1 Model Description

The Geoplat focus mission is an outgrowth of work performed by Ford Aerospace and Communications Corporation for the Marshall Space Flight Center on contract NAS8-36104,' GEOSTATIONARY PLATFORM BUS STUDY FOR EARTH OBSERVATION SCIENCES". This activity is part of the National Aeronautical and Space Administration's (NASA's) continuing efforts to fully identify and exploit the attributes and capabilities of the geostationary orbit. Figure 3 presents a detailed drawing of the Ford Aerospace Geostationary Platform. The platform consists of four major structural components: 1) the main housekeeping module, 2) the payload support module, 3) the payload support truss, and 4) the Orbital Maneuvering Vehicle (OMV)/Orbital Transfer Vehicle (OTV) interface cylinder. The required payload support truss structure provides structural support primarily for the Passive Microwave Radiometer (PMR) payload dishes, during SB-OTV launch, and high dimensional and alignment stability during the on-orbit operational lifetime of the platform.

The truss is a 3.0 m total cross section structure assembled 'erector set' style using techniques that have been demonstrated on NSTS flight 61B. It consists of 51 mm diameter by 1.59 mm wall thickness graphite tubes attached to graphite end fittings. The tube/end fitting interfaces are pinned and bonded to insure rigid joints and to minimize thermal or structural creep. The PMR's are attached to the main truss structure through tubular substructures which are essentially extensions of the main truss.

Few mechanisms are employed on the structure because of the intended use of the low thrust mode SB-OTV. As a result, the majority of the appendages can be deployed manually at the Space Station prior to GEO insertion. At LEO the solar array is partially deployed, though the solar sail would most likely be deployed at GEO.

Program details regarding design considerations for propulsion, thermal control, electrical power, telemetry, command and data handling, attitude and orbit control, and platform servicing can be found in Reference 1.

2.1.2 Sensor Suite

As shown in Figure 4, there are eighteen payloads which must be pointed with some level of accuracy [see Ref. 1]. The instruments with the tightest pointing requirements are mounted on the instrument payload module (i.e., ozone monitor, IR sounder, Vis/IR Imager, Multispectral Imager, and the Lightning Mapper). The only subsystems not having any pointing requirements are the Active Cavity Radiometer, Energetic Particle Sensor, High Energy Proton Alpha Detector, Triaxial Magnetometer, and the Static Charge Control device. For systems with modest pointing requirements the devices are mounted on the platform truss.

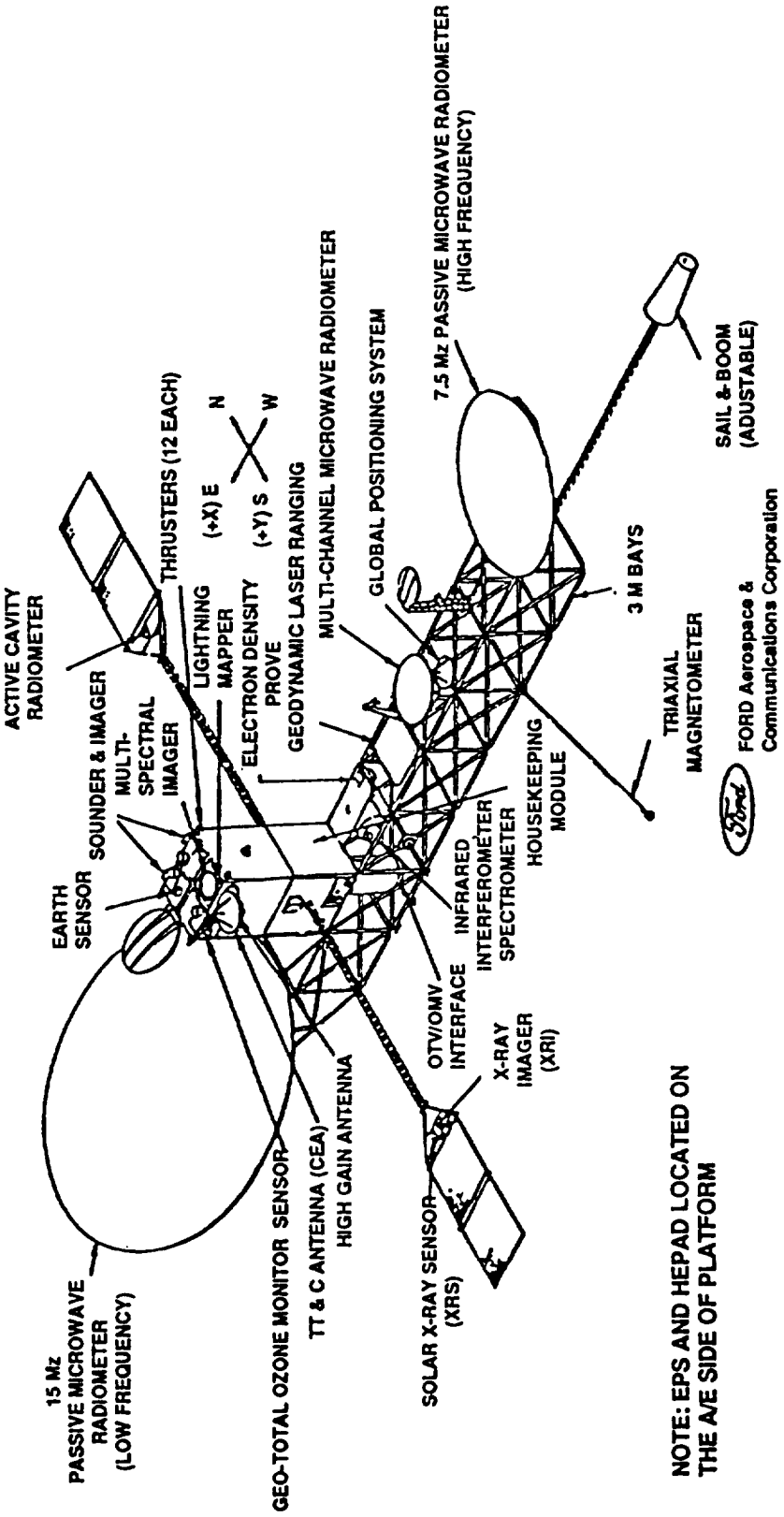

Figure 3: PRELIMINARY FORD AEROSPACE EOS GEOSTATIONARY PLATFORM CONCEPT

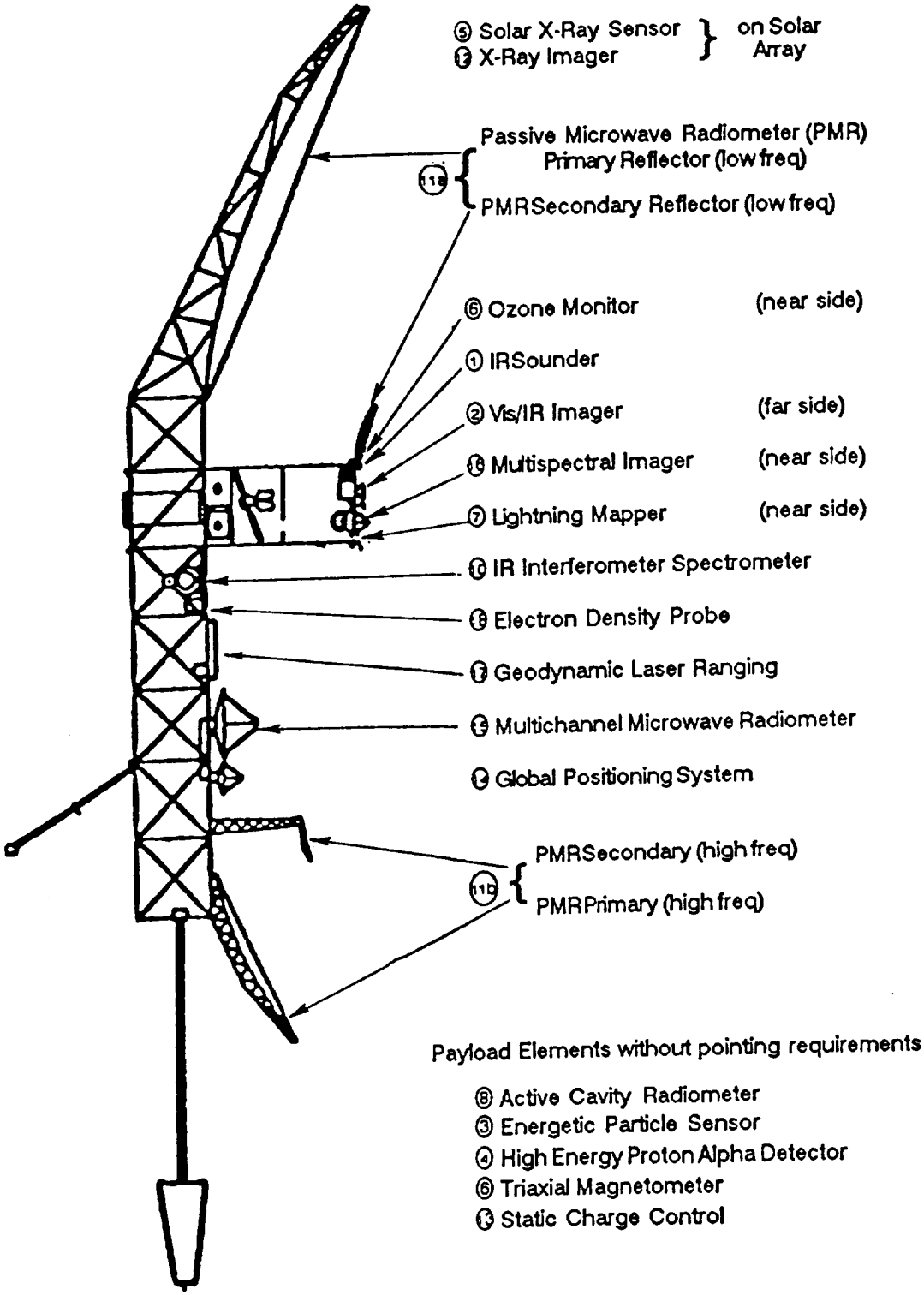

Figure 4: INSTRUMENT PAYLOADS FOR PRELIMINARY GEOPLAT DESIGN

Table 7 presents a detailed description of the sensor suite pointing means, field of view (FOV), satellite pointing requirements, and the short-term pointing requirements. The difference between the satellite pointing and short term pointing requirements is not clearly specified in Ref. 1, but probably indicates that the steering mirrors have enough travel to compensate for the satellite pointing deviations given, and the accuracy to which they compensate must be to the short term pointing values. All of the data in the table must be assumed to be approximate.

Table 8 lists the parameters for each of the PMR's at the minimum and maximum frequencies mentioned in Ref.1. Three values from this table for each radiometer can be used as requirements in preliminary structure and control work, namely the entries at the higher operational frequency value for Figure, Primary Angle, and Secondary Displacement. In this preliminary analysis, small overall displacements between mirrors and the feed which can cause the defocus and higher order aberrations that lead to degradation of the gain, beamwidth, sidelobes, and spillover characteristics of the projected beam pattern are ignored.

2.1.3 Finite Element Model

The LaRC developed FULLFORD finite element model is described in this Section (Ref. 70). Figure 5 presents an overall view of the finite element model used for defining the behavior of the Geoplat. Figure 6 presents the 3.0 meter box truss structure which is composed of beam elements with six degrees of freedom at each node. The physical and material properties of these beams are based upon those in the Geostationary Platform Bus Study Final Report prepared by Ford Aerospace [Ref. 1]. The truss members are constructed of graphite, having a 51 mm outer diameter with a 1.5 mm wall thickness, and a modulus of elasticity, E, equal to 275 X 10^9. Rigid bars are used to model the payload module, the housekeeping module and the thrust tube. Rigid bars are also used to connect the spacecraft truss structure and the microwave reflectors. Figure 7 shows the physical location of the c.g. of the spacecraft finite element model, as well as its overall mass and inertia properties.

Table 9 presents a summary of the mass properties used in the finite element model. The top section gives the properties used for the beam elements that are used to model the truss members and the three deployable booms. The lower section of the table describes the various lumped mass elements used to represent the rest of the spacecraft's mass and inertia. The rigid elements used in thermal analysis have infinite stiffness and zero mass.

Table 10 lists the frequencies for the model and describes the deformation behavior qualitatively. Figures 8-10 show several representative structural mode shapes.

TABLE 7: SENSOR POINTING DATA

SENSOR	POINTING MEANS	FOV	SATELLITE POINTING (DEG)	SHORT-TERM POINTING
Solar X-Rays (5)	Entire	$\pm 1^0$ N-S $\pm 1^0$ E-W	+0.10	0.0
X-Ray Imager (12)	Entire (?)	38x38 ARC MIN	0.017	
PMR (11A) (15M. 19-37 GHz)	Feed Assembly	$\pm 10^0$ Off EC		
Ozone Monitor (9)	Mirror	10^0 OFF EC	Roll $\pm$ 0.1 Pitch $\pm$ 0.15 Yaw $\pm$ 0.20	0.00095 0.001 0.0017
IR Sounder (1)	Mirror	60^0 N-S 60^0 E-W	Roll $\pm$ 0.1 Pitch $\pm$ 0.15 Yaw $\pm$ 0.20	0.00095 0.001 0.0017
VIS/IR Imager (2)	Mirror	60^0 N-S 60^0 E-W	Roll $\pm$ 0.1 Pitch $\pm$ 0.15 Yaw $\pm$ 0.20	0.00095 0.001 0.0017
Lighting Mapper (7)	Entire	10.4^0	$\pm$ 2	
Multispectral Imager (16)	Entire	$20^0/180^0$	0.0001	

TABLE 8: PASSIVE MICROWAVE RADIOMETER REQUIREMENTS

DIAMETER (M)	15		7.5	
Frequency (GHz)	19	36	50	250
Wavelength (Δ) (mm)	16	8.1	6	1.2
Figure Reqmt. (mm) (Δ/10)	1.6	0.8	0.6	0.12
Beam Width (BW) (mr) BW Δ/D	1.1	0.54	0.8	0.1
Primary Reflector Angle Reqmt. BW/10 (mr)	0.1	0.05	0.08	0.016
Pri-Sec Spacing(s) (m)	12			
Secondary Reflector (mm) Displacement Reqmt. BW/10 . s	1.2	0.6	0.4	0.08

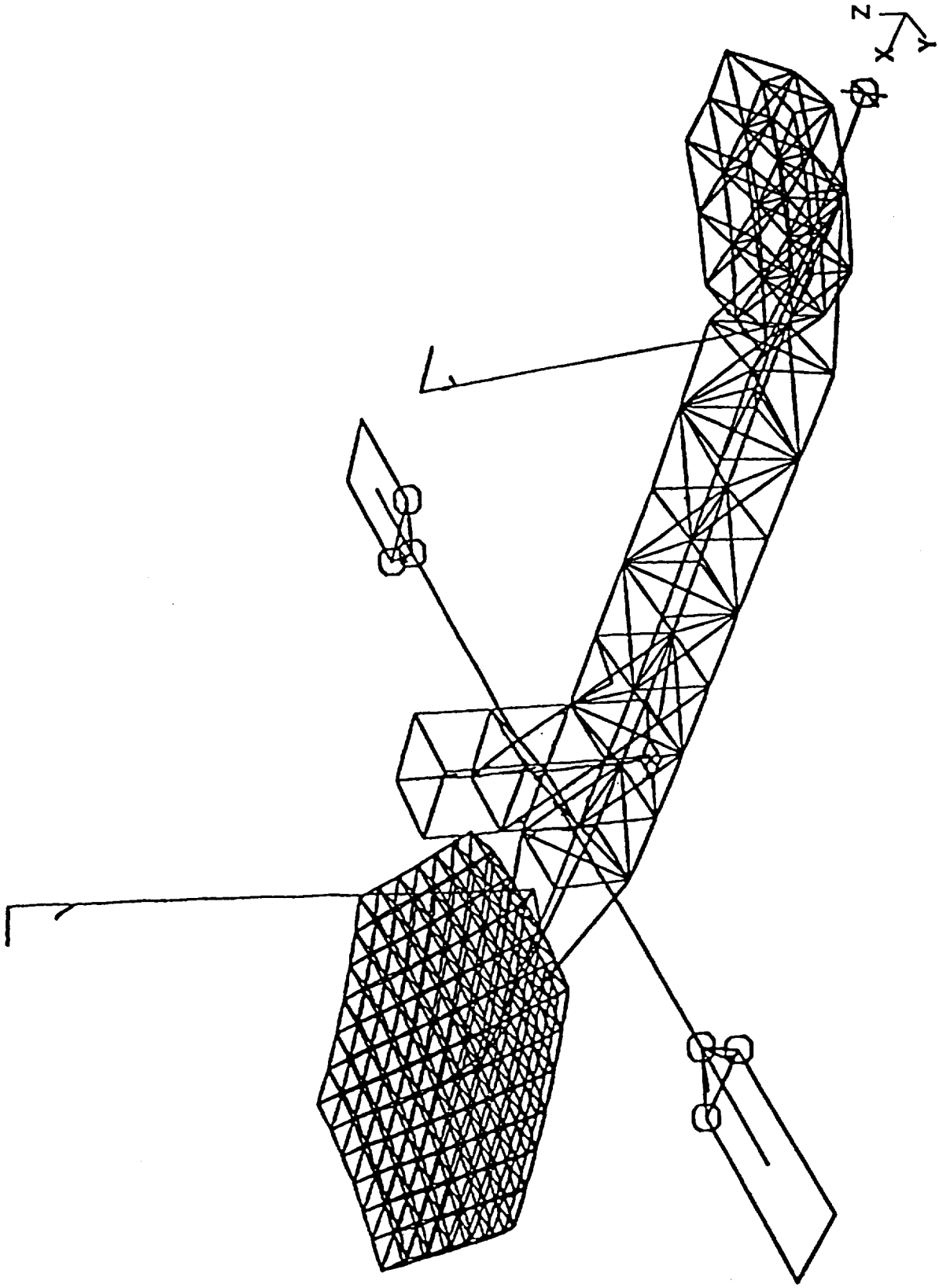

Figure 5: GEOPLAT FINITE ELEMENT MODEL (FULLFORD)

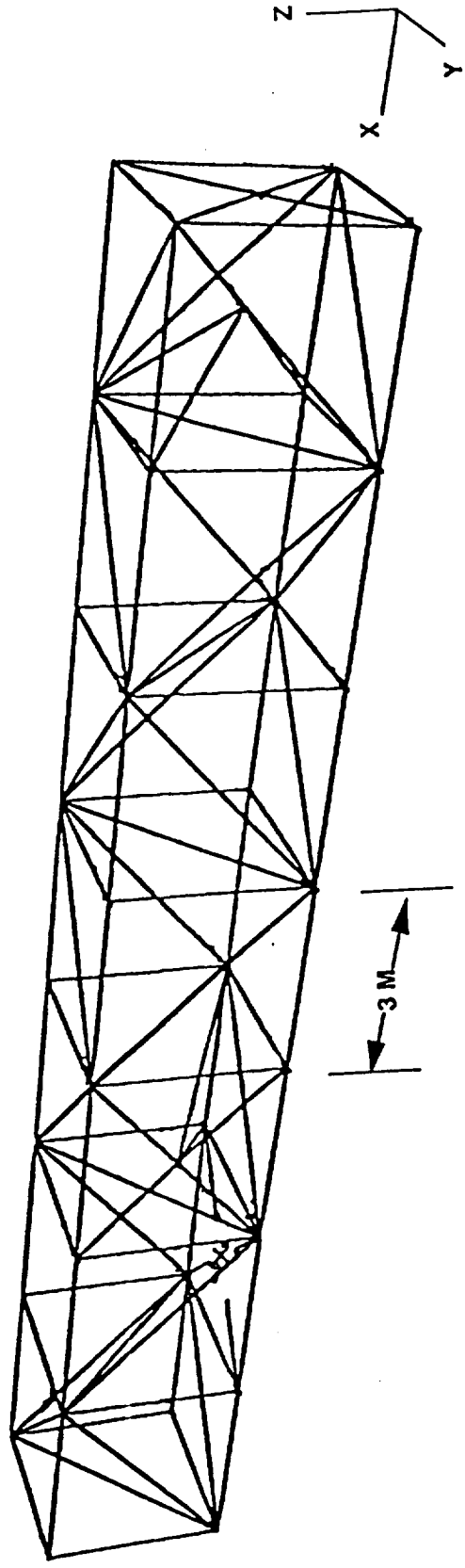

Figure 6: BOX TRUSS STRUCTURE PLATFORM

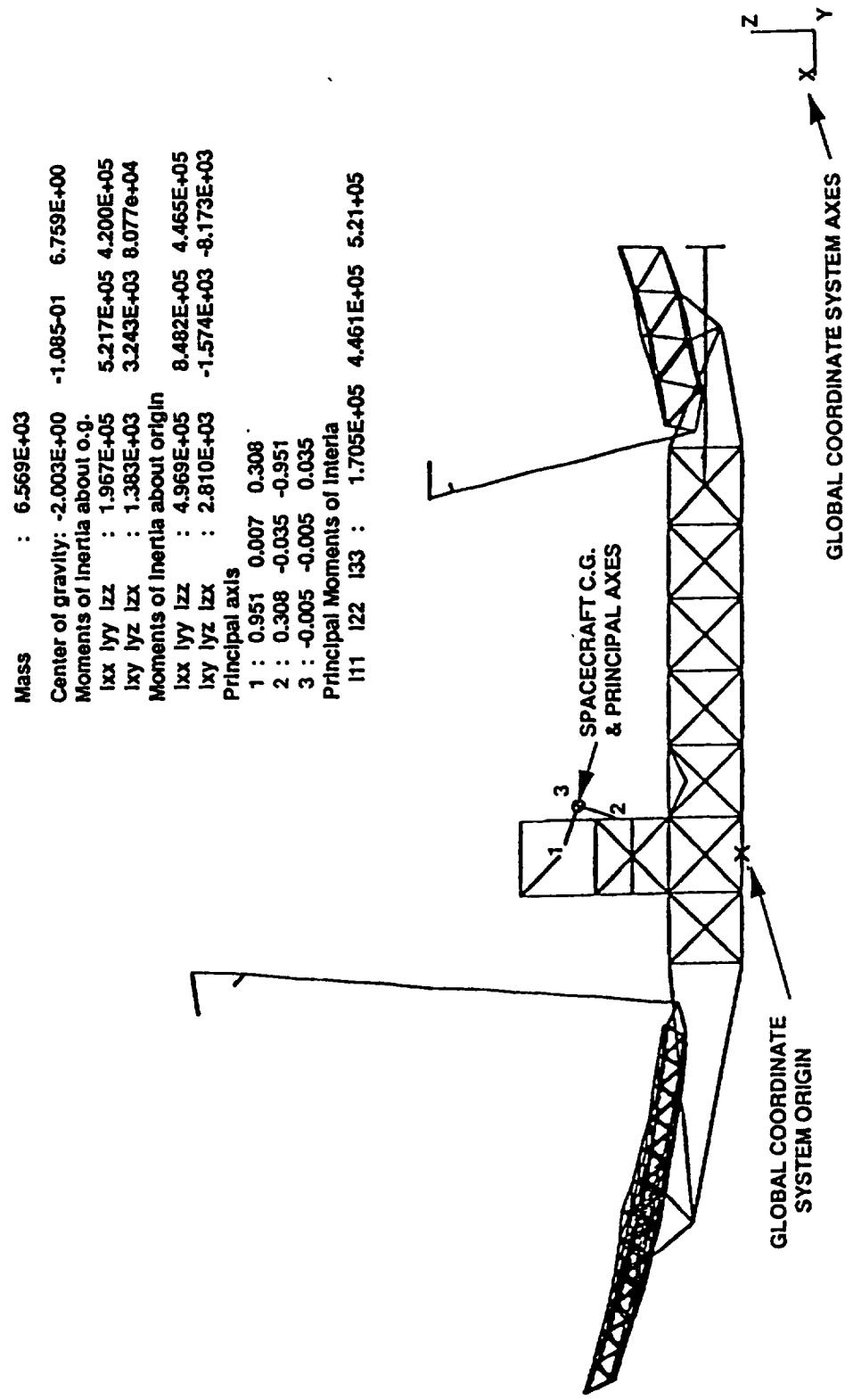

Figure 7: GEOPLAT SIDE VIEW

TABLE 9: MASS SUMMARY CHART FOR FULL ORDER FINITE ELEMENT MODEL

BEAM ELEMENT PROPERTIES	# ELEMENTS	CROSS-SECTIONAL AREA (M^2)	NON-STRUCTURAL MASS (kg/m)	DENSITY (Kg/m^3)	YOUNG'S MODULUS	BENDING INERTIA	TORSIONAL CONSTANT
Spacecraft Truss	108	0.00024681	0.04558	1690	2,759E11	7.540E-8	1.508E-7
Deployable Longeron	18	0.0002072	0.0	2076	5.2E10	5.364E-6	1.532E-8
Feed Mast	28	0.001015	1.482	1026	1.139E11	1.074E-4	2.404E-5
15-M Dish Truss Struts	630	4.88386E-5	0.0	1520	1.38E11	2.735E-9	5.470E-9
15-M Dish Truss Diagonals	324	3.34838E-5	0.0	1520	1.38E11	1.932E-9	3.865E-9
7.5-M Dish Truss Struts	66	0.0002356	0.0	1740	2.07E11	8.073E-9	0.01
7.5-M Dish Truss Diagonals	36	0.0002356	0.0	1740	2.07E11	8.073E-9	0.01

MASS ELEMENT PROPERTIES	# ELEMENT	MASS(kg)	Ixx($kg.m^2$)	Iyy($kg.m^2$)	Izz($kg.m^2$)	Ixy($kg.m^2$)	Iyz($kg.m^2$)	Izx($kg.m^2$)
S/C Truss Nodes & Fittings	32	7	0.028	0.028	0.028	0	0	0
15-M Dish Feed Array	1	443.7	73.95	73.95	73.95	0	0	0
15-M Dish Subreflector	1	52	17.9841	17.9481	35.8963	0	0	0
7.5-M Dish Feed Array	1	72	3	3	3	0	0	0
7.5-M Dish Subreflector	1	13	1.12447	1.12447	2.24352	0	0	0
Solar Array	2	45	135	3375	168.75	0	0	0
X-Ray Imager	1	15.75	0.1641	0.1641	0.1641	0	0	0
X-Ray Sensor	1	15.75	0.1641	0.1641	0.1641	0	0	0
Solar Sail	1	4	1.125	192.563	192.563	0	0	0
Active Cavity Radiometer	1	27.5	1.1458	1.1458	1.1458	0	0	0
GPS Antenna	1	15.3	2.152	2.152	4.303	0	0	0
Geodynamic laser Ranging	1	100	133.3	133.3	98.7	0	0	0
IR Interferometer	2	430	141.1	120.95	141.1	0	0	0
Payload Module	1	3008	4512	4512	4512	0	0	0
Housekeeping Module	1	500	750	750	750	0	0	0
7.5-M Dish Surface	12	34.641	0	0	0	0	0	0
15-M Dish Surface	127	0.024992	0.01	0.01	0.01	0	0	0
Feed Mast Nodes	30	2.3325	0	0	1.7554	0	0	0

TABLE 10: MAXIMUM ANTENNA DIAMETER FOR A 250 GHz SYSTEM

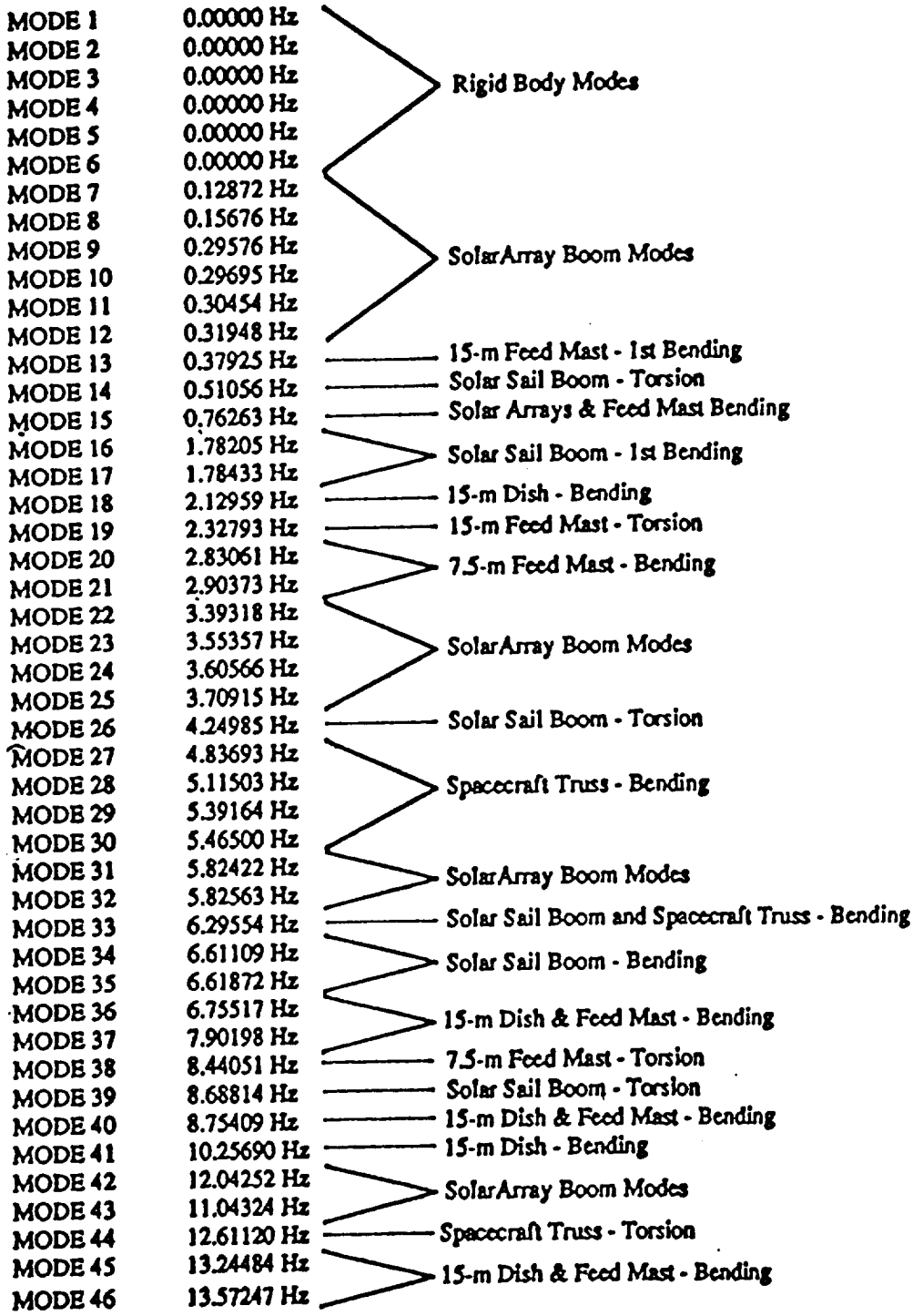

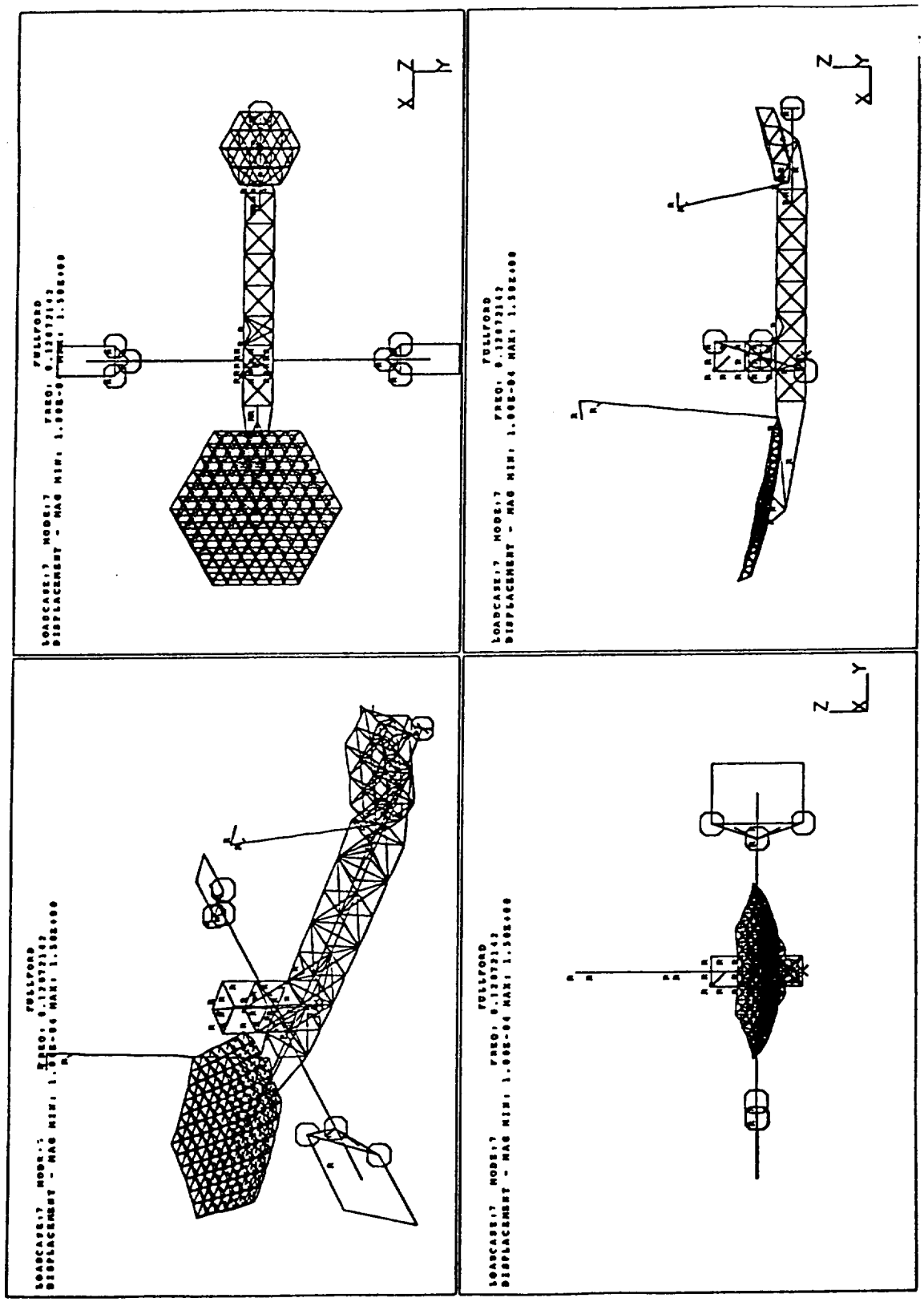

Figure 8: FIRST FLEXIBLE BODY MODE (SOLAR ARRAY BENDING)

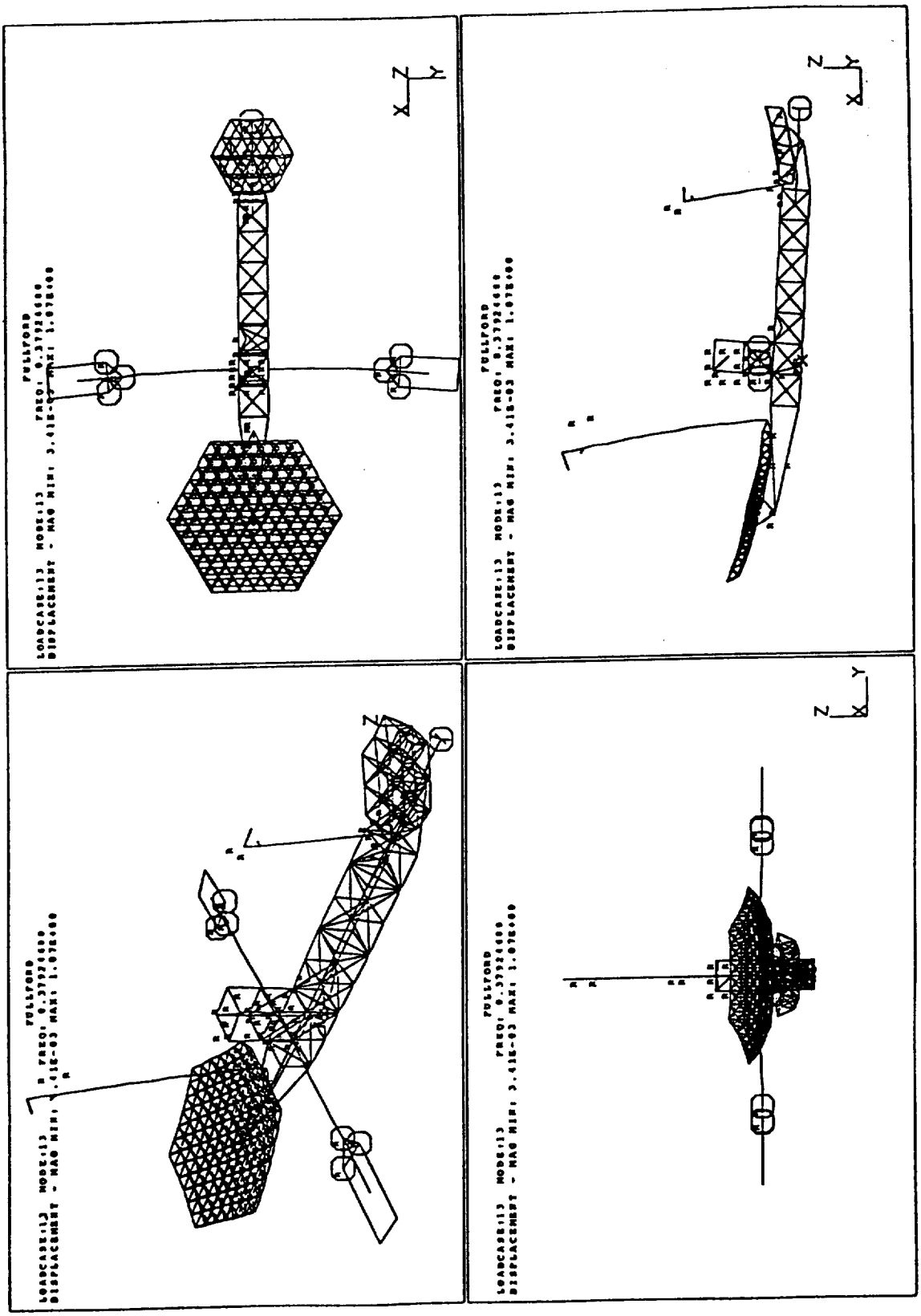

Figure 9: FIRST SUBREFLECTOR BENDING MODE

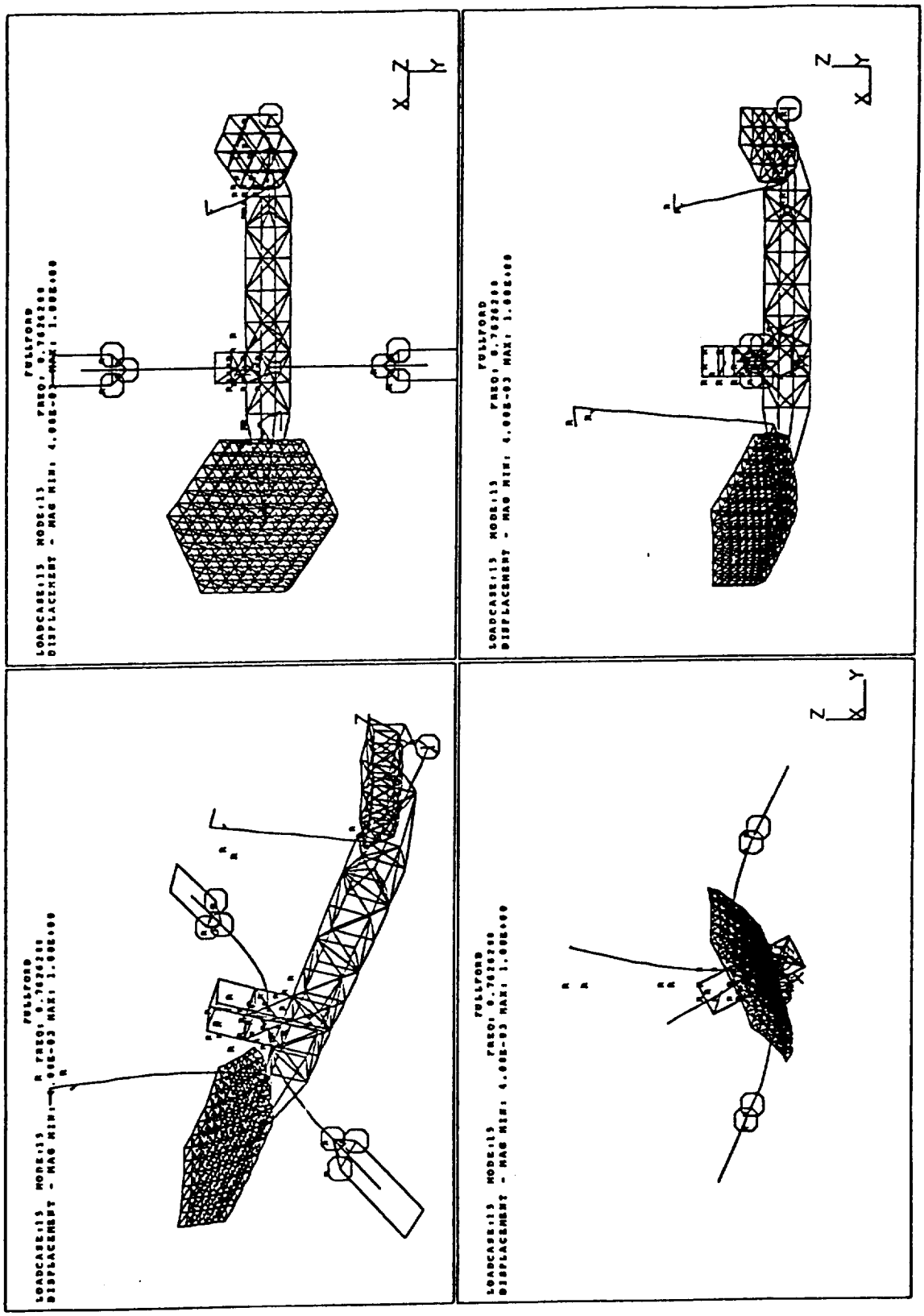

Figure 10: GENERAL STRUCTURAL BENDING MODE

2.1.4 Disturbance Models

Several disturbance sources have been considered as potential mechanisms for inducing a CSI problem. Gravity gradient and solar radiation pressure have been found to be insignificant for this study. However, there may be some possible long-term orbit influence in the case of very large antennas. Reaction wheel imbalances have also been considered when periodic inputs can excite the structure. The spin rate for the attitude control wheels is 33 1/3 Hz, as defined by the Ford Aerospace report [Ref. 1]. Because the FULLFORD model only retained structural frequencies in the range 0-13.57 Hz, the effect of wheel imbalance could not be observed. To bound the potential impact these mass imbalances can have on the stability of the Geoplat structure, a State-of-the-Art (SOA) survey by Sperry Corporation was reviewed in order to establish what reasonable assumptions can be made regarding the levels of disturbance inputs from this class of devices. On reviewing the documentation it follows that the current manufacturing capabilities can achieve static imbalances of 0.02 Oz-In and dynamic imbalances of 0.10 Oz-In-In, with force imbalances of approximately one newton in both cases. These numbers suggest that reaction wheel mass imbalances are unlikely to present CSI problems, though a more complete study should reconsider this issue when higher frequency models become available.

Disturbance models have been considered for several of the earth scanning instruments using the approach defined in Ref. 8. In all cases considered, instrument pointing disturbances were shown to be infinitesimally small. It should be recognized, however, that all of the instruments on the platform truss have been modeled as lumped masses and inertias; as a result, it is not possible to investigate the potential for interactions of pointing control systems with the internal degrees-of-freedom of the instruments. For the pointing systems which have stringent accuracy requirements, more detailed models are needed in order to assess this type of CSI issue. This problem has been discussed in detail in Ref's. 9 and 51 for the GOES geostationary weather satellites.

Thruster firings during station keeping maneuvers have also been considered as a potential source of disturbance. Figure 11 presents the location of the thrusters on the platform truss and the instrument deck. These locations have been selected to produce the largest possible inputs to the structure; accordingly, the thruster firing disturbance represents a worst case system input. During normal operations the station keeping firing occurs once a day with 30 minutes allowed after firing for the structural response transients to decay to normal operational levels. As shown in Section 2.3.5 the thruster disturbance inputs produce the largest structural responses.

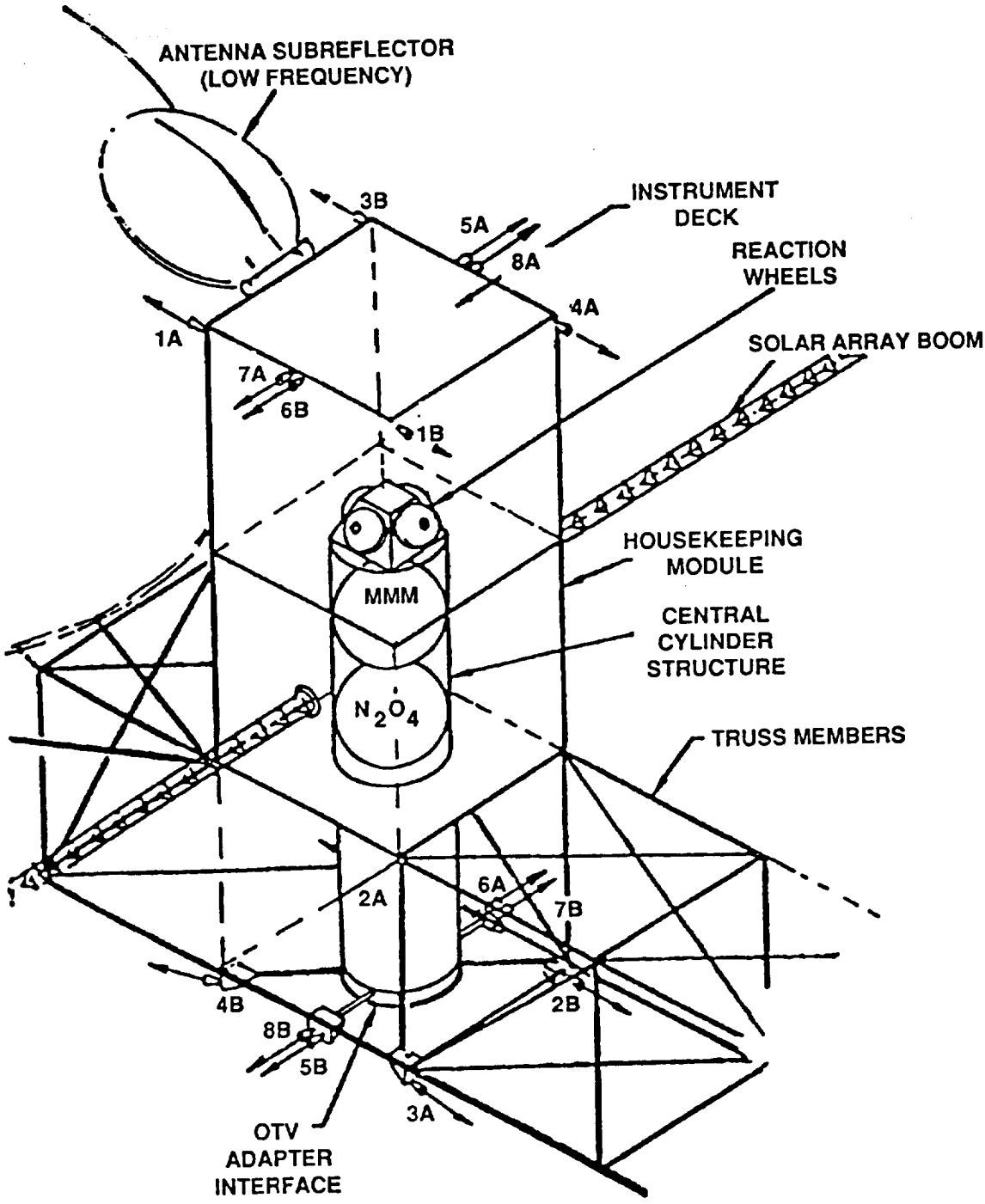

Figure 11: PLATFORM ACTUATOR LOCATIONS

The final disturbance considered in the study is the subreflector scanning motion for the 15 m antenna. This disturbance represents the largest nominal input source for the structure. The 13th structural mode produces the largest pointing error for the subreflector and is shown in Figure 9. A worst case scanning input to the structure is considered, where the scanning period of the subreflector is taken to be approximately equal to the period of the 13th mode with a structural frequency of 0.379 Hz and period of 2.64 sec. To reverse the direction of the scanner a momentum impulse is computed and applied to the structure. The calculation for the momentum impulse assumes that there are no frictional losses in the scanner motion and that an ideal impulse is executed each time.

The required impulse is computed by knowing the required field of view (approximately 17 degrees at geostationary orbit) and the scan rate (which must be specified). Simple calculations lead to a scan rate of w = 0.1125 rad/s, from which it follows that the scan rate momentum is given by:

$$Hy = Iy \cdot w = (17.95\ Kg\text{-}m^2) \cdot (0.1125\ rad/s.)$$
$$= 2.02\ Kg\text{-}m^2/s$$

where the subreflector scanning axis moment of inertia, Iy, is defined in Table 9. To reverse the scan rate an input of -2Hy must be applied to the system.

The results of applying these disturbances to the Geoplat model are discussed in Section 2.1.5.

2.1.5 CSI Assessment

The disturbances described in Section 2.1.4 have been applied to the three Geoplat models are shown in Table 6. The GEORIG and GEORED models have been found to have no significant CSI, all pointing goals can be achieved without structural interference. The FULLFORD model has been found to be sensitive to only the subreflector scanning disturbance and the station keeping thruster firing disturbances. The basic conclusion from this study is that the Ford Aerospace Platform Bus design is not susceptible to major CSI problems. This conclusion is, however, subject to the assumption that the instruments are modeled as rigid bodies without internal flexible degrees-of-freedom, and fixed antennas sizes. When larger antennas are considered, the potential for CSI increases because the structural frequencies decrease thereby increasing the likelihood that disturbances can excite an unacceptable response.

Section 2.3 presents various trade studies for investigating the impact of antenna size, operational frequency, weight, and control requirements for a range of system concepts. The results obtained in the dynamics studies of Section 2.1 are used in Section 2.3 to provide traceability for scaling law predictions.

2.2 Large Space Structures Control Technologies

The design effort for a complex LSS application combines many technical disciplines in order to achieve a workable structural configuration. For early spacecraft applications the structural and control design processes have been successfully carried out by treating each process as independent. This approach has worked because the structural frequencies and control bandwidths have been well separated. As structures have become larger and more flexible the bandwidths for the structure and the control have moved closer together and now in fact overlap for many systems of interest (see Figure 12). When these bandwidths are either close or overlapping there is a potential for these systems exchanging energy, which can lead to structural instabilities.

When the open-loop response of a structure exceeds allowable performance tolerances, control can be used to create artificial stiffness in parts of a structure in order to shape a surface or suppress a response. The success of these approaches, however, critically depends on the designer having available a precise knowledge of the dynamics models for the sensors, actuators, and structure to be controlled. The sensitivity of the control arises because the control design attempts to exploit the frequency domain characteristics of the structure, disturbances, and sensors/actuators in order to minimize the response. Uncertainty in the parameters describing the control system directly affects the performance of carefully shaped frequency domain characterization of the control, because an optimized control attempts to minimize energy in narrow bands around structural frequencies (often by many orders of magnitude). A by-product of the optimization process is that even small errors can lead to large increases in the energy available for exciting a response. To overcome this problem control approaches have been developed which seek to minimize sensitivity of the control system to anticipated levels of parameter uncertainty, leading to "so-called" robust control designs.

For early spacecraft applications where problem structural modes have appeared (typically solar array modes) the classical controls approach has been to design notch filters which eliminate energy in the applied control at specific structural frequencies. This approach has proven to be successful for many spacecraft. The notch concept becomes unmanageable for large systems when many modes must be considered, because it degenerates into a so-called "comb" filter. The notch filter concept generally represents an

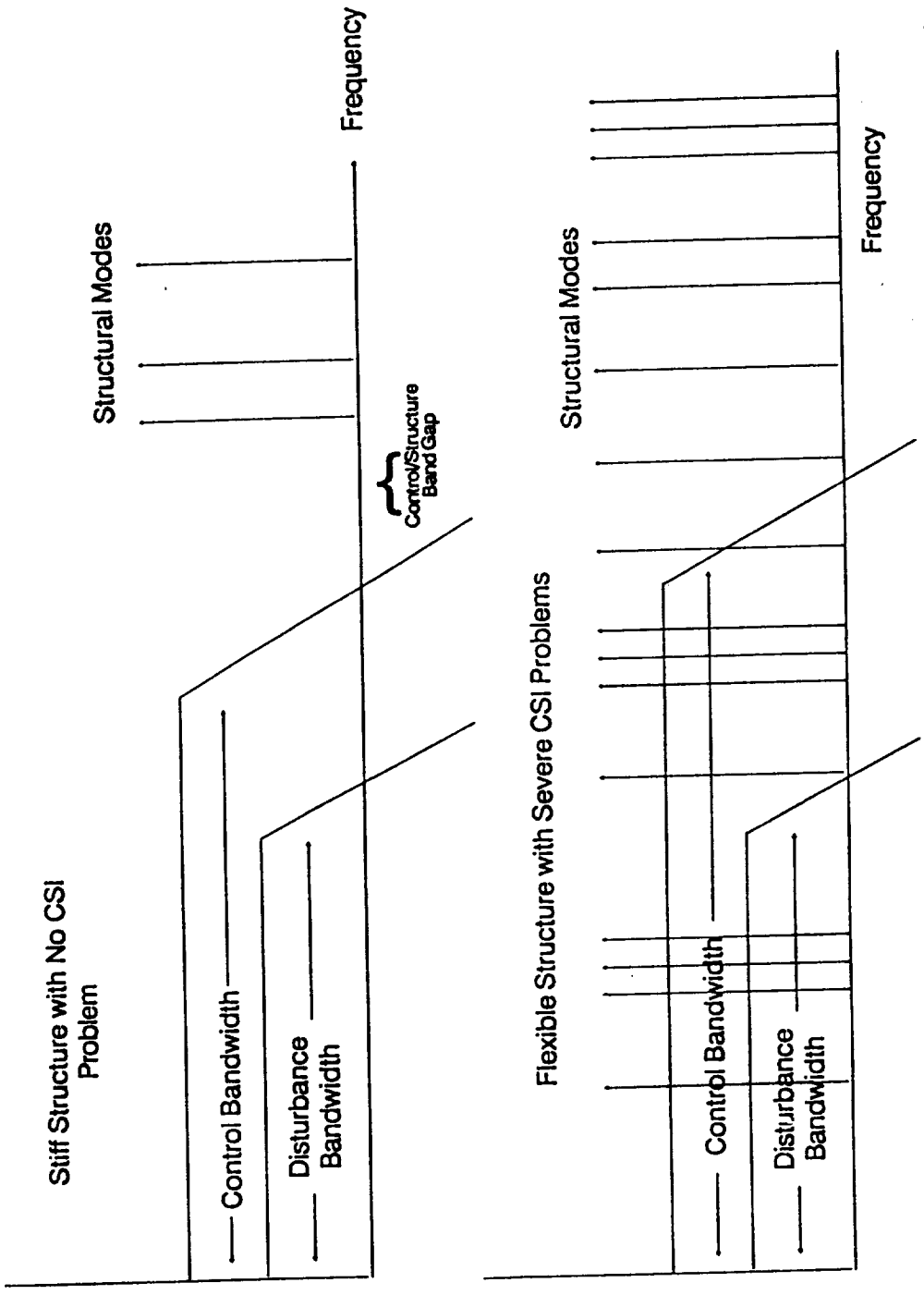

Figure 12: CONTROL, STRUCTURE, AND DISTURBANCE BANDWIDTHS

open-loop methodology in that the selection of notch locations in the frequency domain is generally done a priori. If the system parameters change during the operational life of a satellite (i.e., through the use of expendable fuels, c.g. shifts, material aging due to exposure to the space environment) then the notches must be moved to dynamically track the changing system parameters. Classical control methods are generally limited to single-input-single-output (SISO) design methodologies, whereas the multi-input-multi-output (MIMO) nature of the LSS control is most naturally handled using modern control methods. The design of MIMO modern controls represents an integration of several methodologies. Each of these methods are described in Sections 2.2.1 through Section 2.2.3.

Model Reduction Methods are described in Section 2.2.1. These techniques are required to establish a suitable control design model when finite element modeling approaches are used to develop mathematical structures models. Section 2.2.2 describes system identification techniques. System identification is required in order to correct errors (usually due to unmodeled or nonlinear behavior) in the math model used to describe the structure and the control system sensors and actuators. This capability is important because of the inherent sensitivity of modern control design to uncertainty in the knowledge of the plant to be controlled. A brief review of the available modern control techniques is presented in Section 2.2.3. The ground-based experiments that have been performed to verify the performance predictions of modern control are presented in Section 2.2.4. Section 2.2.5 reviews the lessons learned from both theory and experiment as it relates to LSS control methodology.

2.2.1 Model Reduction Methods

A basic problem in the design of control systems for LSS is defining a suitable math model for describing the behavior of the system in its operational environment. For geometrically simple structures analytical models can readily be developed. Unfortunately, typical applications are characterized by asymmetric designs with complex geometries which defy simple analytical characterizations. As a result, approximate modeling techniques provide the only viable means for generating the required math models. The standard approach is to use finite element techniques.

The finite element technique approximates the elastic continuum in terms of many subdomains where the local motion of individual elements is constrained in order to produce the correct system-level motion. The goal of the finite element modeling technique is to replace the rigorous PDE distributed parameter description of the system behavior with a computationally simpler ODE description. To accurately capture the low frequency behavior the finite element model typically consists of hundreds to thousands of elements. This approach describes the motion of the

individual elements in terms of physical coordinates (i.e., motion measured relative to the inertial frame). By introducing translational and rotational constraints between adjacent elements to account for the correct local connectivity of the individual elements, and defining the elastic behavior of each element, a mathematical model for the structure is obtained.

The second step in the process is to introduce a coordinate transformation which maps the system response to an uncoupled modal description, where each transformed equation describes the response of an individual structural deformation shape. The number of equations is equal to the number of degrees of freedom (DOF) in the original physical coordinate model. Because of various approximations which have been made, the transformed model estimates for the structural frequencies are only valid for the lowest modes (i.e., approximately the first 25%). To further reduce the number of DOF retained in the model it is necessary to define the following system inputs and potential performance measures:

* Mechanical loads

    -On board disturbances
    -Environmental disturbances
    -Sensor and actuator dynamics
    -Thermal inputs

* Performance metrics

    -LOS pointing accuracy
    -Jitter stability
    -Settling time after slews
    -Vibration suppression
    -Shape Control
    -percent critical damping in controlled modes

The mechanical loads define inputs to the structure which can induce a response. The performance metrics define how well the structure is performing relative to the tolerances required for fulfilling mission objectives. This information is then used in a generally iterative process whereby the structural model, disturbances, and the control design are refined in an effort to achieve performance goals, work within operational capabilities of the available sensors and actuators, and minimize control and estimation spillover effects to modes not included in the control design model.

Five currently useful model reduction methods are presented in Table 11. Each method seeks to provide a qualitative measure for the importance of retaining individual modes. Several of these methods can also provide insight into sensor and actuator placement as part of the model order reduction process. A common area where

TABLE 11: MODEL REDUCTION METHODS SURVEY

TECHNIQUE	THEORETICAL BASIS/DESCRIPTION	FEATURES	COMMENTS
Gain Factor Analysis	DC gain of transfer function between 2 nodes at mode of interest	- can weight spectrally to include known disturbances - easily computed - can include performance measures - closely approximates more complex methods	- system must be lightly damped
Singular Value Decomposition (SVD)	Use SV's as measures of contribution of dynamical elements to input-output relationship & eliminate modes with lowest SV's	- relative weight is obvious	- plant variations may make stable system unstable; not evident from SV's - can't handle unstable system - SV's lose significance when loop is closed
Internal Balancing	Balance modal states to replicate impulse response of evaluation model	- can evaluate sensor/actuator placement	- difficulties with closely spaced modes - computationally complex for highly damped systems
Modal Cost Analysis	Discard controller poles which have small performance influence	- can tailor optimization to application	- difficult to implement - assumes zero mean, time uncorrelated input disturbance
Chained Aggregation	Partition system into aggregated & residual subsystems based on observability of modes using transformation matrix	- straight forward procedure to partition strongly & weakly observable modes	- weak coupling of modes not easily identified

all the methods experience difficulties is when two or more modes are closely spaced.

It should be realized, however, that structural damping has not been addressed in the process just described. This omission represents standard modeling practice because the basic theory is not available for reliably predicting the modal contributions to structural damping. At best the techniques used for incorporating damping can only be described as being ad hoc. System identification is required, nevertheless, for refining the parameters which are used to characterize the assumed models for structural damping (See Section 2.2.2).

2.2.2 System Identification

System identification (ID) and parameter ID are required to accurately determine system transfer functions, modal damping, and modal parameters. System ID can provide needed parameter values for analytical simulation, analysis and design as well as validating a mathematical model. Since all dynamic simulations and controls algorithms must use reduced order models (ROM's), a system ID test establishes the parameter values needed for a successful control design, as well as uncovering any previously unmodeled dynamics which affect the performance of the control system.

Key problems in parameter ID methods are parameter recovery accuracy, algorithm complexity, and the ability to identify closely spaced modes. Several methods are available where each has both strengths and weaknesses. These methods include: traditional transfer function techniques, Kalman filtering, cross-correlation techniques, linear prediction methods, maximum likelihood techniques, maximum entropy formulations (Refs 54-62), and the eigensystem realization algorithm.

The transfer function method utilizes fast Fourier transforms (FFT) to generate transfer functions using the power spectral density (PSD) of input and measured output. This much-used and easily implemented method is sensitive to non-white noise disturbances and non-zero initial conditions.

The Kalman filter approach yields time-varying optimal estimates of system parameters. This method is designed to handle MIMO systems which must operate in the presence of measurement noise. The method is computationally intensive and may also lead to biased estimates.

The cross-correlation method evaluates the error between the sensor measurement output and the estimated output by identifying input parameters. The formulation and implementation is straightforward but convergence properties for MIMO systems are poor.

The linear prediction method is least squares based. A model is selected which minimizes the mean square output prediction error. The method is computationally simple but is insensitive to non-white noise measurements and non-zero initial conditions.

The last three methods appear most promising for high-order MIMO systems. The maximum likelihood method is a least squares based method which selects parameter values to minimize a cost function, which is defined as a function of the error between the measured and computed time histories, and the noise covariance matrix. This method can handle nonlinear systems and provides a reliability measure. It has a history of successful implementation. The minor drawbacks of the approach include complicated modifications for handling non-white noise disturbances, and the need for iterative solution techniques.

The maximum entropy method generates a stochastic design model to compensate for the dimensionality and parameter sensitivity. The probability model is generated from limited parameter data and is used to account for large modeling errors in high-order modal parameters. Drawbacks for this approach include assumptions about the parameter probability distributions, and model uncertainties are difficult to account model, even when they possess well-defined structure (e.g., additive or multiplicative errors).

The eigensystem realization algorithm (ERA) constructs minimum order linear state variable representations for the dynamics system using measurements of the unforced structural response (Refs 86-88). This method provides quick convergence to parameters of complex structures. It is computationally simple and stable but requires a large number of computations and is sensitive to structural non-linearities.

2.2.3 Modern Control Techniques

Modern control, in contrast to classical control, provides a direct approach for dealing with the MIMO nature of complex spacecraft applications. The standard methodology first defines a measure or performance index (i.e., typically an integral which penalizes the control effort used as well as the system response and response rate) which permits an optimization process to be defined. There are two classes of problem formulations which are of general interest, finite and infinite time problems.

First, finite time problems correspond to applications where the structure must achieve specific boundary conditions in a specified amount of time, leading to so-called two-point boundary-value problems (TPBVP). Examples of this class of applications include slewing or retargetting maneuvers where the structure has an initial orientation in inertial space and it is desired to maneuver the vehicle to a new orientation. Because the problem is

finite in time, there are concerns about the applied torques, which are applied for repointing the rigid part of the structure, exciting the flexible part of the structure. Without proper shaping of the maneuver commands the vehicle will likely experience an unacceptably large induced response. There are many approaches for incorporating the beneficial effects of command shaping in the design of the control. Most of the approaches ultimately depend on some form of prescribing the bandwidth and roll-off characteristics of the control. The frequency domain characteristics of the control roll-off are extremely important because any high frequency control content can potentially excite unmodeled structural modes not retained in the ROM, leading to the so-called spillover effects. (See Figure 12 where spillover corresponds to the overlapping of the control and/or structure and/or disturbance bandwidths.)

The second class of control formulations consists of infinite time problems, where the final boundary conditions for the structural response are free, though subject to a constraint that the steady-state motion is less than some prescribed tolerance. Examples of this class of control problem include shape and vibration suppression applications. The control law must typically operate in a persistent disturbance environment. Because control must be applied continually it is of great concern that overall system stability be preserved. This class of control problem is at the very heart of most CSI technology concerns. The challenge for successful control designs is to achieve structural performance goals within a reasonable time period (i.e., not a sluggish response) while maintaining overall system stability.

The methodologies for generating modern control algorithms basically split into the following two classes (See Table 12):

* Parameter Optimization Techniques

* Integral-Variational Methods

The parameter optimization techniques basically assume some mathematical form for the optimal solution. The unknown parameters are determined by imposing a performance criteria. Typical performance criteria include closed-loop pole locations in the complex plane and various forms of signal orthogonality. A limitation of these approaches is that the optimization procedures generally do not directly account for the system dynamics. As a result, they can be prone to exciting unmodeled dynamics unless precautions are taken in the design process. Many of these approaches are conceptually easy to understand and implement.

TABLE 12: MODERN CONTROL METHODS SURVEY

TECHNIQUE	THEORETICAL BASIS	FEATURES	COMMENTS
Direct Output Feedback	Pole Placement or LQG	- Pole placement method straightforward - Adds damping without instability from residual modes	- Subject to control spillover - Number of sensors = number of actuators - Collocated sensors and actuators
Parameter Optimization	Optimization Theory	- Can customize optimization to the application	- Subject to spillover - Desing depends on choice of optimization parameter
Orthogonal Filter	Nonlinear	- Can compensate simultaneously for parameter errors, residual errors, disturbances, and nonlinearities	- Computationally intensive - Error states are modeled in the controller residual states
Positivity/ Characteristic Gain (PCG)	Stability Theory	- Can accommodates non-linear and time varying plants - Stability assured - Low Sensitivity to modal data	- Asymptotic stability assured if plant or compensator is strictly positive and other is positive real - Designer expertise necessary to translate performance spec into loop requirements
High Authourity Control/Low Authourity Control (HAC/LAC)	LQG, Frequency Shaping	- HAC provides high damping and/or mode shaping in selected modes - LARC provides low damping in wide bandwidth	- Requires a Large Number of Sensors and Actuators - Designer expertise necessary to determine weightings - Generally requires collocated sensors and actuators
Model Error Sensitivity Suppression (MESS)	LQG	- Low modeling error sensitivity - Damping of suppressed modes results in a more positive controller transfer matrix	- Stability not assured - Robust only if control inputs decoupled by modes - Iterative LQG design to remove spillover
LQG with Loop Transfer Recovery (LQG/LTR)	LQG	- Ability to design LQG transfer function based on full state feedback and utilize recovery proceedure for an approximation	- Sensitive to spillover - Frequency ranges exist where uncertainties won't allow recovery

TABLE 12: MODERN CONTROL METHODS SURVEY (Continued)

TECHNIQUE	THEORETICAL BASIS	FEATURES	COMMENTS
H^{∞}	Optimization Theory	- Straightforward & Comprehensive - Handles stability, sensitivity, response shaping, singular value optimization simultaneously	- Based on L norm of frequency response - Computationally intensive
Adaptive Methods	Nonlinear	- Able to handle time varying plants and not well known parameters	- Includes model reference techniques, lattice filters, signal shaping, & adaptive modal control - Success depends on ROM - Large modal separation usually necessary
Maximum Entropy	LQG	- Ability to include uncertainty measures to eliminate modeling & dimensionality errors	- Algorithm convergence not guaranteed - Difficult to incorporate uncertainties - Method assumes complete knowledge of parameter probability distributions

Integral-variational methods, on the other hand, define integral performance indices which penalize the control, states, and the corresponding rates. Many generalizations of the basic approach have been proposed [Ref. 11]. When the performance index has been defined, the equations of motion and the terminal boundary conditions for the problem are appended to the performance index via Lagrange multipliers. Application of the integral-variational methodology then generates the governing necessary conditions which define the optimal control solution. The models are generally linear, though it is possible to handle nonlinear problems. The solutions are frequently defined in terms of time-varying matrix differential equations (e.g., Riccati and Lyapunov Ref. 11).

The integral-variational methods directly handle the MIMO nature of the control design problem. Many problem formulations are related to Linear Quadratic Gaussian (LQG) methodologies. Without modification the basic LQG approach will not produce useful results because of parameter sensitivity. To overcome this limitation one typically seeks to invoke some form of frequency shaping and robustness to parameter uncertainty. Three very different approaches to this problem are presented in Table 12. The high and low authority control (HAC/LAC) presented in Figure 13 captures many of the basic objectives of many of the methods [Refs. 19, 23, 36, 38]. For example, for the part of the structure which is well known and most significantly impacts the performance goals, an advanced LQG frequency shaped approach is applied. For modes in the HAC bandwidth, the system performance meets the specifications, though some of the HAC spills over into modes outside the HAC bandwidth leading to overall system instability. To overcome this high frequency excitation, a second control procedure is invoked (i.e., LAC) for adding high frequency damping so that the combined HAC/LAC system is stable. Frequency shaping is not used for the high frequency modes because of uncertainty in parameter values for these DOF.

An alternative approach is used in the Model Error Sensitivity Suppression (MESS) algorithm [Ref. 41]. In this approach the control design is altered to directly account for uncertainty in the structural parameters. The process tends to be iterative because it is impossible to directly control the spillover behavior of the resulting control.

One of the most advanced LQG-based control techniques is the Maximum Entropy method [Ref. 25, 54 through 62]. This approach has the theoretical ability to directly account for modeling uncertainties. Though the method can be difficult to apply, it has the advantage that stability can be assured for both the control design model and a specified number of out-of-band modes.

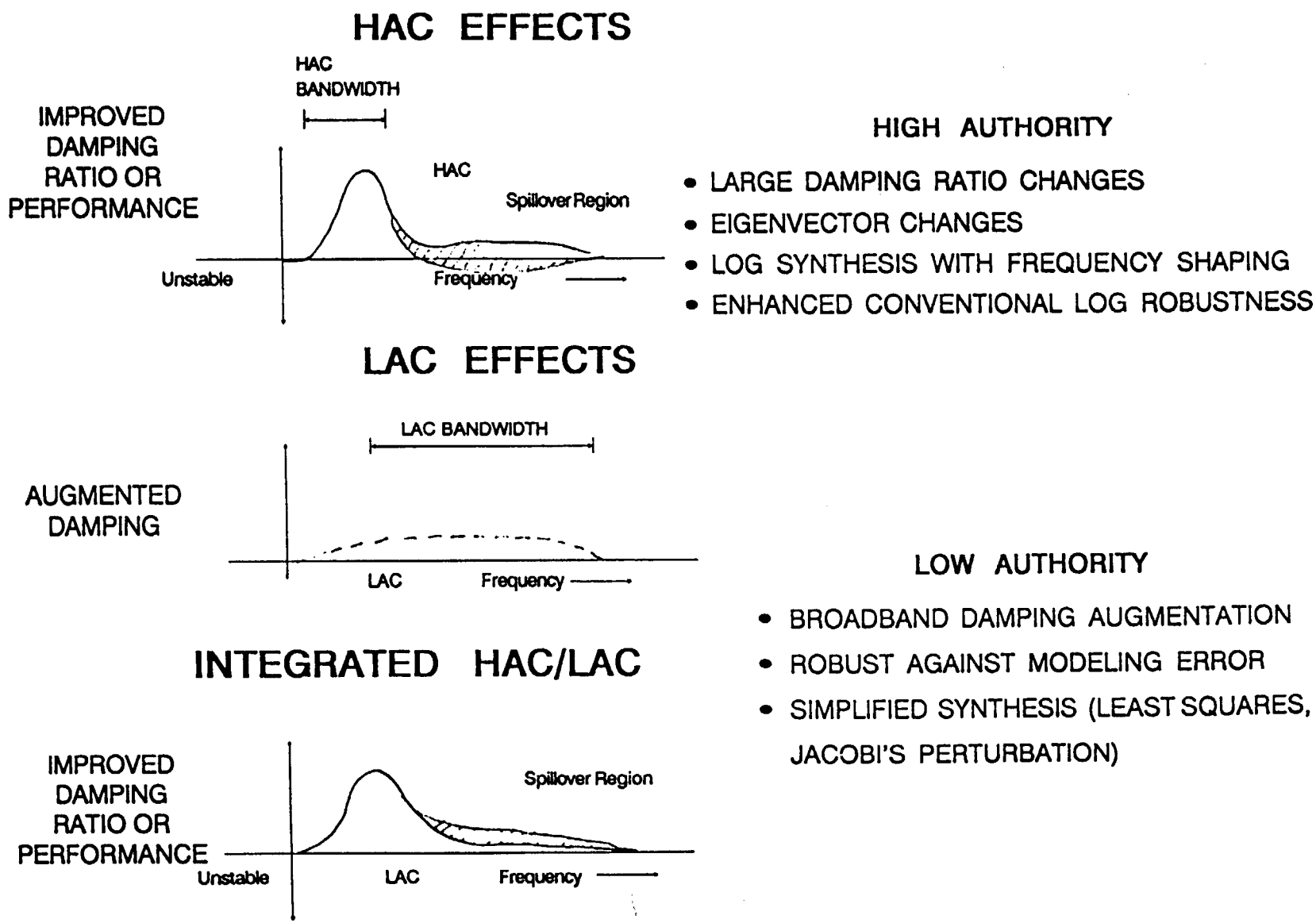

Figure 13: HIGH AND LOW AUTHORITY CONTROL

Many of the modern control methods have been developed in response to the 1978 to 1984 DARPA-initiated Active Control of Space Structure (ACOSS) program [Ref's. 42 through 45]. ACOSS was a broad-based technology program which was fundamentally interested in developing control methodologies for controlling LSS. The program preceded the establishment of the Strategic Defense Initiative (SDI) and was focused on the requirements of surveillance-like applications, though the resulting technology directly supports the generic needs of SDI and NASA applications.

There were seven industrial research efforts which focused on different aspects of the theoretical and experimental demonstrations of the emerging technology. The seven research efforts are described as follows:

CORPORATION	PROJECT DESCRIPTION
Control Dynamics Co.	Dynamic modeling/Digital Control
Convair/General Dynamics	FAMESS (Filter Accommodated Model Error Sensitivity Suppression) Plus a Hardware Experiment
Draper Laboratory	Vibration Suppression/Disturbance Rejection/Rapid Retargeting
Honeywell	System Stability/System Identification
Hughes	Control Theory Development/Electronic Damping Plus a Hardware Experiment
Lockheed	HAC/LAC Plus several Hardware Experiments
TRW	Positivity Control Design Plus a Hardware Experiment

Section 2.2.4 describes a number of the experiments listed above as well as more recently undertaken control experiments.

2.2.4 Ground-Based Experiments

Ground-based experiments are required to demonstrate the capabilities and limitations of various advanced control design approaches. The ACOSS program has provided a unique opportunity to develop and test many advanced LSS control approaches on simple structural models. Table 13 describes the ACOSS experiments. All

TABLE 13: ACOSS EXPERIMENTS

COMPANY	TYPE	DESCRIPTION	SENSOR	ACTUATOR	DEMONSTRATION
Lockheed	Beam	Fixed-free 1/4 x 1 x 60 in. aluminum	Piezoelectric accelerometers	Electrodynamic Shaker	Observation/control spillover modern modal control
	Beam	Fixed-free 40in. magnesium	Optical rate sensor	Proof-mass	Low-authority control
	I-Beam	Fixed-free 26 x 16 in. (400 lb) aluminum	Optical rate sensor	Single gimbal CMG	Low-authority control
	Vertical beam	Fixed-free 6in. aluminum lead tip masses	Accelerometers, quad-detector photodiodes	Pivoted proof-mass	Low-authority control system identification
	Circular plate	Suspended 2 m-diam aluminum	Multichannel microphase optics	Pivoted proof-mass	Low-authority control Low/high-authority control system identification
	POC	Suspended 4.5m boom, 3mreflector, aluminum	Accelerometers, rate gyros, laser	CMG, proof-mass	Classical and modern control of vibration and slew
	TOYSAT	Suspended rigid body 1.6 m cantilever beams aluminum	Accelerometers, LVDT velocity pickoffs	Electrosesis actuators	Open-loop torque profile high-authority control
Convair	Plate	Fixed-free 68 x 103 in. aluminum 4 x 5/16 in. welded beams	Rate gyros	Torque wheels	Model error sensitivity suppression
JPL	Beam	Pinned-free 150 x 6 x 1/32 in. stainless steel	Eddy current position sensor	Brushless dc torque motor	Modern modal control
LaRC	Beam	12 x 6 x 3/16 in. aluminum	Noncontacting deflec- tion sensor, load sensor	Electrodynamic shaker	
TRW	Plate	Clamped 1.73 m x 1.22 m x 1.66 mm aluminum	Rate sensors, accelerometers	Bending moment actuator	Vibration suppression and damping augmentation

of the experiments shared a desire to develop a structural model which emulates the important structural behaviors of LSS. Typical structural design goals include: first mode less than 1 Hz, closely spaced modes, discrete and continuous disturbance inputs, and planned structural modifications for modeling parameter uncertainties. The structural models have generally been very simple (i.e., beam-like models, square or circular plates,) though the Lockheed proof-of-concept (POC) resembles a space based radar concept.

Figure 14 presents two of the early Lockheed experiments. The Slim Beam experiment considered 3D boom motion using a LAC-based control approach [Ref. 15]. Non-colocated sensor and actuator placement allowed system stability assessments to be conducted. The disturbance input consisted of a proof-mass actuator. A major goal of the experiment is to verify that the LAC controller adds expected high frequency damping to the model. This class of experimental structure has provided the basis for many experiments [Ref's 13, 17-18, 20-22, 24-25, 30].

The TOYSAT experiment presented in Figure 14 represents the earliest attempt to verify the use of modern control methods for a maneuvering flexible structure [Ref. 23]. The experimental setup limited the rotational motion to small angles. An open-loop control command is generated to maneuver the structure. A combined HAC/LAC is used to provide closed-loop performance.

The control is provided by two Electroseis linear actuators which act on the rigid central body. The linear actuators are commanded to provide equal but opposite forces, resulting in a pure torque on the rigid central body. Two sets of sensors have been used, accelerometers and linear potentiometers. The accelerometers were mounted on the ends of the flexible bar. Linear potentiometers were connected in parallel with the Electroseis linear actuators, which measure the rotation of the central body. Parameter uncertainty is incorporated by adding tip masses to the flexible bar. Digital control implementation issues are directly considered in the theoretical and hardware implementation.

Figure 14 presents the experimental setup for the Lockheed circular plate control problem [Ref. 40]. This application is a 2D surface emulating a mirror- or antenna-like LSS. The control approach consists of using the VAMP system identification technique with HAC/LAC for the control. The LAC approach considered colocated rate feedback, while the HAC approach employed noncolocated state estimation using both analog and digital implementations. The unique feature of the structure is that there are nearly repeated modal frequencies. Purely optical sensing is used for the control. Four corner-cube mirrors are mounted on the plate. They are used in conjunction with the mu-phase sensor, which measures position along an axis normal to the undeformed plate by comparing the phase between outgoing and reflected laser

SLIM BEAM HARDWARE SETUP

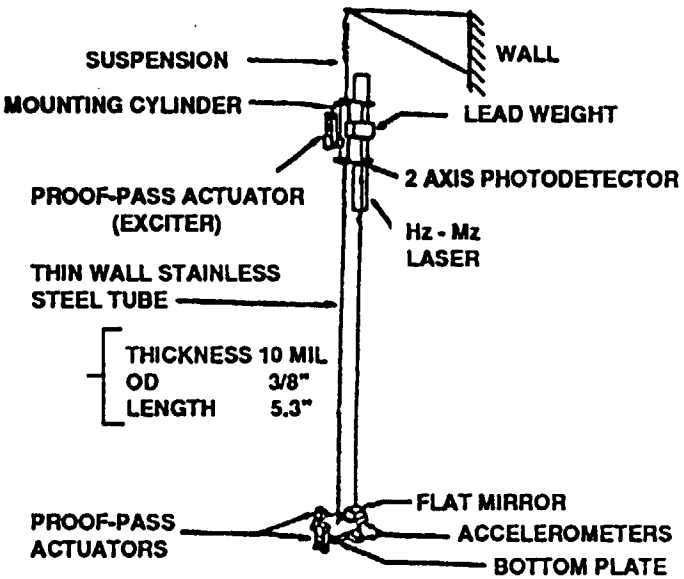

SLIM BEAM SENSOR/ACTUATOR

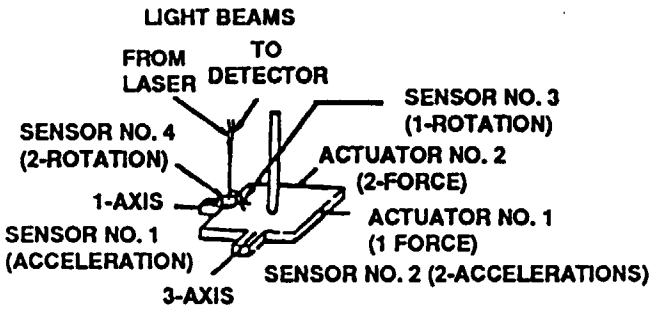

SLIM BEAM EXPERIEMNT

GOAL

LAC on 3D Structure
Compared Predicted and Actual Damping
Cross-Axis Coupling
Noncolocation
Nonconsistency of Sensor and Actuators
Parameter Sensitivity

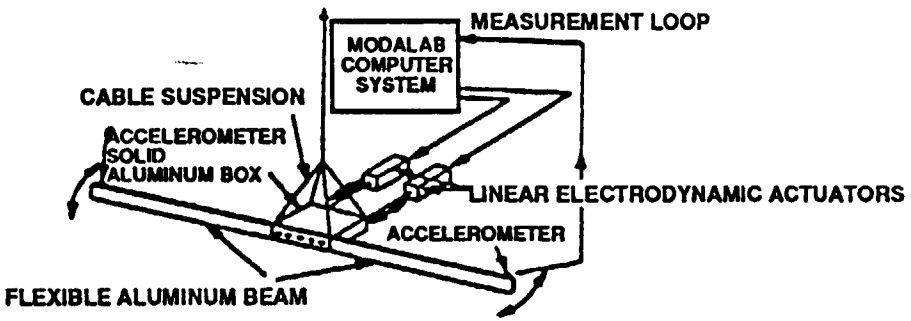

TOYSAT TEST SETUP

GOAL

Slewing
HAC/LAC
Digital Control
Agreement Between Theory/ Experiment
Spillover & Parameter Sensitivity
Low Sample Rate

beams. Plate rotation is measured by using two-dimensional linear photodetectors which measure reflected laser beams from two flat mirrors mounted on the top of the plate. Actuation is provided by three contactless actuators, for attitude and vibration control, and two Pivoted Proof Mass (PPM) actuators for vibration control and disturbance injection. Six sensors and four actuators are used for control purposes. The remaining actuator (i.e., a PPM) is used to excite the specimen with various disturbances. The LAC has been shown to produce about 1% damping in the high frequency mode, whereas the HAC system achieved more than 10% damping as predicted.

Figure 15a and 15b presents Lockheed Proof-of-Concept (POC) [Ref. 14]. This structure combines features of the Slim Beam, TOYSAT, and Circular Plate experiments. The experiment emulates the slew and vibration suppression control requirements for a space-based radar LSS application. Discrete time control approaches have been considered.

General Dynamics active control experiment for ACOSS is presented in Figure 16. The experimental device is a flat grillage, appropriately known as the fly swatter structure. The test article is clamped at the top to a very heavy support structure. The test article is composed of 4 in. x 5/16 in. thick aluminum beams welded together to form the structure. The sensor and actuator suite consists of four components, mounted as indicated by the small arrows in Figure 16. The mass of the sensor and actuator components has been accounted for in the design by mass loading the beam intersections without components with an equivalent amount of lead. This approach preserves the symmetry of the modal response behavior. Spring-restrained rate gyros are used to sense the structural motion. Torque wheels are used to transmit reaction torques into the structure. Control is provided by the two upper sets of components, while disturbances are introduced by the two lower sets of components. The rigid body mode is suppressed by using the MESS technique. The experiment is intended to demonstrate vibration suppression in the presence of persistent disturbances. This type of grillage structure has been used in many subsequent university and government laboratory experiments [Ref's 12, 16, 35, 39].

The NASA Langley Research Center has been actively involved in demonstrating active control methodology [Ref.13, 22, 31-34]. Figure 17 presents two of these experiments. The first experiment consists of a 12 ft. flexible beam. The control system for the beam is provided by four attached electromagnetic actuators, nine noncontacting sensors for measuring structural deflections, and four strain gauge type load cells which are colocated with the electromagnetic actuators. A large-scale computer is used to provide real-time processing for the sensor data and producing the actuator commands. The beam is supported using two 5 ft. lightweight cables which are attached to the ceiling. The cables must be light in order to avoid support structure coupling effects

AUBRUN, RATNR (LOCKHEED), LYONS (ISI)

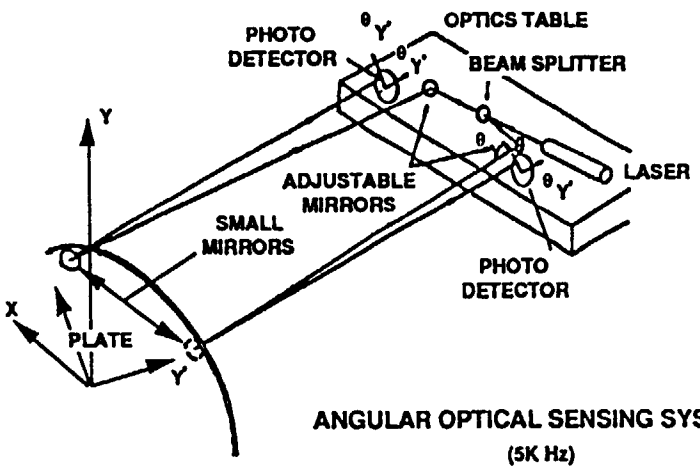

ANGULAR OPTICAL SENSING SYSTEM
(5K Hz)

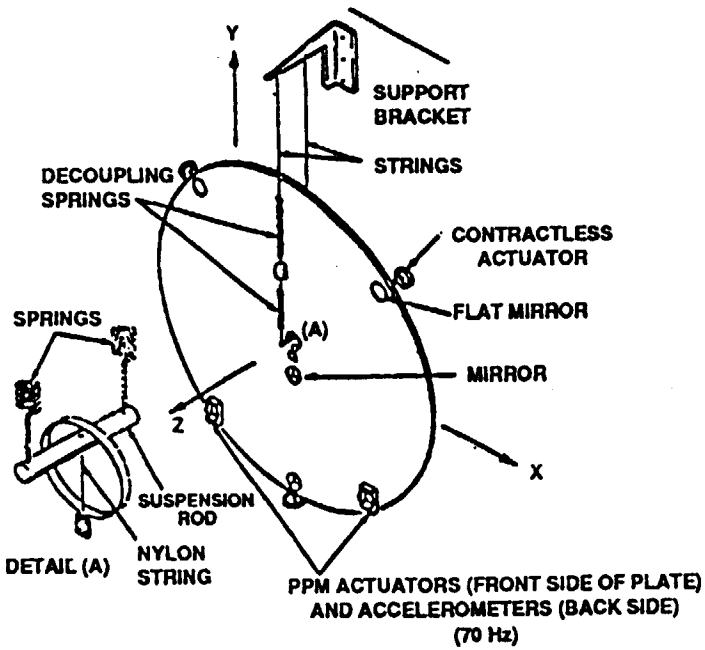

Approach (4 to 16 States)

- Low Authority Control (LAC)
- Low/High Authority Control (HAC/LAC)
- System ID (VAMP)
- Pivioted Proff-Mass Actuator
- Disturbances
- Environmental Noise
- Step Function
- Sinusoidal

Results

- NAC/LAC Methodology Verfied
- Significant Increases in Model Damping (10%)
- Proof-Mass Actuators Used in HAC
- Multi Channel U-Phase Sensor Used
- High-Order Digital Control

Figure 15a: LOCKHEED EXPERIMENT FOR ACOSS

GOAL

Classical and Modern Control
Transient Disturbance Rejection
LOS Control
Distributed Actuators
Optimal Slewing
Control of Dish Dynamic

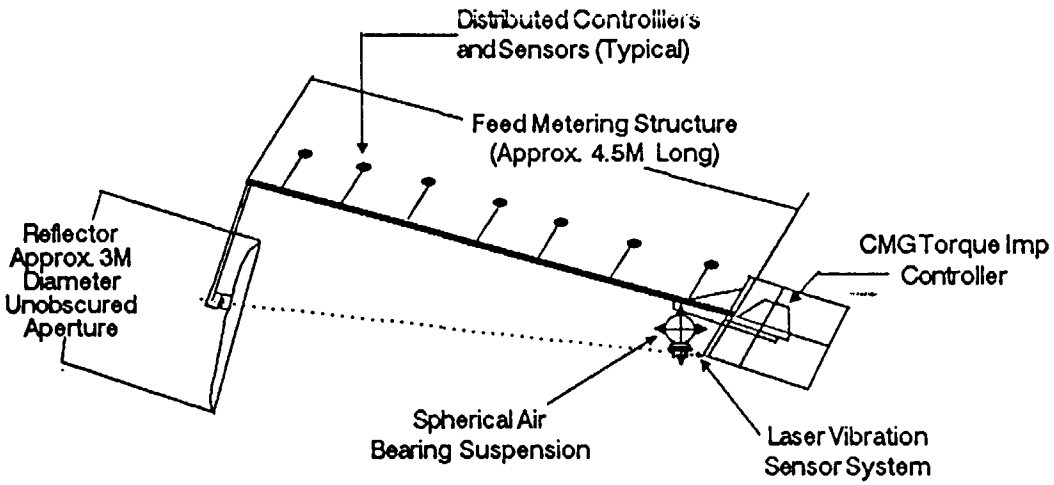

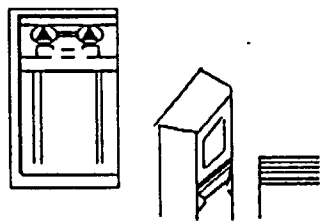

Proof-of-Concept Experiment
- Typical Offset Freed RF Antenna

FEATURES

First Two Bending Modes (1-2 Hz)
Modes 1-6 (<9Hz)
Antenna Dish Modes (>20 Hz)
4 CMG's + PMA

Figure 15b: LOCKHEED POC ACOSS EXPERIMENT

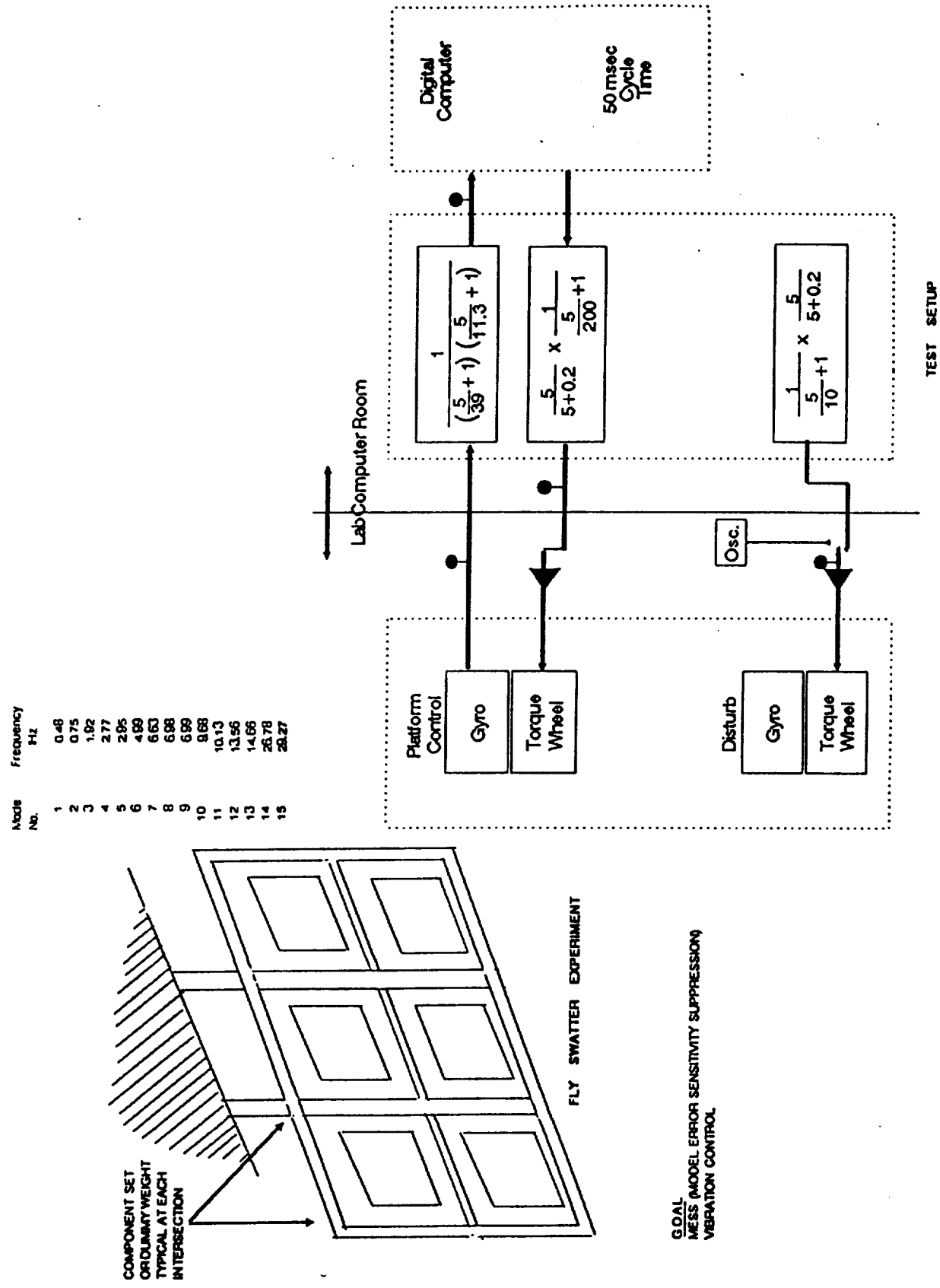

Figure 16: GENERAL DYNAMICS ACOSS CONTROL EXPERIMENT

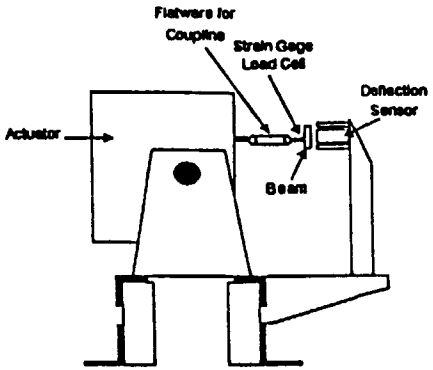

End view of experimental apparatus

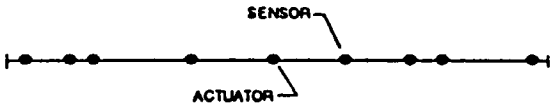

BEAM EXPERIMENTS

- Adaptive Control
- System Identification Via lattice Filters
- Autoregressive Moving Average
- Pole Placement

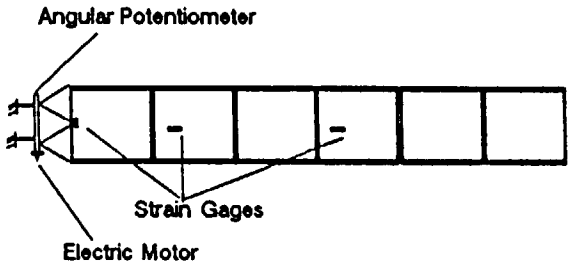

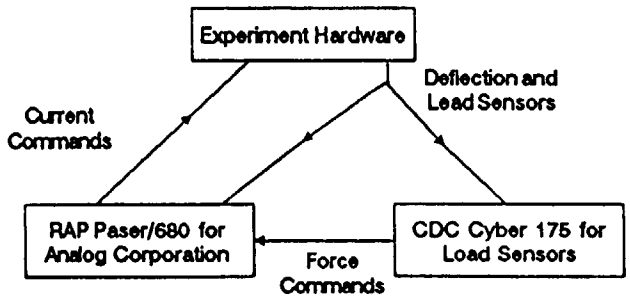

SOLAR ARRAY SLEW EXPERIMENTS

- Constant and Time-Varying Gain Control
- Torque Shaping
- System Identification
- Air Drag Interactions
- Single Axis

Figure 17: LaRC GROUND-BASED VIBRATION CONTROL EXPERIMENTS

to the controlled beam. The problem of designing test fixtures which emulate a space environment is common to all ground-based demonstration applications (e.g., gravity and atmospheric damping). Special actuator compensation is required to avoid artificial structural response damping. Initial control design have been based on pole placement schemes. More advanced control studies consider adaptive control have used recursive least square lattice filters, where an autoregressive moving average (ARMA) is employed for identifying the modal parameters. In this application the lattice filter generates mode shape estimates which are orthonormal in the space of the measurements. A coordinate transformation is introduced, relating the measurement space mode shape to the natural modes, which are orthonormal in the coordinate space. Using this transformation, the lattice filter produces the decoupled modes estimates, and a time series of the decoupled modal outputs are analyzed via the ARMA model. A discrete time control law formulation is implemented in the experiment.

The second experiment presented in Figure 17 consists of a 12.8 ft. aluminum/honeycomb solar panel. The instrumentation consists of three full-bridge strain gages to measure bending moments and two angular potentiometers to measure the angle of rotation. The strain gages are located at the root, at 22% of the beam length, and at the midspan. A finite time terminal controller is used to generate the shaped slew command as well as a constant gain feedback formulation. Tests demonstrated that significant air damping is induced during the slewing maneuvers [Ref's 32, 34].

The Spacecraft Control Laboratory Experiment (SCOLE) located at LaRC is presented in Figure 18 [Ref. 37]. The primary goals of the experiment include 3D rigid body motion for the base Shuttle, antenna pointing, and vibration suppression for the flexible boom connecting the antenna to the Shuttle. The primary interests for the testbed are MIMO control designs which deal with the PDE models for the structure as well as nonlinear beam bending mathematical formulations.

JPL has actively sponsored several active control experiments for LSS applications [Ref. 36]. Figure 19 presents four of the these experiments. The flexible beam is the simplest. The adaptive antenna control experiment deals with 2D surface control and parameter uncertainty. This facility also permits studies of robust and distributed control, shape determination and control, and the use of advanced optical sensing technology. The truss structures provide testbeds for demonstrating precision control for vibration suppression, disturbance rejection, and system identification.

AFAL has sponsored a ground-based slewing control experiment for demonstrating large angle slew motion, terminal fine pointing, and structural vibration suppression [Ref's. 26-29]. A major

SPACECRAFT CONTROL LABORATORY EXPERIMENT

3-D Slew Control
Flexible Modes in Control Bandwidth
Distribute Sensors and Actuators
PDE Modeling
Minimum Time Slews
Nonlinear Beam Models

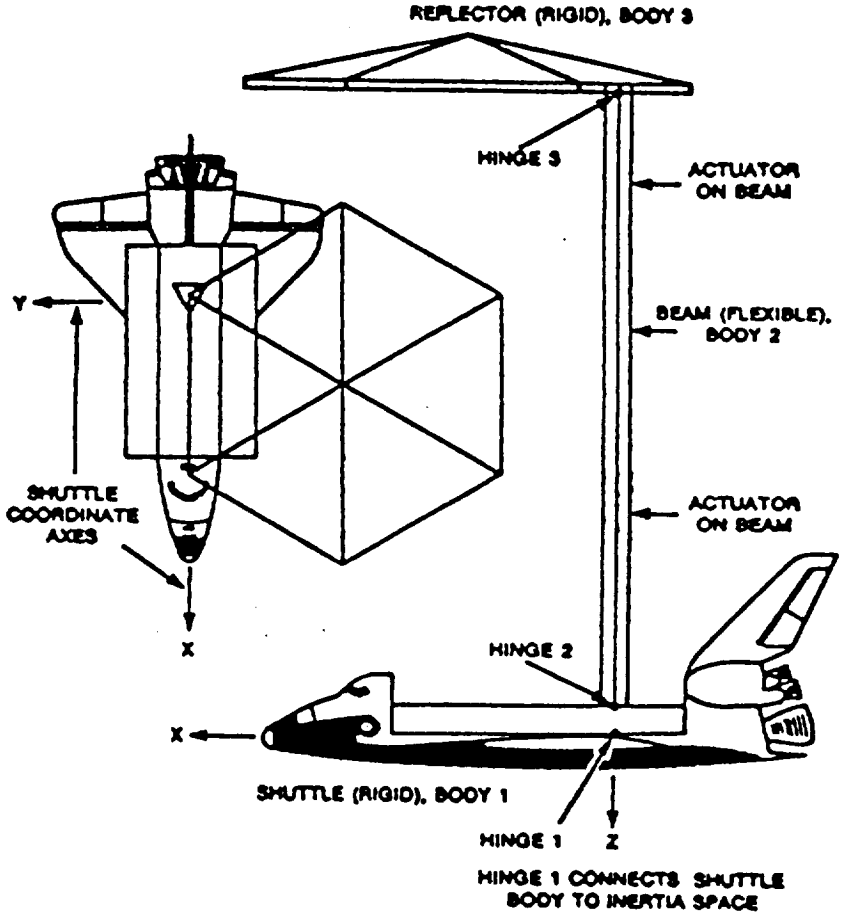

Figure 18: LaRC SCOLE: NASA/IEEE DESIGN CHALLENGE

Figure 19a: JPL LSS CONTROL EXPERIMENTS

Figure 19b: JPL LSS CONTROL EXPERIMENTS

objective of the experiment has been to demonstrate the use of Reaction Control Jet (RCS) thrusters for simultaneously accomplishing both the slew and the terminal vibration suppression. The basic test article consists of a central hub with four attached flexible appendages. The gas for the RCS system is stored on the central hub and cables carry the gas to the thrusters located on the tips of two of the flexible appendages. The facility has been used to demonstrate pole placement and Maximum Entropy modern control designs. The testbed has also been used to demonstrate piezoelectric distributed actuator concepts [Ref's. 48-49]. An advanced version of this experiment is currently in the planning stage, and is known as the Advanced Space Structure Technology Research Experiment (ASTREX). This facility will permit full-scale 3D rapid retargetting maneuvers and vibration suppression studies for a scaled version of a space-based laser.

Marshall Space Flight Center (MSFC) has sponsored the Active Control Technique Evaluation for Spacecraft (ACES) facility. This program tested three promising control approaches developed on the ACOSS program. The three techniques included: Filter Accommodated Model Error Sensitivity Suppression (FAMESS), High Authority Control/Low Authority Control (HAC/LAC), and Positivity. The comparison has been carried out both analytically and experimentally. Each controller is implemented and tested at the NASA/MSFC Large Space Structure Ground Test Facility on the ACES test article. Much planning has been carried out to ensure that identical sensor/actuator suites, computers, disturbances, and performance criteria are applied for each control design /evaluation. An unmodeled low-frequency mode caused some difficulties for the control evaluation studies. A currently planned follow-on for the ACES experiment is the Controls, Astrophysics and Structures Experiment (CASE). This facility will investigate critical control technology applicable to stabilizing and pointing large flexible structures in space. CASES will provide an on-orbit test bed for demonstrating the flight readiness of several key aspects of CSI Technology.

SDI has sponsored the development of the Rapid Retargetting and Precision Pointing (R2P2) test facility. Control experiments are conducted for single-axis slews of various directed energy weapon concepts. The unique aspect of the facility is that extremely high pointing precision can be achieved. The structural modeling is analog in that tuned pendulums are used to characterize the structural behavior of specific systems. SDI had also sponsored the Joint Optics and Structures Experiment (JOSE) which had been designed to demonstrate 100:1 response reduction for controlling a space based laser-like test fixture. Unfortunately this ambitious program has been canceled; nevertheless, experiments are still required to fully demonstrate the levels of control capability that this experiment was attempting to achieve.

The area of LSS control has attracted the interest of many groups of researchers. The experiments discussed in this section represent the early efforts by many organizations to address the key technology areas. A more complete listing of the experiments conducted in the USA since 1982 is presented in Table 14. The test objectives, sensor, actuators and test facility description is briefly provided. The experimentally obtained results are discussed in Section 2.2.5.

2.2.5 Lessons Learned

The control experiments presented in Section 2.2.4 have sought to demonstrate typically a 100:1 response reduction when the closed-loop control is active. Though this goal is reasonable for many vibration problems, some optical systems require performance improvements of 1000:1 to be successful. Theoretical results suggest that extremely high levels of performance can be achieved by using modern control methodologies. The observed experimental performance, however, has been disappointing. Early results with HAC/LAC have demonstrated 10% damping in controlled modes and 1% damping in out-of-band modes as expected. Later experiments have generally demonstrated 10:1-50:1 performance improvements with most results biased towards the lower figure. Clearly, much work remains to be done if modern control technology is to be used in the near-term applications for handling operational space borne systems.

There are many potential reasons for why this promising technology has yet to perform as expected. For example, many experiments have been designed to minimize costs by making maximal use of off-the-self components. A by-product of this approach has been to limit the range and bandwidth of sensors and actuators as well as the computational throughput available for real-time applications. The current status of demonstrated control capabilities is attributable to a lack of a focused mission with clearly defined goals and control objectives.

There are three classes of potential missions which have related but different mission goals. The missions are: i) large platforms (e.g., space station), i)) large antennas (e.g., Geoplat), and iii) large optical platforms (e.g., LDR). Strawman designs exist for each of these concepts and preliminary performance requirements have been defined. It is unlikely that a single experiment can resolve all of the control questions of interest for the three mission classes. Nevertheless, a need exists for defining an experiment which addresses CSI technology issues which cannot be resolved by conventional work-arounds, structural modifications, passive damping treatments, isolation systems, or exotic materials. A useful experiment should have modern control technology as the only viable design option and should demonstrate LSS control methodology for a problem needing response reductions in the range of 100:1-1000:1.

TABLE 14: LSS GROUND-BASED EXPERIMENT SINCE 1982

EXPERIMENT	DESCRIPTION	ACTUATORS/SENSOR	TEST OBJECTIVE
Advanced Beam Experiment (ABE) - AFWAL [Robert W. Gordon]	71 in. aluminum beam, vertically hung, cantilevered at top	Proof mass actuators, accelerometers	active vibration suppression
12 m Truss Control AFWAL [Robert W. Gordon]	Aluminum truss, vertically oriented, cantilevered at base	Proof mass actuators, accelerometers, photodiode	active & passive damping
TRW Truss Experiment [Maribeth Roesler]	115x55 in. truss box	optical sensor	active & passive damping
Compound Pendulum Harris Corp. [John Shipley]	2 beams, connected at middle and bottom end	Harris Linear DC motor, accelerometers	testing of Harris LDCM on lightly damped structure
Plate Experiment Harris Corp. [John Shipley]	4 sq. ft., 1/8 in. thick plate, suspended vertically	microshakers, accelerometers	surface roughness control, sensor/actuator placement studies
Multi-Hex Prototype Experiment (MHPE) Harris Corp.	10 ft diameter, 7 graphite epoxy panel segmented test bed	Harris Linear precision Actuators (LPACTS), piezoelectrics, optical sensor	generic testing of large segmented reflectors, surface shape control
Air Force Planar Truss Experiment USAFA-AFOSR [William L. Hallauer]	23.3ft. 20 bay truss, horizontal on bearing	thrusters, proof mass actuators, accelerometer	actuator-structure interaction studies
Beam Cable - VPI [William L. Hallauer]	80 in. vertical steel beam, with aluminum cross beam, hung by cables	force actuators, velocity sensors	active damping, theoretical/ experimental comparisions
2-D Pendulous Plane Grid VPI [William L. Hallauer]	Aluminum grid with steel top beam	force actuators, velocity sensors	active damping, theoretical/ experimental comparisons
Slewing Grid - VPI [William L. Hallauer]	Aluminum plane grid, pivots about steel shaft	reaction wheels, servo accelerometers	active rigid body slewing a and vibration suppression
Hoop-column antenna Langley [Thomas Campbell]	15 m mesh antenna, supported by outer graphite hoop, a 13 m column in center	accelerometers, proximity probes	deployment, electromagnetic, structural tests
Three-body rapid maneuvering experiment Langley [Jer-Nan Juang]	two flexible, horizontal panels, one on each side of a rigid hub, hub rotates in horizontal plane	gearmotor, strain gauges, potentiometers	rapid slewing experiments
Multi-body maneuvering experiment - Langley [Jer-Nan Juang]	1 m flexible panel, projecting out from a cart, cart travels on a horizontal 3 m beam	gear box motor, direct drive motor, tachometer, potentiometer, strain gauges	rapid translational & rotational control of flexible panel, can be mini-test article for CSI
Daisy Test bed Dynacon Enterprises [P.C. Hughes]	central rigid hub, 10 equally spaced rods projecting out total diameter 19 ft.	thrusters, reaction wheels, accelerometers, digital angular motion encoders	generic test bed for flexible spacecraft studies
Ohio State University Control Research Lab [U. Ozguner]			
Free-Free Beam	1.8 m horizontally suspended aluminum beam	proof mass actuators, accelerometers, strain gauges	system ID, vibration suppression
Slewing Beam	40 in. horizontal aluminum beam, attached at end to hub, counter-weight attached at opposite side of hub	direct drive motor, motor encoders, accelerometers, tachometer	slewing control and vibration suppression
Smart Structure Lab VPI [Harry Robertshaw]			
Variable Geometry Truss	2 module variable configuration truss, with beam suspended vertically in center	electric motors, linear potentiometers, strain gauges	truss configuration, beam control
Planar Truss	1 bay truss, contrained on one side, horizontal on table	jack screws, strain gauges	vibration and slewing control
Free-Free Planar Truss	1 bay truss, free to move horizontally on table	jack screws, strain gauges, linear potentiometers	

TABLE 14: LSS GROUND-BASED EXPERIMENT SINCE 1982 (Continued)

EXPERIMENT	DESCRIPTION	ACTUATORS/SENSOR	TEST OBJECTIVE
Flexible Satellite Slew Test bed - AFAL/CSDL [P. Madden]	hub with 4 horizontal arms (9 ft total diameter), suspended on air table	cold gas jets, proof mass actuators, angle resolver, accelerometers	active vibration suppression, rigid body slewing control
MIT Space Systems Lab [Ed Crawley]	composite beam, horizontally hung by wire	embedded piezoceramic actuators, strain gauges	active vibration suppression
	25ft. brass beam, horizontally suspended bywire	shaker, accelerometer	traveling wave experiments
	Horizontal truss on soft springs	piezoceramic actuators, PCB structcel accelerometers	active structural member studies
Aluminum Beam Expander Structure (ABES) AFWL [David Founds]	SBL Beam Expander model 9 m tripod, 6 m base	shakers, triaxial accelerometers	system identificatoin
Spacecraft Control Laboratory Experiment (SCOLE) - Langley [Raymond Montgomery]	rigid platform, with 10 ft beam with a 40 in. diameter offset reflector frame, all suspended by steel cable	cold gas jets, reaction wheels, control moment gyros, rate gyros, optical sensors, accelerometers	slewing and pointing experiments, with vibration suppression, system identification tests, failure detection and reconfiguration tests
Advanced Structures/ Controls Integrated Experiment (ASCIE)	truss supporting a 2 m diameter, 7 hexagonal aluminum plate, segmented mirror	proportional electromechanical flexure levers, optical sensor	control test bed for segmented reflectors
Space Integrated Controls Experiment (SPICE) - AFWL [Capt. Robert Hunt]	SBL test model	active suspension (SAVI) and passive	
Passive and Active Control of Space Structures (PACOSS) AFWAL/MMDA	Dynamic Test Article (DTA) various components		Active and passive control
Joint Optics Structure Experiment (JOSE) AFAL-TRW-Litton_ITEK [Capt. Robert Hunt]	Primary/secondary reflector optical truss - Halo structure	proof mass actuators	
SUNY - Buffalo [Daniel Inman]	vertically oriented aluminum beam, cantilevered, active hinge conecting beam with second flexible beam	torque motor, strain gauges, tachometer (active hinge)	slewing/vibration suppression control
	cantilevered composite beam	proof mass actuators	transverse vibration control, actuator/sensor interaction
	horizontally cantilevered beam	torque motor	tests eigenfunction based slewing control
	planar truss structure	proof mass actuator	periodic trusses modeling
	cantilevered beam and truss	electric motors	slewing/vibration control, actuator/sensor interaction tests
	horizontal beam, hinged at end, suspended at other end	active track/cart system	active suspension tests
Vibration Control of Space Structures (VCOSS) MSFC-AFWAL-LMSC-TRW [Henry B. Waites]	13 m Astromast with asymmetric crusiform at base, vertically oriented, cantilevered at top	linear momentum exchange devices, LVDT, accelerometers	pre-cursor to ACES
Active Control Technique Evaluation for Spacecraft (ACES) - MSFC [Henry B. Waites]	13m Astromast with 3 m offset antenna, vertically oriented, cantilevered at top	linear momentum exchange devices, accelerometers, laser	general test article, vibration suppression, system ID
Mini-Mast - Langley [Richard Pappa]	vertically oriented, 20 m, 18 bay truss, cantilevered at base	reaction wheels, proof mass actuators, position sensors, accelerometers	vibration damping and system ID, general test structure

2.3 Large Antenna Study

There are typically many options available early in the design process for selecting antenna diameters, operational frequencies, scanning techniques, and myriad other related technical decisions. Unfortunately, the basic problem is highly nonlinear when all of the competing criteria are considered. Sorting through the many competing, and often conflicting, design criteria represents a significant challenge for those involved. As systems become larger, the potential for concern about CSI issues increase. CSI concerns can manifest themselves on several levels, and it is important to bound the level of complexity of the problem. Figure 20 presents a preliminary CSI assessment decision tree, which can be used to identify the magnitude of CSI. The assessment is based on comparing the open-loop performance of the system relative to the performance goals. The process requires that a series of questions be answered. The responses then identify the complexity of the CSI solution. There are four main questions which must be addressed: i) can passive damping treatments be used to meet the performance goals?, ii) is the disturbance a single frequency input to the system requiring less than a 10000:1 response reduction?, iii) is the disturbance a broad-band input to the system requiring less than a 100:1 response reduction?, and iv) can isolation techniques be used to meet performance goals? For systems falling outside the bounds of these questions a potentially severe CSI design problem exists. If this process is repeated for every structural concept, then the effort required to generate the models becomes prohibitive. To minimize the modeling effort scaling laws are developed to facilitate comparison of generic classes of missions.

Section 2.3.1 presents the basis approach for developing the methodology. Section 2.3.2 presents the Geoplat-specific modeling issues used in the study. The modeling assumptions are reviewed in Section 2.3.3. The structural performance scaling laws are presented in Section 2.3.4. The CSI trade study for Geoplat-class missions is presented in Section 2.3.5.

2.3.1 Technical Objectives

This section develops a methodology for assessing the CSI impact for Geoplat-class systems. The methodology is generic and can be applied to different classes of spacecraft applications. A basic idea behind the approach is to use an example application which accounts for the correct physics of a structure. The nominal and worst case system responses are determined by applying anticipated disturbances to a preliminary structural model. Scaling laws are developed for extrapolating the observed system responses for variable vehicle parameters such as antenna diameter and operational frequency. Guidelines for the complexity of control law design requirements can be established by plotting the

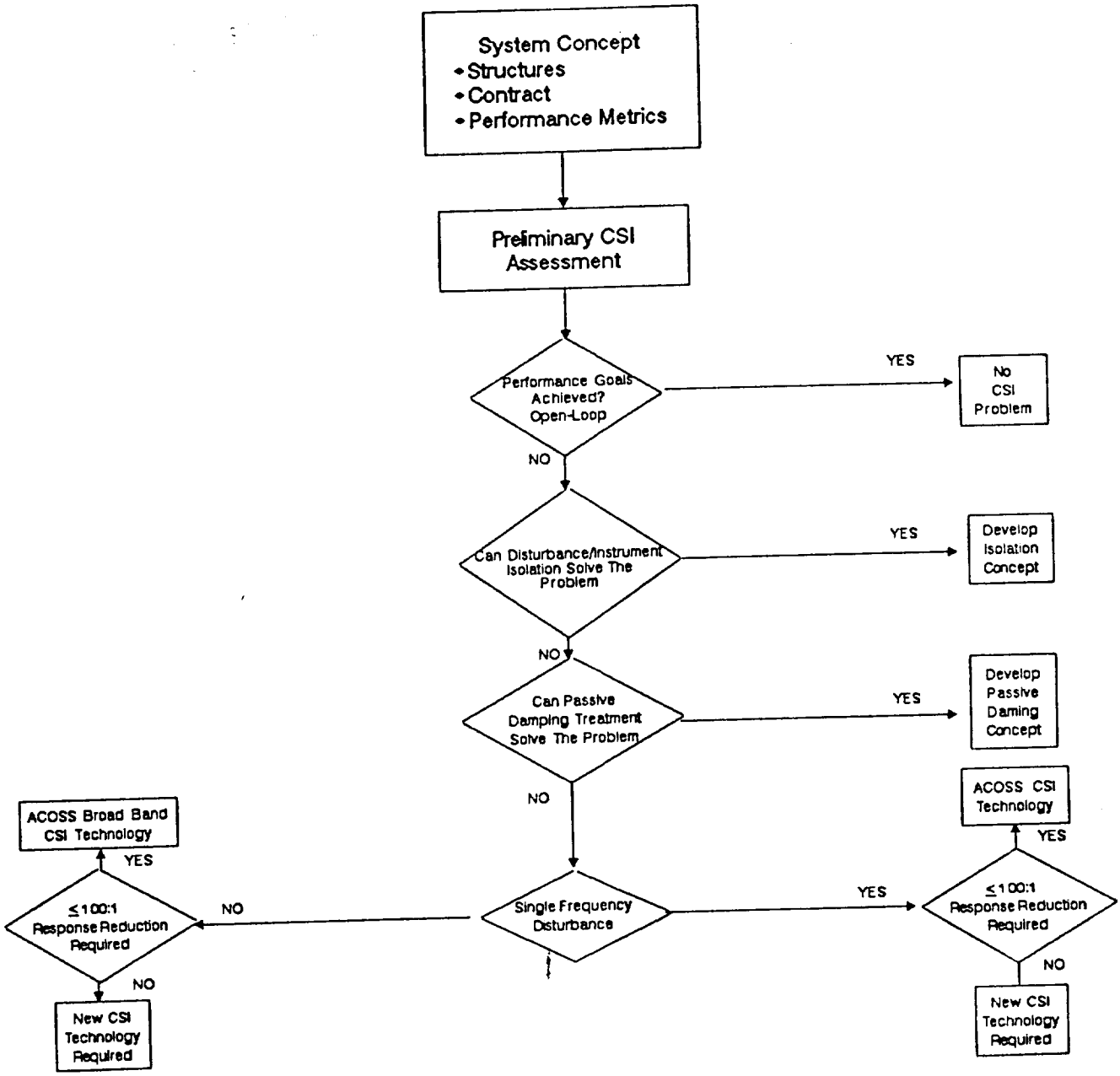

Figure 20: CSI PRELIMINARY ASSESSMENT DECISION TREE

extrapolated system responses for larger diameter systems. Because the extrapolated estimates are anchored in predictions for a realistic structural model, the conclusions can be considered approximations for a more exact analysis. The key issues to be extracted from the analysis are trends indicating the potential for CSI problems. These assessments are useful because mission risk is a function of the technology which must be invoked to solve a particular control problem. The risk being highest for applications which require technology developments beyond the current state-of-the-art. If problem areas are identified, then more detailed studies can be conducted to ascertain the exact behavior of a specific satellite configuration. It is anticipated that an early identification of potential problem areas can have a significant impact on the design process.

2.3.2 Study Methodology

The FULLFORD model presented in Figure 5 is used to develop system responses for both nominal and off-nominal operational conditions. The nominal system responses have been obtained by applying a subreflector scanning torque to the feed boom for the 15m antenna. The subreflector scanning torque has been found to induce the largest system response (see Section 2.2.4 for details). To explore a worst case scenario, the scan frequency has been selected to be close to the structural frequency of the first bending mode of the 15 m feed boom. The off-nominal operational condition corresponds to thruster firing for daily station keeping. These operational conditions bound the expected range of induced structural behaviors.

One significant limitation of the model used for this analysis is that the instruments, other than the antennas, are modelled as lumped masses. If, on the other hand, the instrument models included both rigid and flexible body degrees of freedom, then a possibility could exist of CSI arising because of instrument scanning motions exciting internal instrument DOF. Detailed simulation studies should not over look this possibility for CSI problems [Ref's. 8-10, 51].

2.3.3 Modeling Assumptions

To compute the line-of-sight (LOS) pointing errors induced by the nominal and off-nominal disturbances described in Section 2.3.2 one has to make a number of modeling assumptions. The first assumption is that the antenna is treated as being rigid (Ref. 1). This implies that induced surface deformations do not influence pointing direction calculations. The second assumption is that the subreflector scanning torques are not momentum compensated. The third assumption is that the scan configuration is idealized. These assumptions allow preliminary assessments to be conducted

while some aspects of the design have not been firmed up. In selecting modeling goals the objective has been to err on the side of conservatism.

When very large antenna systems are of interest, the rigid antenna assumption needs to be revisited (Ref. 72, 73), since surface deformations can become a significant contributor to the pointing error. One aspect of the approach described in this section is that no assumptions are made regarding the potential for overlap between the structure and control bandwidths. For the baseline Geoplat model this idealization can be justified; however, for larger systems studied exclusively through extrapolation of the baseline system response, the performance and control requirement predictions may prove to be optimistic rather than pessimistic. More work is required in this area to develop a complete understanding of all of the interacting phenomenologies.

2.3.4 Response Scaling Laws

The nominal responses computed for the Geoplat baseline configuration provide data for a point design. Because the effort involved in developing similar point designs for many competing concepts is prohibitive, there is a need for developing scaling laws which allow trade studies for related systems. The baseline Geoplat results provide traceability for the extrapolated system response predictions. The scaling law predictions are not exact, but rather provide trends in assessing the general behavior of complicated systems. To gain greater confidence in the extrapolated predictions several additional point designs should be studied (e.g., 20 - 40 m systems).

There are three structural frequency and response scaling laws which are of interest. The generic scaling laws are obtained by investigating analytic solutions for a variety of simple geometrical forms and determining the functional dependence of the response on parameters such as lengths, diameters, structural mass and nonstructural mass. The first scaling law relates antenna structural frequency to antenna diameter, as follows:

$$F = FN*(DN/D)^2 \qquad (1)$$

where FN denotes nominal antenna structural frequency, F denotes scaled antenna structural frequency, DN denotes nominal antenna diameter, and D denotes scaled antenna diameter. Equation (1) indicates that the scaled structural frequency decreases as the scaled diameter increases. This scaling law follows from simple models for circular membranes, as well as comparison of the structural behavior for several antenna models.

The scaling law for predicting the antenna response and the feed boom response can be shown to be:

$$R = RN*(D/DN)^4 \qquad (2)$$

where R denotes the scaled system response, RN denotes the nominal system response, D denotes the scaled system diameter, and DN denotes the nominal system diameter. Equation (2) indicates that the scaled system response increases as the scaled system diameter increases, and that the scaling is nonlinear. This result follows from analytical results for beam-like structures under a variety of load conditions.

The scaling law for predicting the antenna structural frequency change as a function of structural mass scaling is given by:

$$F=FN*[(1+C)*\rho/(1+C*\rho)]^{1/2} \qquad (3)$$

and

$$C = MS/MNS \qquad (4)$$

where F denotes the scaled frequency, FN denotes the nominal frequency, MS denotes the structural mass, MNS denotes the non-structural mass, ρ denotes scaling parameter for the structural mass. This result is empirically derived.

The scaling laws permit extrapolations for structural frequencies and responses. For this study the nominal structure is taken to be the 15 m antenna for Geoplat. An implicit assumption in the use of the scaling laws is that the spacecraft configuration is fixed and that the subreflector scan support boom scaling laws follow the changes in the antenna scaling laws. This assumption is made in order to bound the number of potential problem variations which must be considered. To gain greater confidence in the predicted results, there is a future need for verifying the scaling laws with additional large point designs.

The nominal frequencies and responses are obtained by using the FULLFORD model described in Section 2.1 and the disturbance inputs presented in Section 2.1.4. This model is used to insure that the extrapolated system responses are anchored to results of a physically meaningful mathematical model.

2.3.5 Trade Studies

This section presents several trade studies which evaluate the behavior of a large range of antenna-like systems. The goal of the effort is to establish the relative complexity of several competing design concepts, in terms of: i) open-loop performance relative to LOS stability goals for different operational frequencies, ii) passive damping treatment performance relative to LOS stability goals for different operational frequencies, iii) open-loop performance relative to demonstrated broad band vibration control technology, iv) open-loop performance relative to theoretically predicted vibration control for single structural frequency disturbances, and v) open-loop performance relative to structural mass variation trade studies.

The LOS pointing stability is defined by an optical measure of system performance. The basic idea is to use a two-dimensional Fourier transform of the aperture field distribution. This approximation is used because of the severe obstacles attending the rigorous solution of the coupled vector wave equations for electric and magnetic fields, while addressing the boundary conditions imposed by Maxwell's equations. The first step in the approximation process is to use scaler rather than vector diffraction theory. Scaler diffraction theory leads to the so-called Rayleigh criterion which states that two point sources of monochromatic light of the same wavelength are said to be just resolved if the maximum intensity of one source occurs at the position of the first diffraction minimum of the other source.

The mathematical description for the intensity can be shown to be:

$$I(p) = \pi^2 * d^4 (2 * j1(k * \theta * d) / (k * \theta * d)) \qquad (5)$$

where p denotes the point at which we wish to calculate the amplitude of the intensity, d denotes the aperture diameter, j1(*) denotes the Bessel function of the first kind, k denotes the wave number, θ denotes the off-axis angle measure relative to the aperture plane, and I(*) denotes the field intensity. The first zero of I(*) occurs at the first root of the j1(*), which can be shown to be 3.832. Since θ represents the half-angle measure for the distribution pattern, it follows that the desired angle is given by:

$$\phi = 1.22 * \lambda / d \qquad (6)$$

where the wave number, k, has been replaced by $2*\pi/\lambda$, and λ denotes wavelength. The LOS pointing stability is obtained by dividing Eq. (5) by five, leading to

$$LOS\ Stability = (0.2)*(1.22)*\lambda/d \qquad (7)$$

This equation is used to identify when an induced structural response exceeds the pointing stability performance goal. The important thing to observe about Eq. (7) is that LOS stability is inversely proportional to the antenna diameter for a fixed operational wavelength. This result implies that as larger and larger systems are considered, the basic physics of the observation process leads to tighter performance requirements.

In the results presented in Sections 2.3.5.1 through 2.3.5.4, the ultimate interest is in assessing the magnitude of CSI for systems of various sizes. Figure 21 presents scaled response curves for the nominal and off-nominal thruster firing cases. These curves bound the expected structural behaviors for systems up to 100 m in diameter where Eq. (2) has been used. As in all results presented, the responses are for the 15 m. Geoplat system responses are marked on the plot.

Figure 22 presents similar response curves except that only the nominal behavior is shown. The solid line represents the system response when 0.5% natural damping is assumed. The dashed line presents the system response when passive damping treatments have been applied to reduce the induced response. Clearly the use of passive damping treatments offer significant improvements in the system performance. To be meaningful for CSI investigations, these curves are combined with LOS pointing stability curves, control technology curves, and mass variation curves to permit simple trade studies for competing design concepts.

A typical control stability curve is presented in Figure 23. The solid line represents the LOS stability curve for a 250 GHz system with variable antenna diameter (see Eq. (7)). When system response curves are superimposed, one can determine the complexity of the CSI problem. For example, if the response curves lie within the hatched region, then the LOS Stability pointing goals are achieved by passive techniques. If, on the other hand, the response curves lie between the hatched region and the dashed line, then the control problem can be handled for broad-band disturbance inputs by using ACOSS-like technology. The dashed line represents a two-order-of-magnitude increase over the LOS stability response curve. When a response curve lies within this region ACOSS technology can be used to bring the controlled response back into the hatched region where the performance goals are achieved. The dotted line corresponds to a four-order-of-magnitude increase over the LOS Stability response curve. When a response curve lies

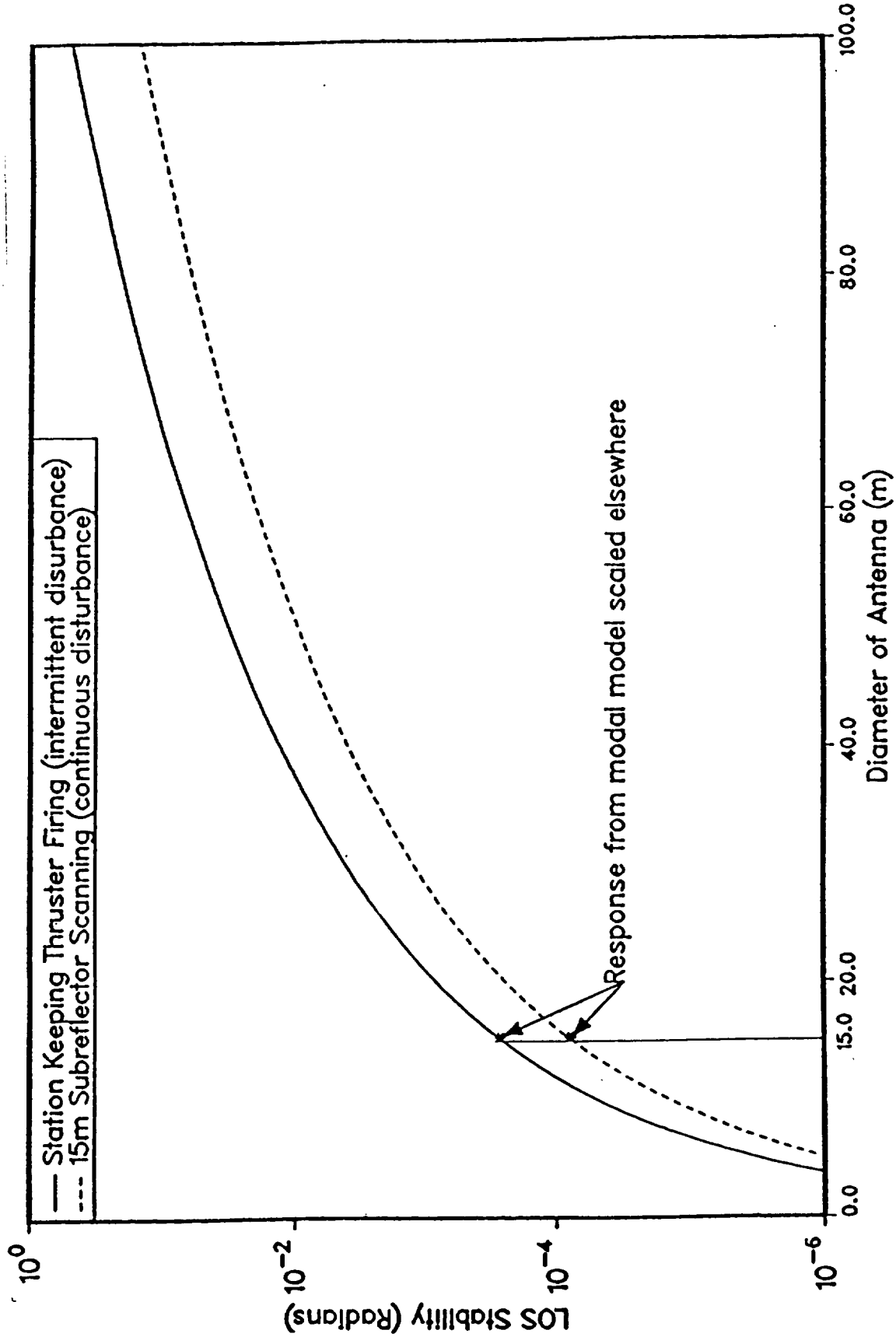

Figure 21: DYNAMIC RESPONSE OF LOS SCALING WITH ANTENNA SIZE

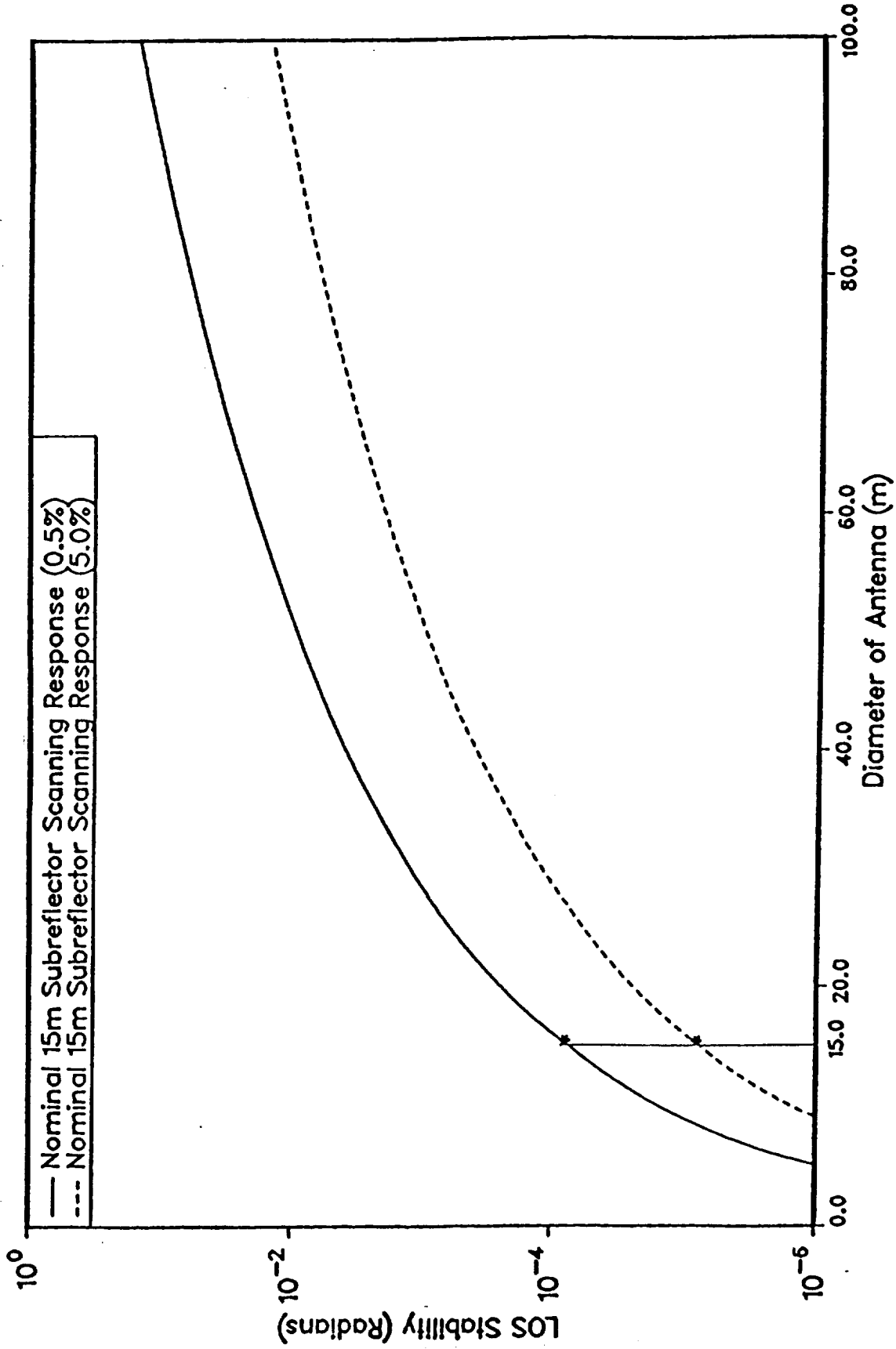

Figure 22: RESPONSE WITH DIFFERENT DAMPING RATIOS

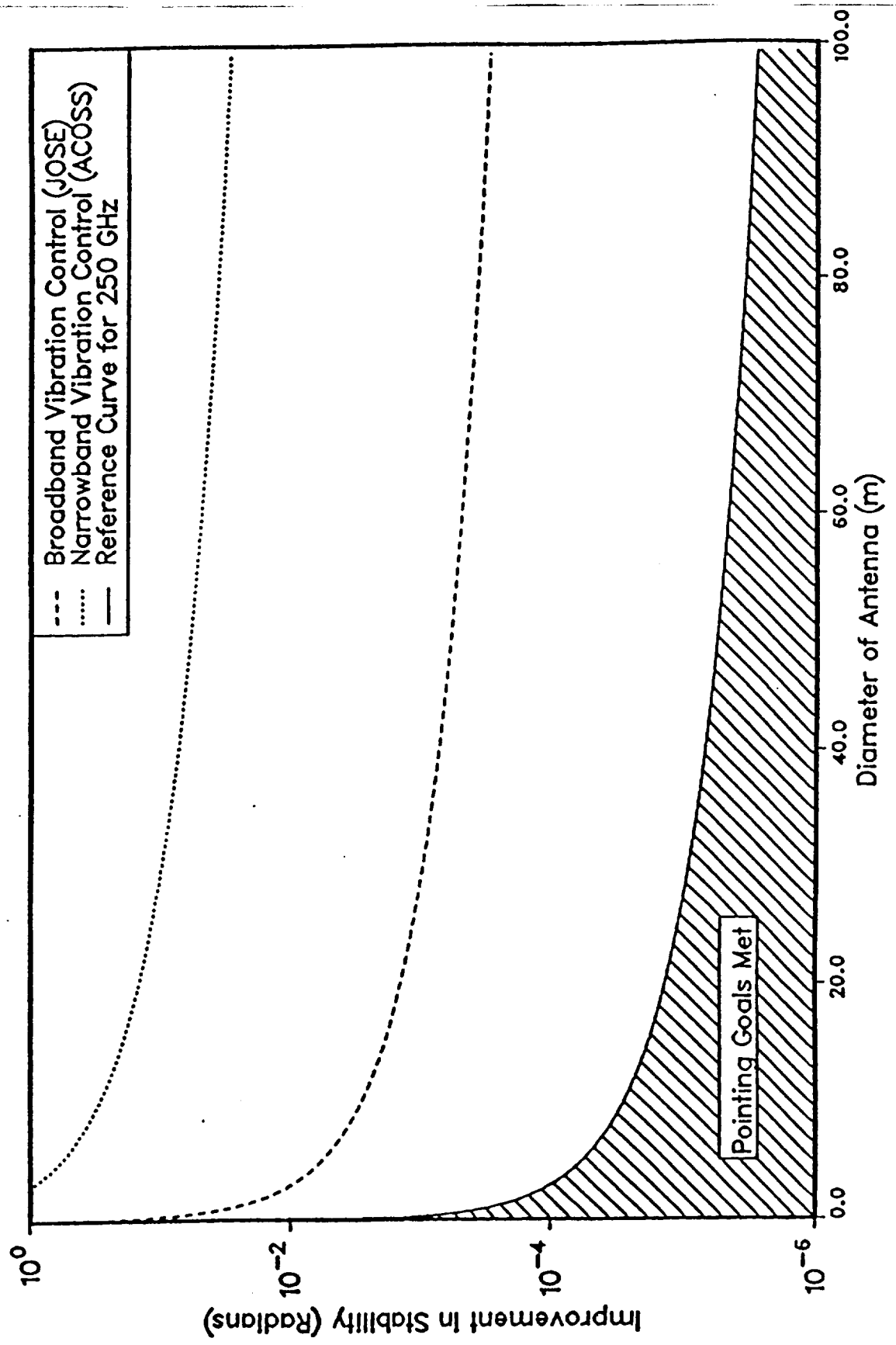

Figure 23: CONTROL TECHNOLOGY PERFORMANCE FOR 250Hz SYSTEM

between the dotted line and the reference curve for the 250 GHz system and is due to a narrow band disturbance (e.g., a single frequency input), then ACOSS technology can be used to bring the controlled system response back into the hatched region where the performance goals are achieved.

On the other hand, if the response is due to a broad band disturbance which lies above the dashed line then the response can not be controlled by ACOSS technology. Accordingly, the dashed line represents a control technology boundary for broad band disturbance applications. Similarly, the dotted line represents a control technology boundary for narrow band disturbance applications. When these curves are superimposed with response curves, a direct measure of the potential CSI control problem is obtained, as a function of the antenna diameter, operational frequency, and control technology.

2.3.5.1 Diameter vs. Operational Frequency

Performance trades are presented in this section for 250 and 19 GHz system design concepts. These results are generalized to determine the maximum antenna sizes when different design options are considered.

Figure 24 combines Figures 22 and 23 for a 250 GHz system and identifies the maximum antenna diameters which can be used for broad and narrow band disturbances as well as natural and passive damping treatment approaches. The maximum antenna diameters are indicated in Figure 24 by thick vertical lines, and the numerical values are summarized in Table 15. It is interesting to observe that the 15 m Geoplat system is only slightly outside of the hatched region, consistent with the results obtained in Section 2.2.5.

The performance curves for a 19 GHz system are presented in Figure 25 and the results for the maximum antenna diameters are presented in Table 16. The maximum antenna diameters are approximately 67% larger than for the 250 GHz case presented in Figure 24. These results indicate that the narrow band control capabilities exist for systems beyond 100 m diameters. Figures 24 and 25 indicate that passive damping offers significant benefits in terms of extending the operational antenna sizes which can be handled without active control means.

The maximum antenna diameters as a function of electromagnetic frequency are presented in Figure 26. The curves correspond to broad and narrow band control technology as well as natural and passive damping treatment concept designs. In all cases, the curves flatten out significantly for high frequency applications. Because the curves are based on extrapolations for system responses obtained for a 15m application, a future study should corroborate

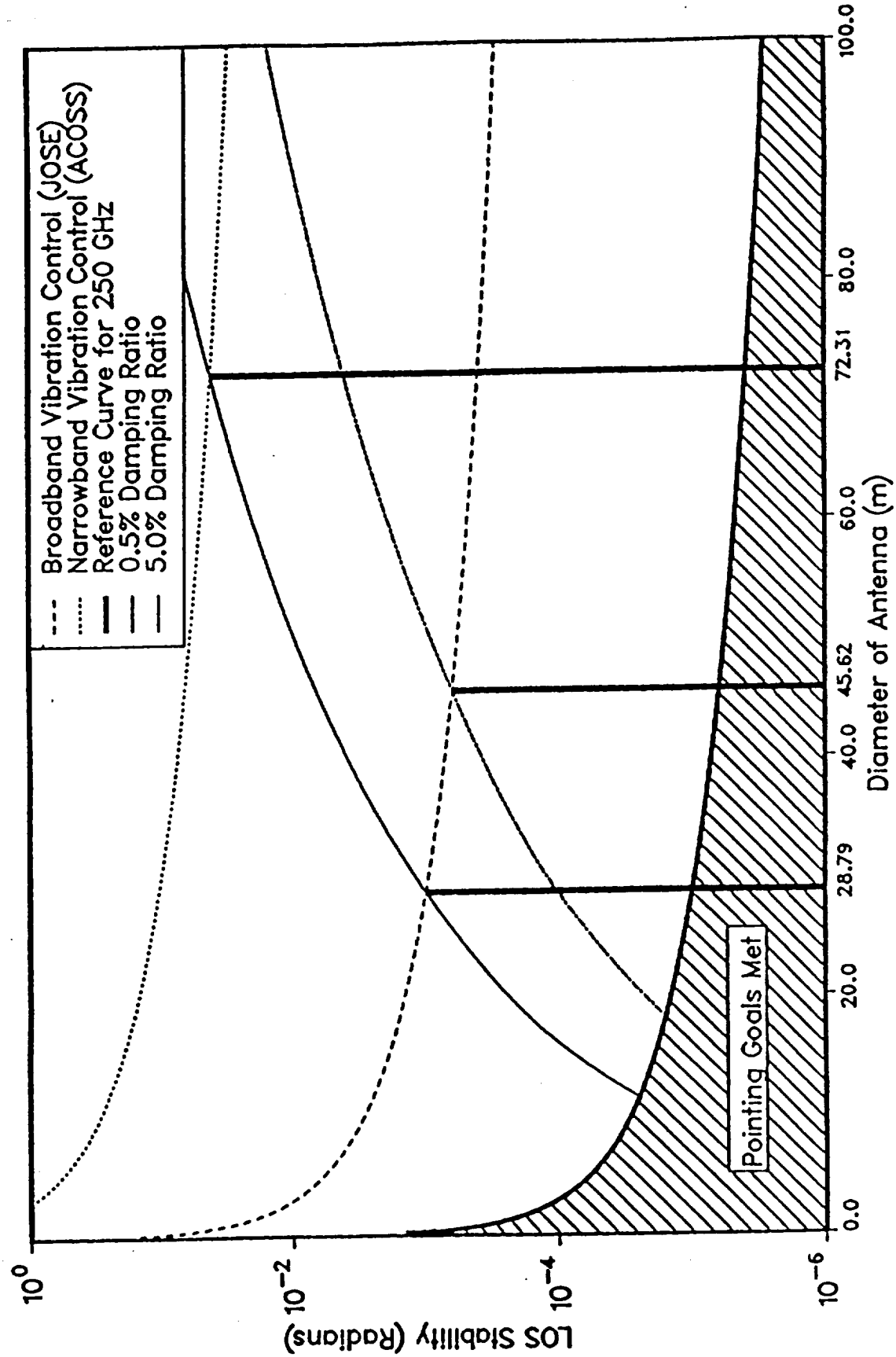

Figure 24: PERFORMANCE FOR A 250 GHz SYSTEM

TABLE 15: MAXIMUM ANTENNA DIAMETER FOR A 250 GHz SYSTEM

DAMPED RESPONSE (%)	BROADBAND CONTROL ANTENNA DIAMETERS (M)	NARROWBAND CONTROL ANTENNA DIAMETERS (M)
0.5	28.79	72.31
5.0	45.62	NOT SHOWN

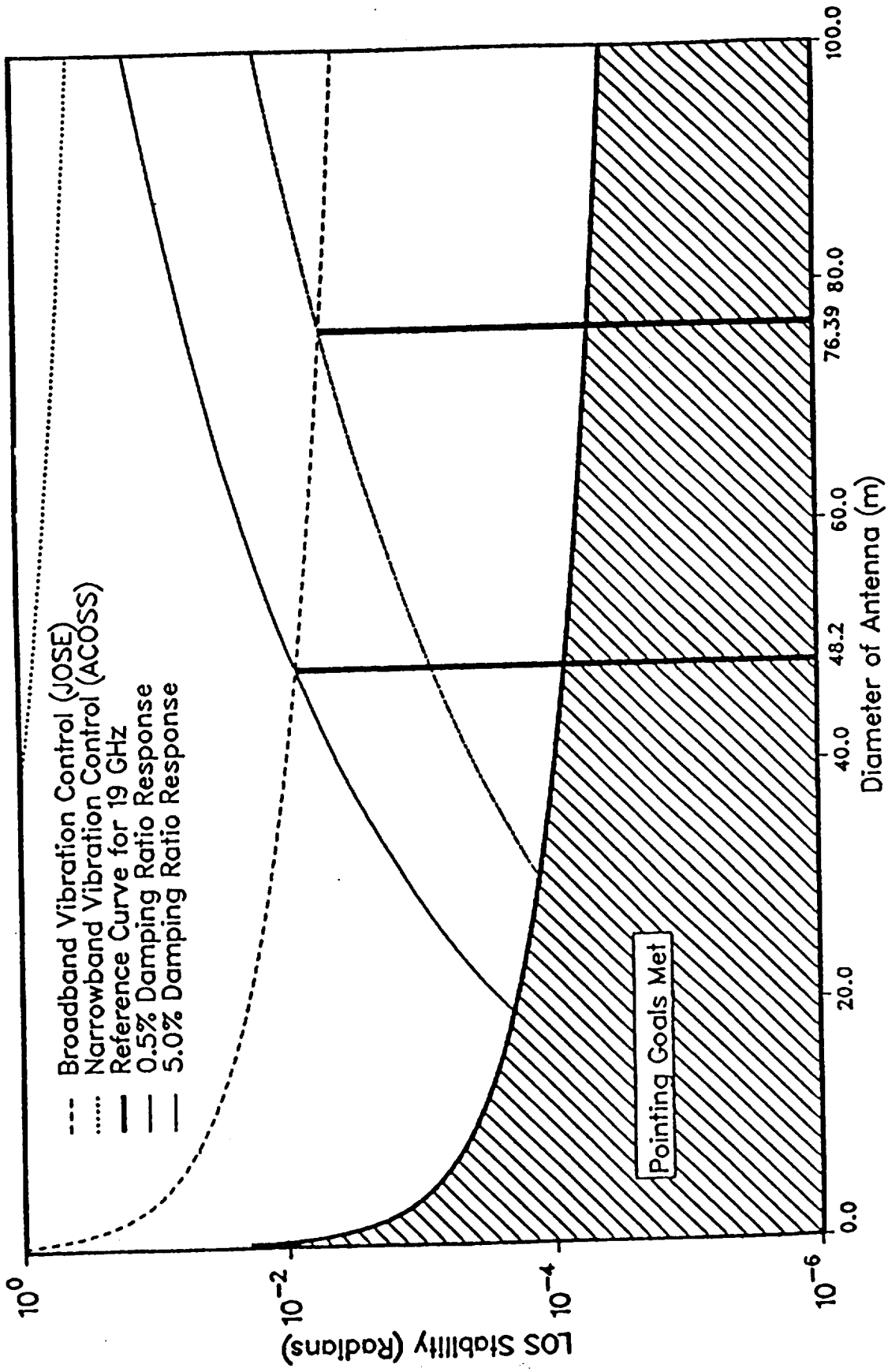

Figure 25: PERFORMANCE FOR A 19 GHz SYSTEM

TABLE 16: MAXIMUM ANTENNA DIAMETER FOR A 19 GHz SYSTEM

DAMPED RESPONSE (%)	BROADBAND CONTROL ANTENNA DIAMETER (M)
0.5	48.2
5.0	76.4

these predictions by developing point designs for one or more larger systems. Such an effort would greatly strengthen understanding about the abilities and limitations of the proposed concept evaluation methodology.

2.3.5.2 Light vs. Heavy Weight Structures

When a potential CSI problem is indicated after a preliminary investigation, it is natural to consider passive solution techniques because of the lower associated risk. Possible passive solutions include: i) modifying the structural design to strengthen it, ii) invoking the use of isolation techniques to minimize the transfer of disturbance inputs into the structure, and iii) applying passive damping treatments to reduce induced vibrations. Perhaps the simplest of the options is to modify the structure. For some problems, it is sufficient to add local stiffening to overcome troublesome behaviors. More complex applications, on the other hand, may require system-level changes in the basic interconnection topology throughout the structure. A basic strategy exploits the fact that the system structural frequencies are proportional to the system mass, so that by increasing the mass, the structural frequencies also increase. Because launch costs are related to the payload weight, there are practical limits to how effectively this re-design approach can be exploited. To be successful the following questions must be addresses: i) how much structural mass can be added and still satisfy the TITAN IV/CENTAUR launch weight constraints (i.e., for the Geoplat focus mission)?, and ii) how much structural frequency shift can be obtained by adding weight?

Table 17 presents the projected TITAN IV/CENTAUR launch capacities through the Mid 1990's. This data provides an upper limit for the payload weight to orbit. Recalling the structural model presented in Section 2.2.1, it can be shown that the structural mass represents approximately 10% of the payload weight. To apply scaling laws, it is assumed that only the structural mass can be changed in order to modify the structural behavior. By scaling the structural mass on the Geoplat subsystems: i) 15m antenna, ii) 15m subreflector support boom, iii) 7.5m antenna, iv) 7.5m subreflector support boom, and v) the platform main structure, the overall changes in the system response by varying the antenna diameter can be predicted.

Table 18 provides a summary of the structural frequency shifts which can be obtained by varying the structural mass using Eq. (3). The results of Table 18 are shown in Figure 27 where the nominal subreflector scanning torque input is assumed to act. These results indicate that adding structural mass to stiffen the structure provides little benefit for resolving potential CSI problems. Figure 28 presents the same data except in terms of %structural mass when the disturbance is assumed to move with the

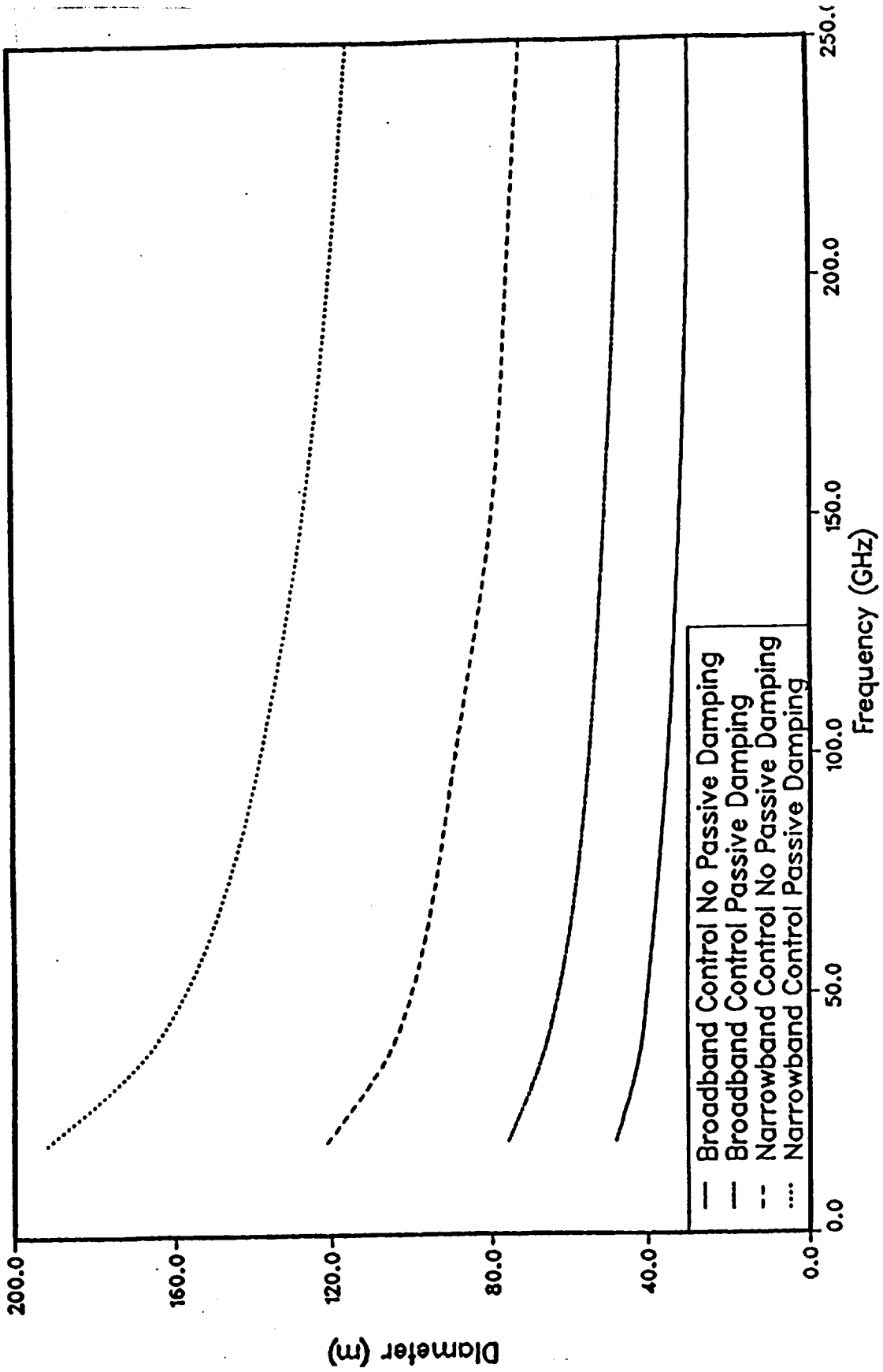

Figure 26: MAXIMUM ANTENNA DIAMETERS AS A FUNCTION OF ELECTROMAGNETIC FREQUENCY

TABLE 17: TITAN IV/CENTAUR LAUNCH CAPABILITY

- Performance to Geosynchronous Orbit
  (0 Deg. Inclination, 0.00 Deg. Eccentricity, 19,323 NM)

1988[1]	1991[2]	MID 1990s[3]
10,300 LB	13,500 LB (GOAL)	15,000 LB (GOAL)

- 86 Foot long fairing allows 40 foot long GEOP

NOTES

1. TITAN IV USER'S HANDBOOK, March 1988, Martin Marietta
2. Requires Solid Rocket motor Upgreade (SRM)
3. Required further SRM and/or 3rd stage upgreades

structural frequency. With the TITAN IV/CENTAUR launch capacity for the mid 1990's indicated, it is further reinforced that the increased mass option for Geoplat provides little benefit.

A further view of the mass variation response curves is provided by Figure 29. Here the performance gains are considered for a 250 GHz system, with both natural and passive damping treatment designs evaluated. This figure indicates that most systems under 30m can be controlled when broadband disturbances are present. Clearly, the greatest benefit occurs when passive damping treatments are used to minimize the structural response.

2.3.5.3 Passive vs. Active Control

In all instances, the use of passive control approaches for resolving CSI represent the preferred solution approach. This is because passive approaches require no active intervention during the operation of the system. Active control implies that on-board systems attempt to damp or suppress induced motions which affect the ability of the satellite to achieve mission performance goals. Unlike passive systems, active systems always carry with them the potential for inducing a resonant response in the structure. This is because passive systems tend to act as energy absorbing systems through damping mechanisms, whereas active systems represent a source of energy, which if not properly designed, can leak energy into the structure. A major design goal of closed loop control approaches is to develop stable techniques which meet the performance goals.

Table 19 presents a summary of the maximum antenna diameters which can be used when different electromagnetic operational frequencies are of interest. The predictions for narrowband control are (perhaps very) optimistic because the reliability of the response scaling laws must be questioned, for systems beyond 100m.

2.3.5.4 Theoretical vs. Experimental Studies

The results presented in Section 2.3 provide a means for conducting trade studies between competing technologies. A key assumption in the development of the control technology trade studies has been that the theoretically predicted two orders of magnitude for broadband control and four orders of magnitude for narrowband control can be achieved in practice. From the results presented in Section 2.2.4 it is clear that all of the experiments conducted to date have failed to achieve these performance objectives. Accordingly, for near-term systems, there are concerns over the availability of advanced control designs able to handle challenging control problems at the limits of theoretically predicted capabilities. To assess these potential concerns, Figures 30 through 32 present trade studies for 6, 19, and 250 GHz

TABLE 18: SUMMARY OF STRUCTURAL FREQUENCY SHIFTS FOR GEOPLAT SUBSYSTEMS

COMPONENT	NOMINAL FREQ.RATIO	-50% FREQ. RATIO	+50% FREQ. RATIO	+100% FREQ. RATIO	+200% FREQ. RATIO
15M Antenna	1.00	1.00	1.00	1.00	1.00
15M Boom	1.00	.73	1.20	1.32	1.51
7.5M Antenna	1.00	.74	1.16	1.29	1.47
7.5M Boom	1.00	.76	1.16	1.27	1.43
Platform	1.00	.71	1.22	1.40	1.69
AVERAGE NEGLECTING 15M ANTENNA	1.00	.75	1.18	1.30	1.50
RESPONSE SCALING $(f_1/f_2)^2$	1.00	1.78	.72	.58	.44

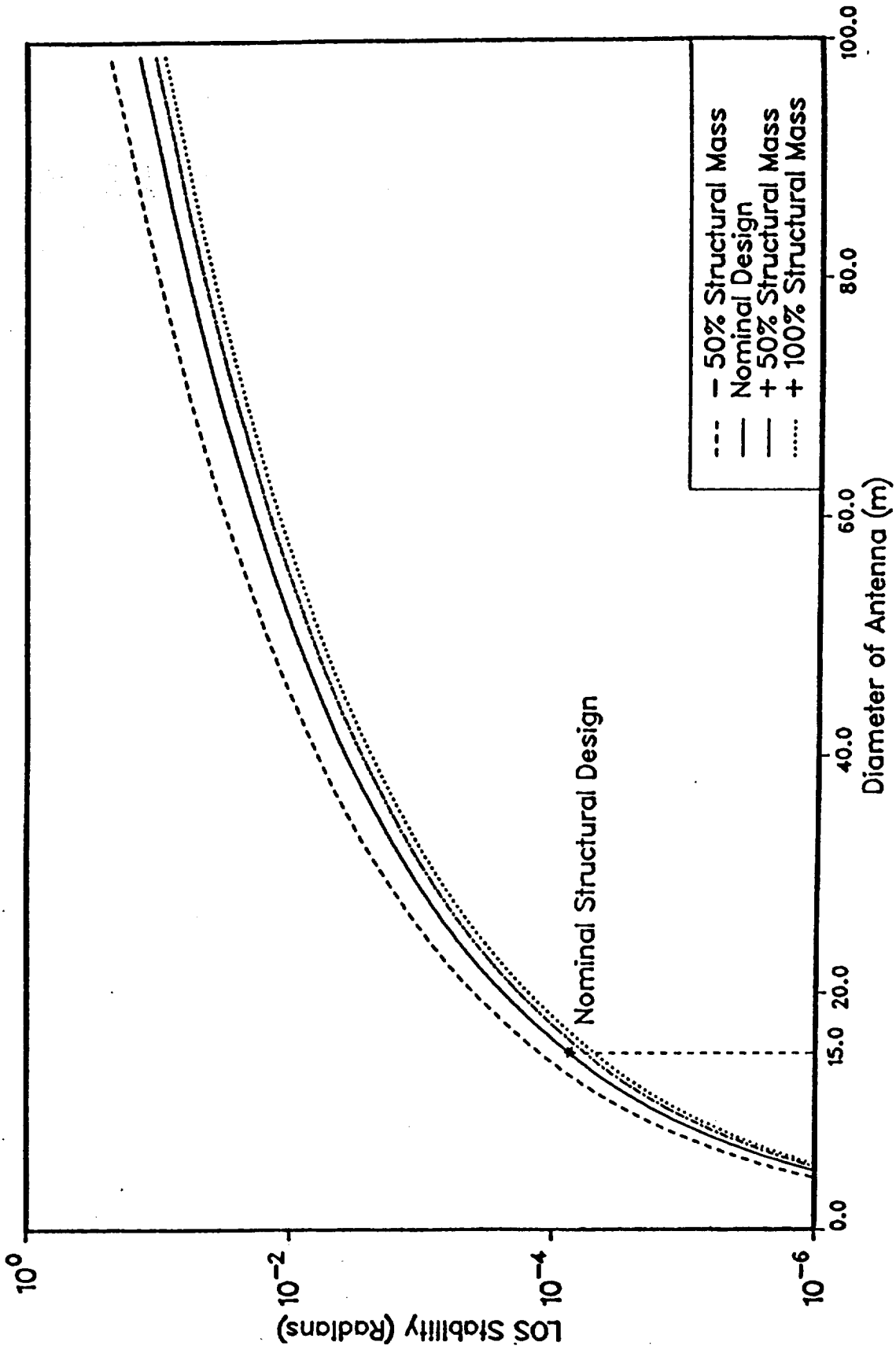

Figure 27: STRUCTURAL MASS VARIATION RESPONSE CURVES

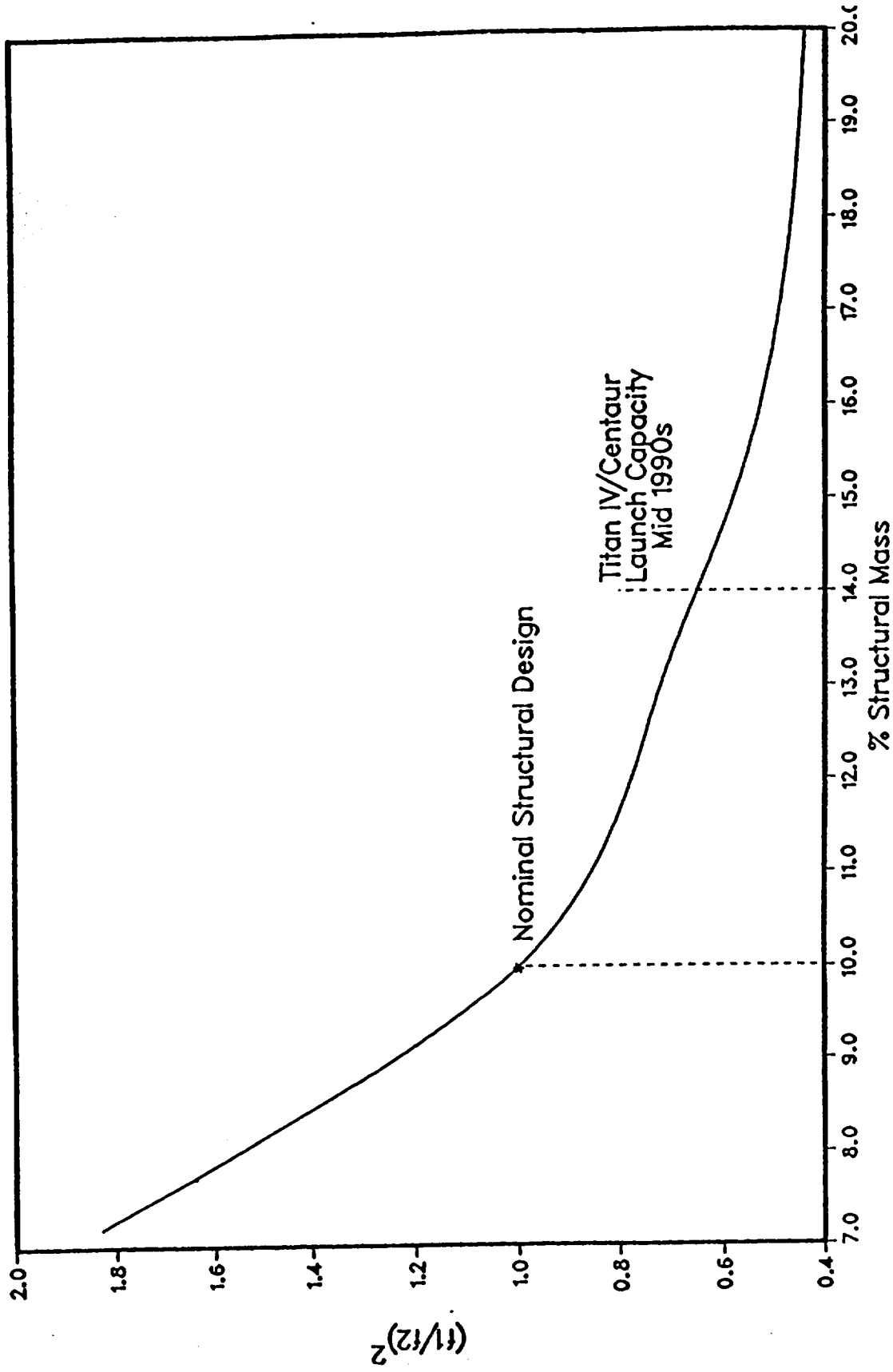

Figure 28: RESPONSE IF DISTURBANCE MOVES WITH STRUCTURAL FREQUENCY

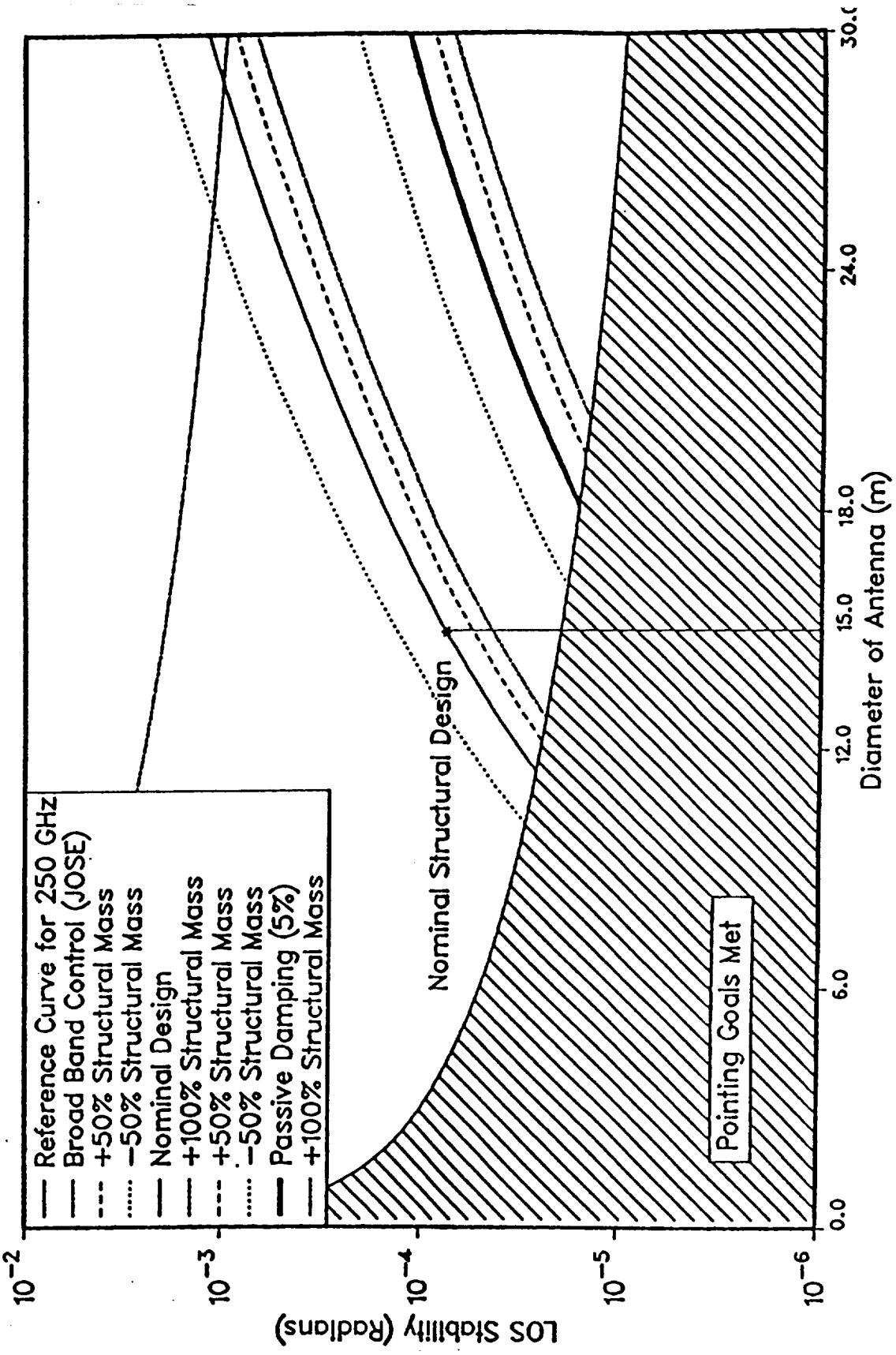

Figure 29: STRUCTURAL MASS VARIATION RESPONSE CURVES

TABLE 19: MAXIMUM ANTENNA DIAMETER FOR OPEN/CLOSED LOOP CONTROL APPROACHES

METHODOLOGY	GHZ 6	14	19	50	250
NO PASSIVE DAMPING					
Open-Loop	24	20	19	16	12
Broadband Control	61	51	48	40	29
Narrowband Control	152	129	121	72	72
PASSIVE DAMPING					
Open-Loop	38	32	30	25	18
Broadband Control	96	81	76	63	46
Narrowband Control	242	204	192	158	1115

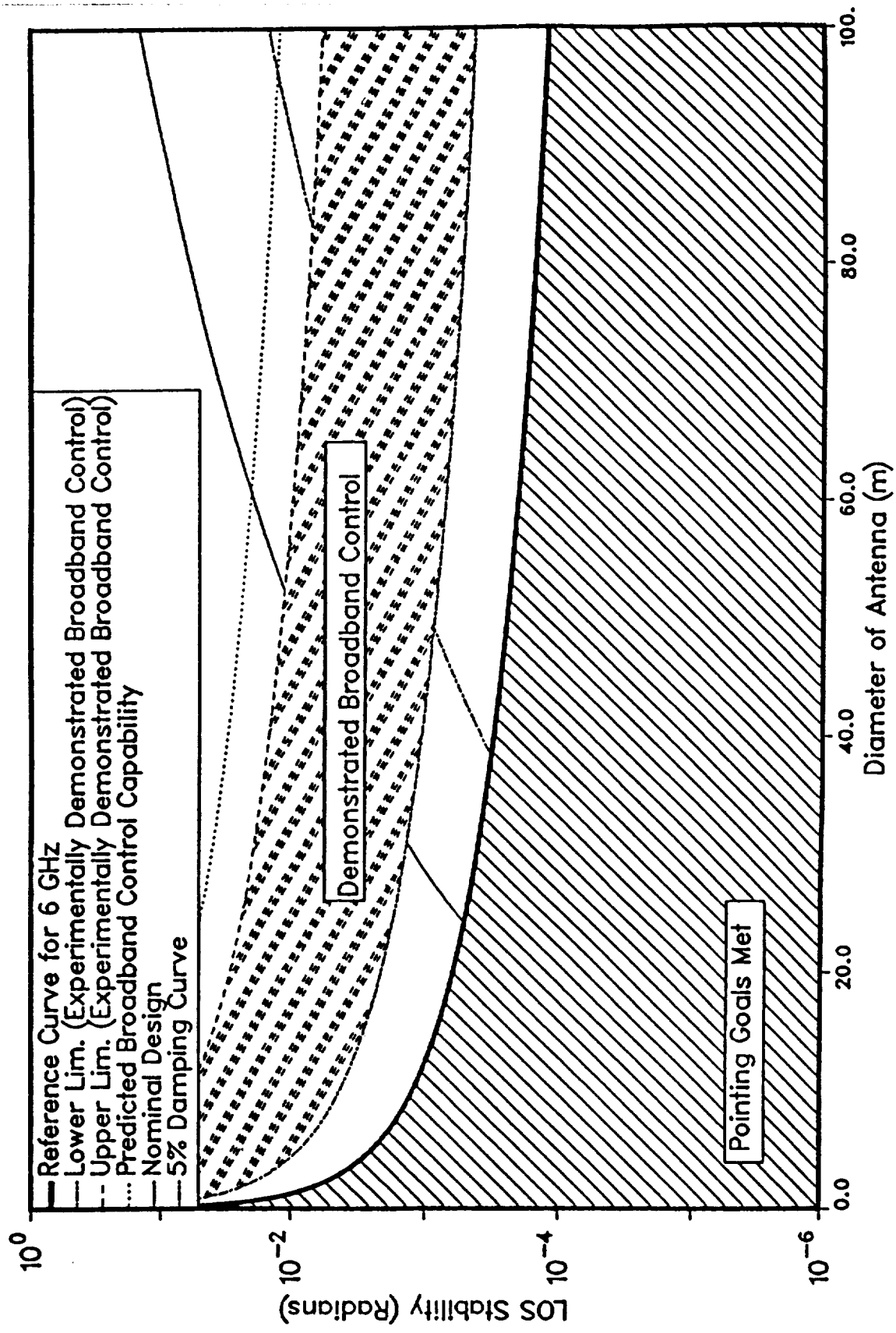

Figure 30: 6 GHz SYSTEM

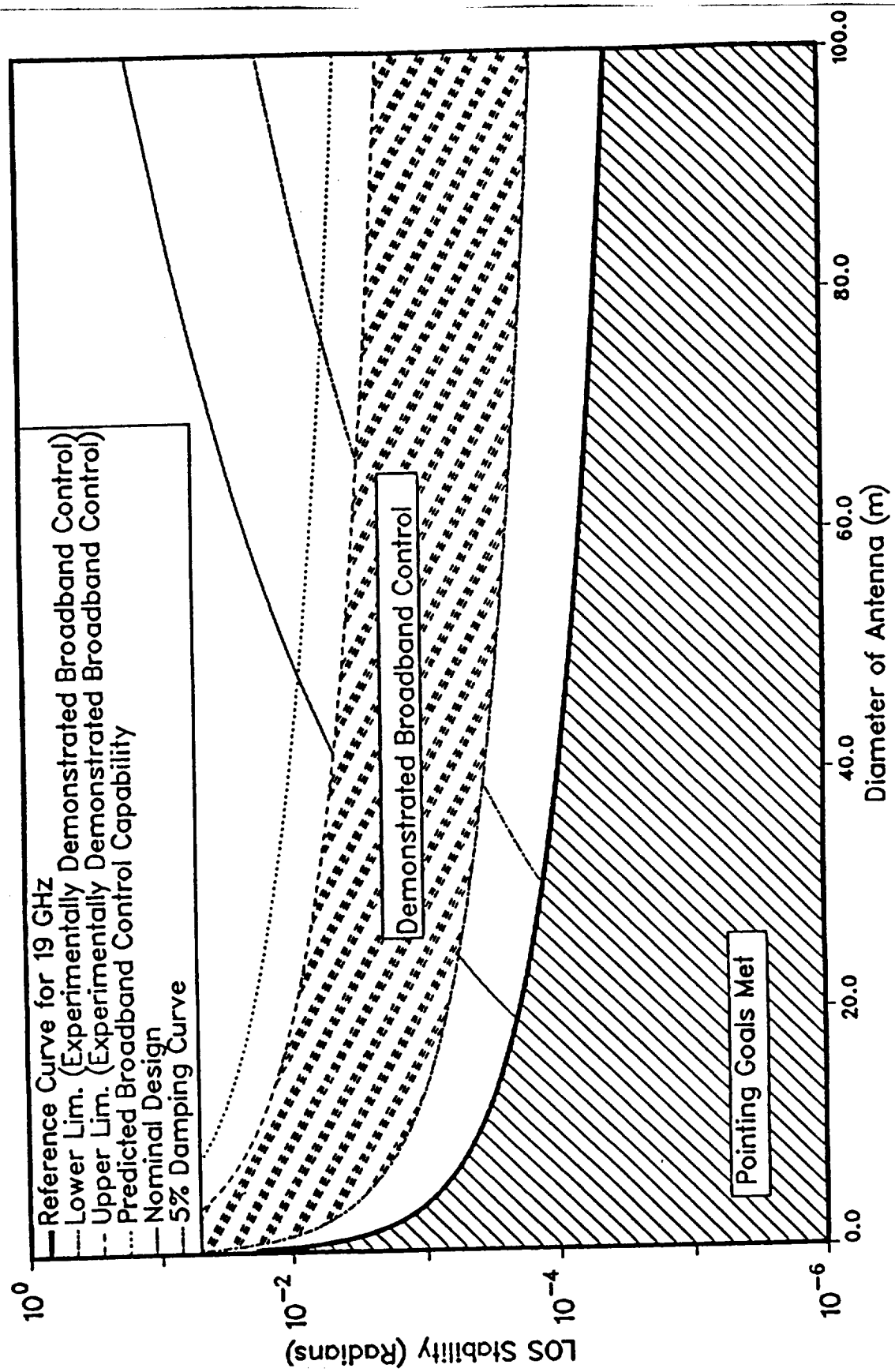

Figure 31: 19 GHz SYSTEM

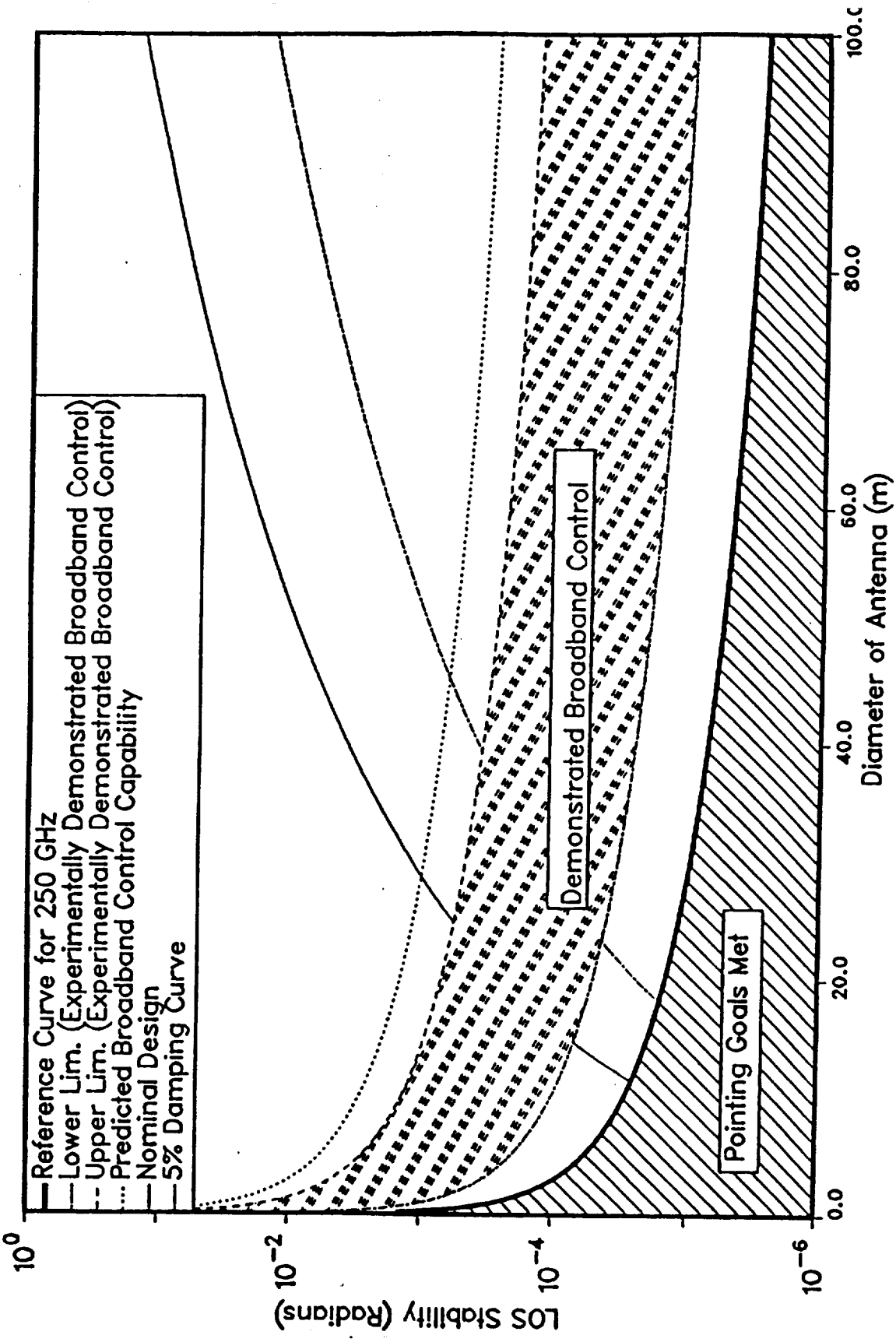

Figure 32: 250 GHz SYSTEM

systems. These results are similar to previously presented material, except that within the broadband control region, a hatched area has been included which represents the demonstrated hardware capabilities for control.

These results lead to a significant conclusion that there is a critical need for conducting detailed ground-based experiments which stress control capabilities at or very near the limits of theoretically predicted capabilities. By exploring the limits of achievable performance, one can carry out meaningful trade studies for a wide range of operational design concepts. Without dedicated experiments, many large scale system concepts may be subject to significant mission risks if there are uncertainties about the maturity of control related technologies.

3.0 CONCLUSIONS AND RECOMMENDATIONS

The basic conclusions which follow from the study presented in this report are:

* Passive damping approaches provide significant benefits

* Increasing the structural mass does not significantly reduce the interaction of the control and structural system

* Control and/or passive damping technologies are required for most missions beyond 20m.

* Demonstrated levels of broadband control capabilities will likely require further experimentation to establish the predicted two orders of magnitude response suppression capabilities

Beyond these top-level observations there remains a basic need to refine the CSI methodology presented here. Issues which need further attention include: i) performance verification for large-order point designs, ii) control/structure/disturbance bandwidth overlaps for larger order systems, iii) generic platform, antenna, and optical system scaling laws, and iv) interactions between enough different control technology options.

C.2

4.0 REFERENCES

1. Geostationary Platform Bus Study: For Earth Observations Sciences, Contract NAS8-36104, VOL II Comprehensive Report, Final Report, Sections 1.0 Through 10.0, September 1987, Ford Aerospace Corporation.

2. Dr. Sally Ride, Leadership and Americas's Future in Space, August 1987.

3. Space Technology to Meet Future Needs, Aeronautics and Space Engineering Board, NRC, 1987.

4. Earth System Science--A Closer View, Earth system sciences Committee, NASA Advisory Council, January 1988.

5. Thomas Paine, Pioneering the Space Frontier, National Commission on Space, 1988.

6. Space Science in the 21st Century, Space Science Board, NRC, June 1988.

7. Space-Based Remote Sensing of the Earth, A Report to the Congress, September 1987.

8. Taback, Israel,"Spacecraft Disturbances Caused By GOES-M Imager," Bionetics Memorandum, March 7, 1989.

9. Chu, Peter Y. "Slew Disturbance Compensation for Multiple Spacecraft Payloads," Paper no. AAS 89-369,Presented at the AAS/AIAA Astrodynamics Specialist Conference, Stowe, Vermont, August 7-10, 1989.

10. Bell, C. and Rudin, D., "Survey of State-of-the-Art Attitude Transfer Technology," JPL Interoffice Memorandum:IOM 343-88-276, April 7, 1988.

11. Junkins, J.L., and Turner, J.D.,"Optimal Spacecraft Rotational Maneuvers," Elsevier, 1986.

12. Hallauer, L.L., Skidmore, G.R., Gehling, R.N., "Modal-Space Active Damping of a Plane Grid: Experiment and Theory'" J. of Guidance, Dynamics, and Control, Vol. 8, No. 3, May-June 1985, pp. 366-373.

13. Meirovitch, L., Baruh, H., Montgomery, R.C., and Williams, J.P., "Nonlinear Natural Control of an Experimental Beam," Journal of Guidance, Control, and Dynamics, Vol. 7, No. 4, July-August 1894, pp. 437-442.

14. Bauldry, R.D., Breakwell, J.A., Chambers, G.J., Johansen,K.F., Nguyen, N.C., and Schaechter, D.B., "A Hardware Demonstration of Control for a Flexible Offset-Feed Antenna," The Journal of the Astronautical Sciences, Vol. 31, No.3, July-September 1983, pp. 455-470.

15. Schaechter, D.B., "Hardware Demonstration of Flexible Beam Control," Journal of Guidance, Control, and Dynamics, Vol. 5, No. 1, January-February 1982, pp. 48-53.

16. Forward, R.L., "Electronic Damping of Orthogonal Bending Modes in a Cylindrical Mast Experiment," Journal of Spacecraft and Rockets, Vol. 18, No. 1, January-February 1981, pp. 11-17.

17. Cannon, R.H., and Rosenthal, D.E., "Experiments in Control of Flexible Structures with Noncolocated Sensors and Actuators," Journal of Guidance, Control, and Dynamics, Vol. 7, No. 5, September-October 1984, pp. 546-553.

18. von Flotow, A.H., and Schafer, B., "Wave-Absorbing Controllers for a Flexible Beam," Journal of Guidance, Control, and Dynamics, Vol. 9, No. 6, November-December 1986, pp. 673-680.

19. Aubrun, J.N., Gregory, C.Z., Lyons, M.G., Kosur, R.L., and Woods Jr., A.A.,"Vibration Control of Space Structures VCOSS: High and Low-Authority Hardware Implementations," AFWAL-TR-83-3074, July 1983.

20. Schafer, B., and Holzach, H., "Experimental Research on Flexible Beam Modal Control," Journal of Guidance, Control, and Dynamics, Vol. 8, September-October 1985, pp. 597-604.

21. Herrick, D., Canavin, J., and Strunce, R., "An Experimental Investigation of Modern Modal Control," 17th Aerospace Sciences Meeting, New Orleans, LA, January 15-17, 1979.

22. Montgomery, R.C., Horner, G.C., and Cole, S.R., "Experimental Research on Structural Dynamics and Control," Third VPI & SU/AIAA Symposium on Dynamics and Control of Large Flexible Spacecraft, Blacksburg, VA, June 15-17, 1981.

23. Auburn, J.N., and Breakwell, J.A., "Experimental Results for Active Structural Control, " IEEE Conference on Decisions and Control, San Diego, CA, December 1981.

24. Bailey, T., Gruzen, A., and Madden, P., "RCS/Linear Discrete Actuator Study," Final Report for the period August 1985 - January 1988, AFAL-TR-88-039.

25. Bailey, T., Gruzen, A., and Madden, P.,"RCS/ Piezoelectric Distributed Actuator Study," Final Report for the period August 1985 - March 1988, AFAL-TR-88-038.

26. Ginter, S., Gelderioos, H., Jolley, S., and Billing-Ross, J."Slew Actuator System Requirements Study," Final Report for the period August 1986 - January 1988, AFAL-TR-88-034.

27. Vivian, J.C., Blair, P.E., Eldreed, D.B., Fleischer, G.E., Ih, C., Scheid, R.E., and Wen, J.T., "Flexible Structure Control Laboratory Development and Technology Demonstration," Final Report for the period July 1985 to July 1987, AFAL-TR-88-093.

28. Floyd, M.A., "Single-Step Optimal Control of Large Space Structures," M.I.T. Dept. of Aeronautics & Astronautics, Sc.D. Thesis, April 1984, Also CSDL report # CSDL-t-840.

29. Kelly,M.G., Podgorski, W.,and Hubbard jr., J.E., "Mechanical Design of a Flexible Spacecraft Test Model for Active Vibration Control," AIAA preprint No. AIAA-84-1048-CP, Presented at the 25th Structural Dynamics Conference, Palm Springs, CA, 1984.

30. Hubbard Jr., J.E., and Lowe, C.W.,"The Active Vibration Control of a Cantilever Beam Using PVF2 in a Simulated Space Environment," Technical Report CSDL-R-1821, The Charles Stark Draper Laboratory, Inc., Cambridge, MA, December, 1985.

31. Sundararajan, N., and Montgomery, R.C., "Adaptive Control of a Flexible Beam using Least Square Lattice Filters," Proceeding of the Fourth VPI&SU/AIAA Symposium on Dynamics and Control of Large Structures, Held in Blacksburg, VA, June 6-8,1983, pp.1-16.

32. Juang,J-N, Horta,L.G. and Robertshaw,H.H.,,"A Slewing Control Experiment for Flexible Structures,"Proceedings of the Fifth VPI&SU/AIAA Symposium on Dynamics and Control of Large Structures, Held in Blacksburg, VA, June 12-14, 1985,pp.547-570.

33. Belvin, W.K. and Edighoffer, H.H.,"Experimental and Analytical Generic Space Station Dynamic Models," NASA TM-87696, March 1986.

34. Juang, J-N, and Horta, L.G.,"A Slewing Control Experiment for Flexible Structures," Journal of Guidance, Control and Dynamics, Vol. 9, No. 5, September-October 1986,pp. 599-607.

35. Hallauer, W.L., Skidmore, G.R., and Gehling, R.N., "Modal Space Active Damping of a Plane Grid: Experiment and Theory," Journal of Guidance, Control, and Dynamics, Vol.7, July-August 1984, pp. 437-442.

36. Schaechter, D.B., and Eldred, D.B., "Experimental Demonstration of the Control of Flexible Structures," Journal of Guidance, Control, and Dynamics, Vol. 7, No. 5, September-October 1984, pp. 527-534.

37. Taylor, Larry, "3rd Annual NASA SCOLE Workshop 1986," NASA Technical Memorandum 89075, Held at NASA Langley Research Center, Hampton, VA, November 17-18, 1986.

38. Eldred, D.B., and Schaechter, D.B.,"Experimental Demonstration of Static Shape Control," Journal of Guidance, Control, and Dynamics, Vol. 6 May-June 1983, pp. 188-192.

39. Ih, C-H.C., Bayard, D.X., Wang, S.J., and Elred, D.B., "Adaptive 'Control Experiment with a Large Flexible Structure," AIAA GNCC, Aug 15-17,1988, Minneapolis, MN, pp. 833-857.

40. Aubrun, J.N., Lyons, M.G. and Ratner, M.J., "Structural Control for a Circular Plate," Journal of Guidance, Control, and Dynamics, Vol. 7, No. 5, September-October 1984, pp. 535-545.

41. Irwin, R.D., Jones, V.L., Rice, S.A., Tollison, D.K., and Seltzer, S.M., "Active Control Technique Evaluation for Spacecraft (ACES)," Final Report for Period Aug 1986 - July 1987, AFWAL-TR-88-3038.

42. Aubrun, J.N., et. al, "ACOSS Five (Active Control of Space Structures) Phase 1A," LMSC-D811889 under DARPA order 3654, March 1982.

43. Aubrun, J.N., and Margulies, G., "Low Authority Control Synthesis for Large Space Structures," NASA Contractor Report 3495, Langley Research Center, VA, September 1982.

44. Benhabib, R.J., et al, "ACOSS Fourteen (Active Control of Space Structures), RADC-TR-83-51, Rome Air Development Center, Griffiss Air Force Base, NY, March 1983.

45. Sesak, J.R., "ACOSS Seven (Active Control of Space Structures), RADA-TR-811-241, Rome Air Development Center, Griffiss Air Force Base, NY, September 1981.

46. Newsom, J.R., "NASA/DOD Controls-Structures Interaction Technology 1989," NASA Conference Publication 3041.

47. Wright, R.L., and Campbell, T.G.,"Earth Science Geostationary Platform Technology," NASA Conference Publication 3040.

48. Richards, K.E., and Rogers, L.C.: PACOSS Program Overview and Status. NASA/DOD Control/Structures Interaction Technology 1986 (NASA Conference Publication 2447).

49. Morgenthaler, D.R., and Gehling, R.N.,:Design and Analysis of the PACOSS Representative System. Damping 1986 Proceedings, May 1986,(AFWAL-TR-86-3059).

50. Balas, G.J., and Doyle, J.C.,"On the Caltech Experimental Large Space Structure and on Control of Flexible Truss Structure," Proceedings of the American Control Conference, Atlanta, GA, June 1988, pp. 1701-1702.

51. Lightsey, E. and Bauer, F., "Design and Analysis of a Flexible Body Instrument Pointing System for the GOES meteorological Satellites, "AIAA Paper No. 89-0542, Presented at the 27th Aerospace Sciences Meeting, January 9-12, 1989, Reno, NV.

52. Kwakernaak, H.A. and Sivan, R., Linear Optimal Control Systems, John Wiley & Sons, 1972.

53. Kailath, T., Linear Systems, Prentice-Hall, 1980.

54. Hyland, D.C., "The Optimal Projection Approach to Fixed-Order Compensation: Numerical Methods and Illustrative Results", AIAA 21st Aerospace Sciences Meeting, Reno, NV, January 1983.

55. Bernstein, D.S. and Hyland, D.C., "The Optimal Projection Approach to Designing Optimal Finite-Dimensional Controllers for Distributed-Parameter Systems", 23rd IEEE Conference on Decision and Control, Las Vegas, NV, December 1984.

56. Hyland, D.C. and Bernstein, D.S., "The Optimal Projection Equations for Fixed-Order Dynamic Compensation", IEEE Trans. Automat. Contr., vol. AC-29, pp. 1034-1037, November 1984.

57. Hyland, D.C., "Optimality Conditions for Fixed-Order Dynamic Compensation of Flexible Spacecraft with Uncertain Parameters", Proc. AIAA 20th Aerospace Sciences Meeting, paper 82-1403, January 1982.

58. Hyland, D.C. and Madiwale, A.N., "A Stochastic Design Approach for Full-Order Compensation of Structural Systems with Uncertain Parameters", AIAA Guidance and Control Conference, Albuquerque, NM, August 1981.

59. Bernstein, D.S. and Hyland, D.C., "The Optimal Projection Equations for Reduced Order State Estimation", IEEE Trans. Automat. Contr., vol. AC-30, pp. 583-585, June 1985.

60. Bernstein, D.S. and Hyland D.C., "The Optimal Projection Equations for Fixed-Order Dynamic Compensation of Distributed Parameter Systems", Proc. AIAA Dynamics Specialists Conference, Palm Springs, CA, May 1984.

61. Hyland, D.C., Mean-Square Fixed Order Compensation-Beyond Spillover Suppression", AIAA Astrodynamics Conference, San Diego, CA, August 1982.

62. Hyland, D.C., "Mean-Square Optimal, Full-Order Compensation of Structural Systems with Uncertain Parameters", M.I.T., Lincoln Laboratory, TR-626, June 1983.

64. Rowell, L.F., and Qualls, G.D., "Structural Analysis of an Earth Sciences Geostationary Platform Concept," NASA TP L-16749.

65. Farmer, J.T., Wahls, D.M., and Wright, R.L., "Thermal Distortion Analysis of an Antenna Strongback for Geostationary High Frequency Microwave Applications," NASA TP 1-16739.

66. Rowell, L.F., and Swissler, T.J., "Advanced Technology Needs for a Global Change Science Program: Perspective of the Langley Research Center," NASA TM L-16748.

67. Rowell, L.F., and Allen, C.L., "Data Base Architecture for Instrument Characteristics Critical to Spacecraft Conceptual Design," NASA TM L-16748.

68. Garrison, J.L., and Rowell, L.F., "Launch Vehicle Integration Options for a Large Earth Sciences Geostationary Platform Concept," NASA TP L-16819.

69. Wahls, D.M., Farmer, J.T., and Sleight, D.W., "On-Orbit Structural Dynamic Performance of a 15-Meter Microwave Radiometer Antenna," NASA TP L-16795.

70. Pidgeon, D.J., and Rowell, L.F., "A Subsystem Design Study of an Earth Sciences Geostationary Platform Concept."

71. Cosgrove, P.A., Farmer, J.T., and Rowell, L.F., "Thermal Distortion Analysis of a Spacecraft Box Truss in Geostationary Orbit," NASA TP L-16828.

72. Scott, A.D., Jackson, C.C., and Duricy, J.A., "Pointing Control Analysis of an Earth Sciences Geostationary Platform Concept," NASA TP L-16796.

73. Rowell, L.F., "A Technology Assessment and Systems Trade Study of an Earth Sciences Geostationary Platform Concept."

74. Air Force Space Technology Center, Air Force Systems Command, Kirtland Air Force Base, NM, "Military Space Systems Technology Plan - Mission Rationale and Requirements (U)" Vol. 1 of 5, Part 1 of 2, January 1985.

75. Air Force Space Technology Center, Air Force Systems Command, Kirtland Air Force Base, NM, "Military Space Systems Technology Plan - Concepts and Definitions (U)" Vol. 2 of 6, January 1985.

76. Air Force Space Technology Center, Air Force Systems Command, Kirtland Air Force Base, NM, "Military Space Systems Technology Plan - Technology Trends and Forecasts" (U), Vol. 3 of 6, January 1985.

77. Air Force Space Technology Center, Air Force Systems Command, Kirtland Air Force Base, NM, "Military Space Systems Technology Plan - Technology Assessment" (U), Vol. 4 of 6, January 1985.

78. Air Force Space Technology Center, Air Force Systems Command, Kirtland Air Force Base, NM, "Military Space Systems Technology Plan - Roadmaps: Contractor Version" (U), Vol. 5-B of 6, Part 1 of 2, January 1985.

79. Air Force Space Technology Center, Air Force Systems Command, Kirtland Air Force Base, NM, "Military Space Systems Technology Plan - Roadmaps: Contractor Version" (U), Vol. 5-B of 6, Part 2 of 2, January 1985.

80. Air Force Space Technology Center, Air Force Systems Command, Kirtland Air Force Base, NM, "Military Space Systems Technology Plan - Contractor Version" (U), Vol. 6-b of 6, January 1985.

81. NASA TM-88174, "NASA Space Systems Technology Model", June 1985.

82. NASA-88176 "NASA Space Systems Technology Model - Data Base Technology Forecasts" Vol. 1, Part A, June 1985.

83. NASA TM-88176, "NASA Space Systems Technology Model - Data Base Technology Forecasts", Vol. 1, Part B, June 1985.

84. NASA TM-88176, "NASA Space Systems Technology Model - Data Base Technology Analysis" Vol. 2, June 1985.

85. NASA TM-88174, "NASA Space Systems Technology Model - Data Base Future Mission Payloads" Vol. 3, June 1985.

86. R.W. Longmear and J.N. Juang, "Recursive Form of the Eigensystem Realization Algorithm for System Identification", Journal of Guidance, Control and Dynamics, Vol. 12, No. 5, Sept-Oct 1989, pp. 647-652.

87. Juang, J.N. and Pappa, R.S., "An Eigensystem Realization Algorithm (ERA) for Modal Parameter Identification and Model Reduction," Journal of Guidance, Control, and Dynamics, Vol. 8, Sept-Oct. 1985, pp. 620-627.

88. Juang, J.N. and Suzuki, H., "An Ergensystem Realization Algorithm in Frequency Domain for Modal Parameter Identification," Proceedings of the AIAA Guidance, Navigation and Control Conference, AIAA, New York, 1986.

5.0 LIST OF ACRONYMS

ACES	Active Control Evaluation for Spacecraft
ACOSS	Advanced Control of Space Structures
AFAL	Air Force Astronautics Laboratory
ARMA	Autoregressive Moving Average
ASTREX	Advanced Space Structure Technology Research Experiment
CM	Center of Mass
CSI	Control Structure Interaction
DARPA	Defense Advanced Research
DOF	Degrees-of-Freedom
EOS	Earth Observation Satellite
ERA	Eigensystem Realization Algorithm
FAMESS	Filter Accommodated Model Error Sensitivity Suppression
FFT	Fast Fourier Transform
FOV	Field of View
GEO	Geostationary Equatorial Orbit
GG	Gravity Gradient
GHz	Gigahertz
GPB	Geostationary Platform Bus
HAC	High Authority Control
Hz	Hertz
ID	Identification
IEEE	Institute of Electronic and Electrical Engineering
IOM	Interoffice Memorandum
IR	Infrared

LIST OF ACRONYMS (Continued)

JPL	Jet Propulsion Laboratory
LAC	Low Authority Control
LaRC	Langley Research Center
LDR	Large Deployable Reflector
LEO	Low Earth Orbit
LOS	Line of Sight
LQG	Linear Quadratic Gaussian
LSS	Large Space Structure
LTR	Loop Transfer Recovery
m	Meter
mm	Millimeter
MESS	Model Error Sensitivity Suppression
mr	Micro Radians
MIMO	Multi-Input Multi-Output
MSFC	Marshall Space Flight Center
N	Newton
NASA	National Aeronautics and Space Administration
NSTS	National Space Transportation System
ODE	Ordinary Differential Equation
OMV	Orbital Maneuvering Vehicle
OTV	Orbital Transfer Vehicle
PDE	Partial Differential Equation
PMA	Proof Mass Actuator
PMR	Passive Microwave Radiometer

LIST OF ACRONYMS (Continued)

POC	Proof-of-Concept
PPM	Pivoted Proof Mass
PSD	Power Spectral Density
rad	Radian
RCS	Reaction Control System
ROM	Reduced-Order Model
R2P2	Rapid Retargeting Precision Pointing
SCOLE	Spacecraft Control Laboratory Experiment
SDI	Strategic Defense Initiative
s	Second
SISO	Single-Input Single-Output
SOA	State-of-the-Art
TPBVP	Two-Point Boundary-Value Problem
VAMP	Vibration Analysis and Measurement Program

NASA
National Aeronautics and Space Administration

Report Documentation Page

1. Report No.	2. Government Accession No.	3. Recipient's Catalog No.
NASA CR-187471		

4. Title and Subtitle

Control-Structure-Interaction (CSI) Technologies and Trends for Future NASA Missions

5. Report Date
December 1990

6. Performing Organization Code

7. Author(s)
Photon Research Associates
Cambridge Research Division

8. Performing Organization Report No.

9. Performing Organization Name and Address
Lawrence Livermore National Laboratory
P. O. Box 5012
Livermore, CA 94550

10. Work Unit No.
585-01-41-01

11. Contract or Grant No.
L-44566C

12. Sponsoring Agency Name and Address
National Aeronautics and Space Administration
Langley Research Center
Hampton, VA 23665-5225

13. Type of Report and Period Covered
Contractor Report - Final

14. Sponsoring Agency Code

15. Supplementary Notes

This report was prepared by Photon Research Associates, Cambridge Research Division, Cambridge, Massachusetts 02138, under contract B063679 for Lawrence Livermore National Laboratory. Technical Monitor: William L. Grantham, Langley Research Center

16. Abstract

The objective of the study is to review Control-Structure-Interaction (CSI) issues which are relevant for future NASA missions. This goal has been achieved by: 1) reviewing large space structures (LSS) technologies to provide a background and survey of the current state of the art (SOA); 2) analytically studying a focus mission to identify opportunities where CSI technology may be applied to enhance or enable future NASA spacecraft; and 3) expanding a portion of the focus mission, the large antenna, to provide in-depth trade studies, scaling laws, and methodologies which may be applied to other NASA missions.

The report is presented in several sections. Section 1 defines CSI issues and presents an overview of the relevant modeling and control issues for Large Space Structures. Section 2 presents the results of the three phases of the CSI study. Section 2.1 gives the results of a CSI study conducted with the Geostationary Platform (Geoplat) as the focus mission. Section 2.2 contains an overview of the CSI control design methodology available in the technical community. Included is a survey of the CSI ground-based experiments which have been conducted to verify theoretical performance predictions. Section 2.3 presents and demonstrates a new CSI scaling law methodology for assessing potential CSI with large antenna systems.

17. Key Words (Suggested by Author(s))	18. Distribution Statement
Large Flexible Space Structures Large Space Antennas Controls-Structures Interaction	unclassified - unlimited subject category - 18

19. Security Classif. (of this report)	20. Security Classif. (of this page)	21. No. of pages	22. Price
unclassified	unclassified	110	A06